Design and Performance Analysis of a Low Complexity MIMO-OFDM System with Walsh Block Coding

Amr Hussein El Mougy

A Thesis

in

The Department

of

Electrical and Computer Engineering

Presented in Partial Fulfillment of the Requirements for

the Degree of Master of Applied Science at

Concordia University

Montreal, Quebec, Canada

Your file Votre référence
ISBN: 978-0-494-20744-4
Our file Notre référence
ISBN: 978-0-494-20744-4

Abstract

Design and Performance Analysis of a Low Complexity MIMO-OFDM System with Walsh Block Coding

Amr Hussein El Mougy

There are many technologies being considered for the next generation of wireless communications. Of these technologies, multi-input multi-output (MIMO), orthogonal frequency division multiplexing (OFDM) and Walsh spreading are drawing the most attention. Although a lot of research has been done in this area, it has not been decided yet as to which technology or combination of the technologies will be used in future wireless generations. The new generation will have to support high data rates and provide excellent performance in order to accommodate several multimedia services. In this thesis, a MIMO-OFDM system that employs Walsh sequences as block coding is designed. Simulation studies show that the proposed system exhibits high performance and comparisons show that it has low complexity compared to some of the previous systems.

Two configurations are considered for the proposed system. The first configuration combines Vertical-Bell Labs Layered Space-Time (VBLAST), OFDM and Walsh block coding, for which a simplified implementation scheme for the proposed coding is

presented. The system is investigated through extensive computer simulations using different system parameters and channel conditions. The proposed system is compared to some of the existing systems in terms of performance as well as computational complexity.

The second configuration integrates space-time block coding (STBC), OFDM and Walsh block coding. In contrast to VBLAST, which aims to increase system capacity and data rates, STBC improves the system's performance through multipath diversity. The performance of the system is studied through computer simulations and the computational complexity of the system is also compared to some typical STBC systems from previous research. The simulations and comparisons of both configurations of the proposed system show its superiority in terms of performance and computational complexity to previous systems.

Finally, to emulate real-life scenarios, the performance of the proposed system is also investigated using some common channel estimation techniques. It is shown that by utilizing a preamble of training symbols, the proposed system provides a satisfactory performance for both the configurations.

"A pessimist sees the difficulty in every opportunity;

an optimist sees the opportunity in every difficulty"

Sir Winston Churchill

Acknowledgments

It would not have been possible to complete this research project without the help and support of many people. First of all, I am truly grateful for the blessings and spiritual support of God which has been a guiding light for me throughout my life. Next, I would like to express my deep gratitude towards my advisors, Dr. W.-P Zhu and Dr. M.O. Ahmad, whose continuous support and invaluable advice have been vastly influential throughout my master's studies. I am much obliged to them and I feel honored and privileged to have had the chance to work under their supervision. I look forward to maintaining a continued friendship with them in the future.

I would also like to thank Dr. M.R. Soleymani for his encouragement and guidance throughout my master's studies. I have gained a great deal of knowledge on the professional and personal level from his direction.

The completion of this thesis would not have been possible without salubrious surroundings. I thank my parents for their love and support throughout my life. I am forever indebt to them for all my achievements and for raising me the person that I am today.

Table of Contents

List of Tables

List of Figures

List of Abbreviations

ADC	Analog to Digital Converter
AGC	Adaptive Gain Control
AMPS	Analog Mobile Phone Service
ASK	Amplitude Shift Keying
AWGN	Additive White Gaussian Noise
BER	Bit Error Rate
BPSK	Binary Phase Shift Keying
CDM	Code Division Multiplexing
CDMA	Code Division Multiple Access
CIR	Channel Impulse Response
CP	Cyclic Prefix
CSI	Channel State Information
DAB	Digital Audio Broadcasting
DAC	Digital to Analog Converter
DBLAST	Diagonal BLAST
DFT	Discrete Fourier Transform
DSP	Discrete Signal Processing
DVB-T	Terrestrial Digital Video Broadcasting
EM	Expectation Maximization
FDMA	Frequency Division Multiple Access
FEC	Forward Error Correction

FFT	Fast Fourier Transform
FWT	Fast Walsh Transform
GF	Galois Field
GI	Guard Interval
GSM	Global System for Mobile Communications
ICI	Inter-Carrier Interference
IFFT	Inverse FFT
IS-95	Interim Standard – 95
ISI	Inter-Symbol Interference
LAS-CDMA	Large Area Synchronized – CDMA
LOS	Line of sight
LRA	Lattice-Reduction-Aided
LS	Least Squares
LST	Layered Space-Time
MAC	Medium Access Control
MAI	Multiple Access Interference
MC-CDMA	Multi Carrier – CDMA
MIMO	Multiple Input Multiple Output
MMSE	Minimum Mean Square Error
MRC	Maximum Ratio Combining
MSE	Mean Square Error
OFDM	Orthogonal Frequency Division Multiplexing
OFDMA	Orthogonal Frequency Division Multiple Access

OWA	Open Wireless Architecture
PAC	Per-Antenna-Coding
PAPR	Peak to Average Power Ratio
PDC	Personal Digital Cellular
PDF	Partial Decision Feedback
PER	Packet Error Rate
PHY	Physical Layer
PIC	Parallel Interference Cancellation
PLCP	Physical Layer Convergence Procedure
PLME	PHY Layer Management Entity
PMD	Physical Medium Dependant
QAM	Quadrature Amplitude Modulation
QPSK	Quadrature Phase Shift Keying
SIC	Successive Interference Cancellation
SISO	Single Input Single Output
SNR	Signal to Noise Ratio
SOMLD	Soft-Output Maximum Likelihood Detection
STBC	Space Time Block Code
TDMA	Time Division Multiple Access
TD-SDMA	Time Division - Synchronous CDMA
VBLAST	Vertical - Bell Labs Layered Space Time
WLAN	Wireless Local Area Networks
ZF	Zero Forcing

List of Symbols

a	Transmit signal vector
$\hat{a}_{k_i}$	Estimated transmitted VBLAST symbol k_i
C	Power constraint of the training symbols
d_{min}	Minimum distance of the code
F	Fourier transform matrix
G	Nulling matrix
H	Complex channel matrix
$\mathbf{H}_{2N}$	Hadamard matrix of order 2N
h_{ji}	Complex channel transfer functions from transmit antenna i to the receive antenna j
I_0 (x)	Bessel function of order zero
K	Rice factor
L	Number of symbols in each preamble
M_T	Number of transmit antennas
M_R	Number of receive antennas
N	Order of the completer Walsh sequence set
P	Matrix of transmitted preambles
p(x)	Probability density function of the channel envelope
R	Code Rate
r	Received data signal
$\mathbf{R_H}$	Channel correlation matrix

$\mathbf{S}$	Matrix of received preambles
S	Number index of the Walsh sequence
$\hat{s}$	Estimated transmitted STBC symbol
T	Period of one Walsh sequence
t	Error correction capability of the block code
$\mathbf{v}$	AWGN matrix
$W_j(t)$	j^{th} Walsh sequence from a complete set of Walsh sequences
$\boldsymbol{w}_{k_i}$	Weight vector
y_{k_i}	Decision Statistic for the symbol i
α	Correlation factor
$\mathcal{E}^2$	Error matrix
θ	Phase shift of the multipath fading
ρ	Attenuation factor of the multipath fading
σ_n^2	Noise variance
Ω_p	Total envelope power

Chapter 1

Introduction

Over the last twenty years the world has witnessed an extraordinary growth of wireless communications from limited analog techniques to complete digital systems. The number of users of wireless applications has rocketed and continues to grow exponentially. As technology advances the demand for complex services also increases. These represent considerable challenges to the development of the next generation of wireless systems. These systems will have to provide and integrate several diverse services such as multimedia and broadband data services. The word multimedia refers to a combination of many signal types such as voice, image, video stream, video conferencing, text, etc, which makes multimedia communications extremely challenging to researchers due to the different types of compression and encoding techniques. There is also increasing demand for fast internet access on mobile phones. Scientists all over the world are struggling to develop technologies to meet these demands.

This chapter provides an outlook on recent developments in the wireless communication industry and technologies proposed to meet the users' demands. At the end of the chapter the motivation to the research topic undertaken in this thesis will be highlighted and the organization of thesis will be presented.

1.1 The Next Generation of Wireless Communications

Table 1.1 [1] shows the evolution of the generations of wireless communications starting with the analog AMPS (1G) which only supported voice to what is now called 4G which is still under investigation.

The newest standard currently deployed is 3G was first "on air" in Japan in 2001 and several countries in Europe followed later. Yet there are several problems and limitations facing the growth of 3G [2]. One of the most important problems is that it takes a huge capital investment to install the network as there are large technological differences between 3G and 2G. Another problem is that the many different standards being developed by the researchers for 3G make roaming very difficult. The 3G systems have also failed to realize their full potential as the signals are still susceptible to multipath fading. Although the data rates have increased from a maximum of 125 kbps in 2.5G to 2 Mbits/sec (a minimum of 384 kbps) in 3G, the increasing demand for higher data rates is forcing scientists to look beyond 3G. Table 1.1 [1] gives a brief description of different wireless network generations and related access technologies as well as key features.

Generation	Access Technology	Features
1G Wireless	• Advanced Mobile Phone Service (AMPS)	Analog Phone Service. No data Service.
2G Wireless	• Code Division Multiple Access (CDMA) • Global System for Mobile Communications (GSM) • Personal Digital Cellular (PDC)	Digital voice service 9.6K to 14.4K bits/sec. CDMA, TDMA and PDC offer one way data transmissions. Enhanced calling features like caller ID. No always-on data connection.
3G Wireless	• Wideband CDMA • Based on the Interim Standard-95 CDMA (CDMA 2000) • Time Division Synchronous CDMA (TD-SDMA)	Superior voice quality. Up to 2Mbits/sec. Always-on data. Broadband data services like video and multimedia. Enhanced roaming. Circuit and packet switched networks.
4G Wireless	• Orthogonal Frequency Division Multiplexing (OFDM) and (W-OFDM) • Multi-Carrier (MC-CDMA) • LAS-CDMA	Converged data and voice over IP. Entirely Packet switched networks. All network elements are digital. Higher bandwidth to provide multimedia services at lower cost (up to 100Mbits/sec)

Table 1.1 The evolution of wireless networks [1]

Until now there is no clear definition of what 4G exactly will be, but scientists have very high expectations for the standard under construction. Hopefully, 4G networks will be able to merge different existing wireless networks, such as WLANs, wireless ATMs and other networks in offices and shopping centers, into a new architecture called the open wireless architecture (OWA) [3]. There are several goals that 4G needs to achieve [1]:

- 4G networks need to have a much better performance at much higher data rates to be able to facilitate high quality video streaming and other multimedia content.

4G is expected to have at least a rate of 20 Mbps and the speed is expected to reach 100 Mbps or even more in hot spots.

- As mentioned before, 4G will permit roaming in an unprecedented manner. There will be seamless interoperability between several types of wireless networks.
- 4G networks will be able to handle the increasing number of users and their changing demands.
- 4G networks are expected to be cheaper than 3G networks.

The industries and academic researchers have separate but dependent roles in realizing this dream [1]. The industry has to standardize the wireless technologies proposed for 4G, if roaming is to be realized. Spectrums have to be regulated to ensure that there will be a specific frequency band for 4G. Networks have to be interconnected and the move from 3G to 4G has to take place with as little inconvenience to the users as possible. It is up to the academic researchers to come up with the technologies that will realize all these goals with as minimum cost as possible.

1.2 Technologies Proposed for the Next Generation of Wireless Communications

There are many technologies proposed for 4G systems and researchers have not yet made up their minds as to which technology or combination of technologies will be used. However, certain key techniques seem to come up in most of the new research papers.

1.2.1 Orthogonal Frequency Division Multiplexing (OFDM)

OFDM is definitely the front runner as the transmission protocol for 4G systems. It was first developed in the 1960's but was exclusively used by the military due to its high cost. As VLSI evolved, DSP chips became easily available and OFDM was revived. OFDM is a multi-carrier modulation scheme where the incoming signal is split into many narrowband signals using an IFFT process and all the carriers are transmitted simultaneously. The carriers are orthogonal which makes the transmission resilient to multipath fading. Fig. 1.1 shows an OFDM signal in the frequency domain.

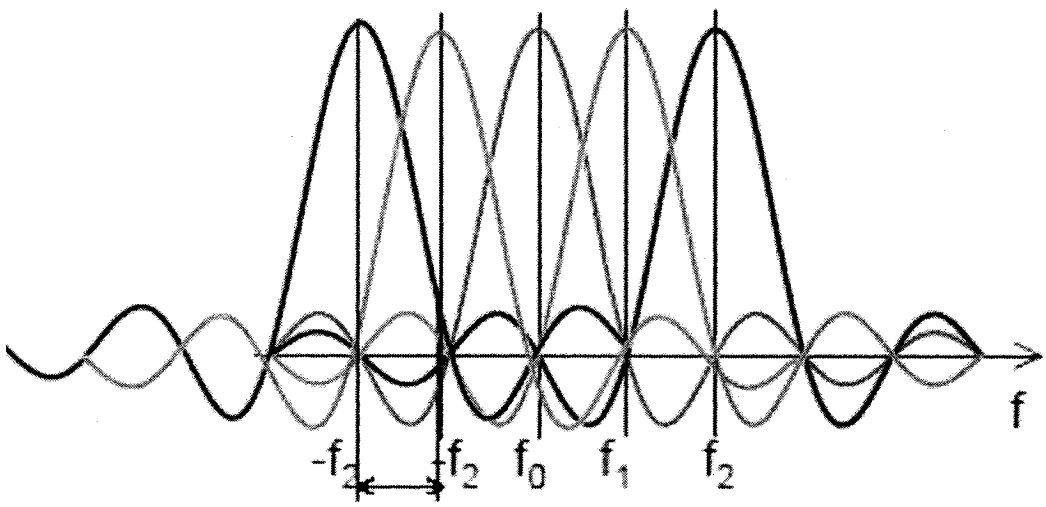

Fig 1.1 An OFDM signal in the frequency domain

In the figure we can see f_0, f_1, …, etc., are the frequencies of the individual subcarriers. Although the subcarriers overlap, at each subcarrier frequency only one signal exists with all the other signals' amplitudes being equal to zero, which implies a high spectrum efficiency. Therefore, theoretically there is no interference among the signals. In practical

conditions the signals lose orthogonality and synchronization has to be performed. OFDM has many advantages over other modulation techniques [4]:

- High resistance to multipath fading.
- High bit rates and high spectrum efficiency due to the overlapping of the orthogonal carriers.
- Low receiver complexity as OFDM is detected using a simple FFT process and equalizers are usually not required.
- Easy implementation (due to the availability of IFFT chips).
- Reduced interference due to the reduced transmission rate of the signal at each subcarrier.

However, OFDM faces certain challenges that have to be addressed:

- Phase distortion and sensitivity to time and frequency synchronization.
- Large peak to average power ratio (PAPR) as the radio components are designed to run at the system's peak value and not its average. This also leads to faster battery consumption.

OFDM has now been adopted in several systems such as DAB (Digital Audio Broadcasting), DVB-T (Digital Video Broadcasting) [6], several IEEE standards which will be discussed in the following chapters, and HIPERLAN/2 [5].

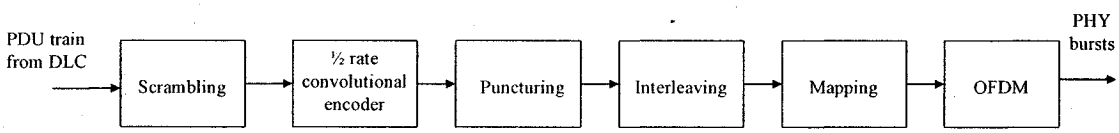

Fig 1.2 Typical HIPERLAN/2 transmitter [5]

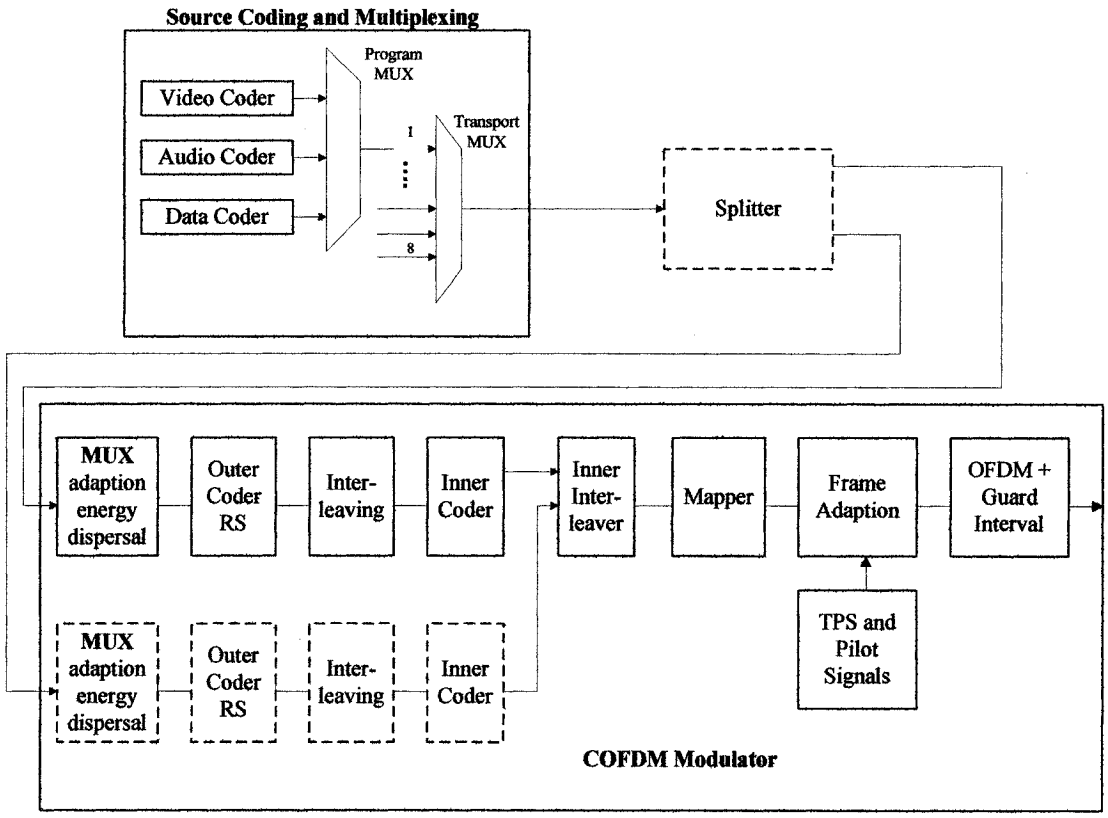

Fig 1.3 Typical DVB-T transmitter [6]

Figs. 1.2 and 1.3 show the transmitter structures of HIPERLAN/2 and DVB-T, respectively. We can see that in both transmitters, OFDM is the final stage before transmission. The blocks before OFDM stage are dependent on the nature of the transmitted data. For example, more coding is applied in the DVB-T transmitter, because the transmission of video streams requires low bit error rates (BER).

1.2.2 Multiple Input Multiple Output (MIMO) Communications

By using multiple antennas at both the transmitter and the receiver we can exploit the space dimension to achieve more diversity. MIMO sends different signals on the different

multipaths, thereby using the effects of multipath fading to the advantage of the transmission instead of trying to eliminate them. In fact, the denser the multipath environment the more spatial diversity we can use. The signals can be encoded in such ways as to improve performance or increase the transmission rate and capacity. These issues will be addressed in detail in the upcoming chapters.

MIMO uses simple encoding and decoding signal processing algorithms at the transmitter and receiver. It operates at the physical layer with no need for the modification of any protocols. For these reasons MIMO is very flexible and could be attached to almost any wireless communication system. MIMO is implemented via signal processing chips and therefore it would be very cost effective to integrate it instead of upgrading LANs. MIMO awards several advantages to the communication process [7]:

- It enables higher rates which permit the handling of rich multimedia content. Since higher rates mean larger bandwidth, the increased rates could also be used to accommodate more users.
- MIMO reduces the effects of interference which means that the signals can still be received over longer distances. This is very cost effective as fewer transmission stations would be required. Less interference, or equivalently, lower transmission power could be used to achieve lower battery consumption and more energy conservation. However, the number of antennas that could be used is limited by the nature of the environment surrounding the transmitting station.
- The power and phase of each antenna could be adjusted separately in what is known as steering so as to further reduce interference.

- Sending different data across antennas could provide more security as the receiver has to gather all the transmitted signals in order to conjure up the whole message.

Though MIMO systems are very cost effective, they still face some challenges [7], mostly because the technology is still new and has not grown wide enough. Most of the available transmissions today use single paths and most MIMO tests have been done indoors. MIMO would be more effective for larger mobile organizations as they have the ability to widely deploy the technology. For example, it would not do much good for an internet user in a small office or home to use MIMO. More research integrated with efficient marketing is needed for the technology to be accepted worldwide.

Since MIMO and OFDM have very promising prospects, it is a very good idea to integrate them. In fact, researchers now consider MIMO-OFDM to be a very popular broadband wireless access scheme. MIMO increases data rates and thus, causes the channel to be more frequency selective. OFDM transforms the signal into multiple narrowband signals and thus reduce the effects of multipath fading. Integrating them both gives great capacity and performance results with low receiver complexity as there is no need for equalization.

1.2.3 MC-CDMA

Multiple Carrier-Code Division Multiple Access (or MC-CDMA) is simply integrating OFDM with CDMA. CDMA is of course the access technology used by 3G systems. Users are assigned orthogonal codes (Walsh codes are normally used) that can be easily separated at the receiver. Integrating CDMA with OFDM eliminates the need for the

wide bandwidth needed by CDMA alone and adds to OFDM a multiple access feature. A typical MC-CDMA transceiver is shown below [18].

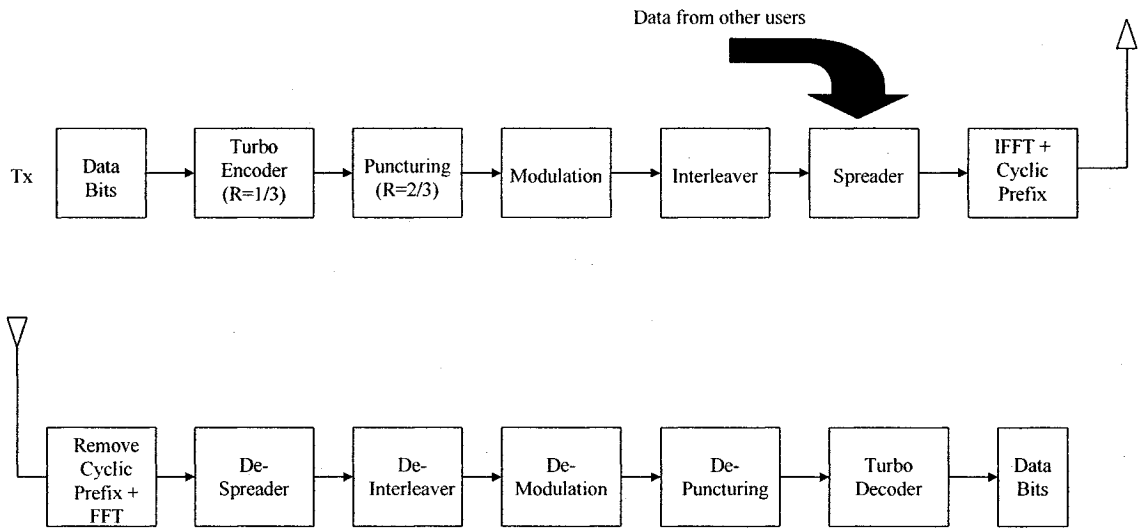

Fig 1.4 Typical MC-CDMA transceiver [18]

Fig. 1.4 shows the transmitter and receiver structure for each user of the MC-CDMA system. The input data is spread using a code from a complete set of orthogonal Walsh codes at the spreader block where data from other users is also added. Afterwards, the spread data passes through an OFDM block where they are converted to the time domain prior to transmission.

1.3 Motivation and Scope of the Thesis

In the preceding sections, we took a close look at the new trends in the wireless communications industry. MIMO, OFDM and CDMA seem to offer promising potential for communication and their combinations offer even better prospects. This is not a new idea; researchers have came up with several different ideas to combine the three technologies and even gave them different names such as MIMO-MC-CDMA, MIMO-

OFDM-CDM, MIMO-OFDM-CDMA, etc. This thesis offers a new way to combine Walsh codes, MIMO and OFDM. The idea is inspired by the CDMA standard IS-95, which uses Walsh sequences in the reverse link in a way similar to block coding. This block code should greatly improve the performance while having low computational complexity.

Most MIMO-OFDM systems proposed so far achieve either good performance results or high data rates by compromising one for the other. Systems that try to achieve both targets usually have high computational complexity. The objective of this thesis is to propose a high-performance and low-complexity system combining MIMO, OFDM and a Walsh block coding scheme. In order to maintain a practical system that could be easily implemented, the design of the proposed system will follow the IEEE standard 802.11a. The performance of the system will be thoroughly investigated by considering different system parameters and channel conditions and in order to emulate real-life scenarios, the system will also be investigated using different channel estimation techniques. The new system will also be compared to some of the existing systems in terms of performance and computational complexity.

1.4 Organization of the Thesis

This thesis is composed of six chapters; the first one is the preceding introductory chapter providing motivation for the investigation undertaken in the thesis.

Chapter 2 deals with the fundamentals of some of the wireless communication systems. Theoretical aspects of MIMO and Walsh codes are explained and an overview of the physical layer of the IEEE standard 802.11a is given. The chapter then outlines some of

the previous research on the combinations of three technologies: MIMO, OFDM and CDM.

Chapter 3 introduces the first configuration of the proposed system which combines, MIMO-VBLAST and OFDM with a new method of implementing Walsh sequences as a block coding scheme. First, fundamentals of the proposed system are presented including a brief review of the VBLAST algorithm. Then, an extensive study of the performance of the system is undertaken. The performance and computational complexity of the system is compared to that of some of the existing systems.

In Chapter 4, the second configuration of the proposed system is discussed. It combines MIMO-STBC, OFDM and the proposed Walsh block coding scheme. As in Chapter 3, we begin with an overview of the fundamentals of the proposed system including STBC techniques. Then, the performance study of the proposed system is carried out through computer simulations with comparisons to some of the existing systems.

In Chapter 5, the performance of the new system is examined using different channel estimation techniques. In the aforementioned chapters a full knowledge of the channel was assumed. The objective of this chapter is to demonstrate the performance of the proposed system in more practical situations, where channel estimation techniques are required.

Chapter 6 concludes the thesis by summarizing and highlighting some of the findings of the thesis and by providing some suggestions for future investigations.

Chapter 2

Fundamentals of MIMO, OFDM and CDM Systems

In Chapter 1, we have described the recent developments in wireless communication systems and the trends followed by researchers around the world. Recent research progress has shown that scientists and engineers are focusing more and more on three candidates for future systems: OFDM, MIMO and CDMA. In particular with the combination of any two of these systems, significant improvements in performance and throughput can be obtained. This thesis demonstrates a new way of combining all three techniques to produce a system that is superior in terms of performance as well as computational complexity.

In this chapter we will briefly review the fundamentals of the main constituent parts of the system to be considered in the upcoming chapters. The chapter starts with a reflection on OFDM, focusing on the physical layer of the IEEE standard 802.11a. Then, a review of Walsh functions and their properties is given with the provision of several methods of

decoding these functions. Next, we will offer an introduction to MIMO systems and the characteristics that define them. Finally, the chapter illustrates some ideas from previous work on how to combine the three systems.

2.1 Systems Employing OFDM Techniques

Extensive work has been done on this topic. The interested reader should go to references [19] - [29] to have a greater insight. In order to maintain a practical system, the OFDM part of the system under study will be consistent with the IEEE standard 802.11a [8]. A brief description of the physical layer of this standard will be presented in the next section.

2.1.1 IEEE Standard 802.11a

The standard gives specifications for the WLAN Medium Access Control (MAC) layer and the physical layer (PHY) for the 5 GHz band. The MAC layer is out of the scope of this thesis and the PHY layer has three functions [8]: Interface the PHY layer to the MAC layer using the Physical Layer Convergence Procedure (PLCP), send and receive data between two stations using the Physical Medium Dependant (PMD) layer and the management of the different functions of the physical layer in communication with the MAC layer using the PHY Layer Management Entity (PLME).

2.1.1.1 OFDM PHY Specifications for the 5 GHz WLAN

The IEEE standard 802.11a specifies the use of OFDM to deliver data rates up to 54Mbit/s. As explained in Chapter 1, an OFDM system could be implemented using an IFFT operation. The standard IFFT size is 64 and the number of data subcarriers is 48 plus 4 pilot subcarriers giving a total of 52. The subcarriers are modulated using BPSK, QPSK, 16-QAM or 64-QAM. The standard specifies data rates of 6, 9, 12, 18, 24, 36, 48 and 54 Mbit/s with the mandatory support of 6, 12, 24 Mbit/s. The specified bandwidth is 20 MHz but according to amendments made in 2004, a half-clocked operation that utilizes a 10 MHz bandwidth is specified giving rates of 3, 4.5, 6, 9, 12, 18, 24, 27 Mbit/s. A summary of the major parameters of the standard is given in Table 2.1

Data Rates	6, 9, 12, 18, 24, 36, 48 and 54 Mbits/s for the 20 MHz Bandwidth 3, 4.5, 6, 9, 12, 18, 24 and 27 Mbits/s for the 10 MHz Bandwidth
Modulation	BPSK, QPSK, 16-QAM and 64-QAM
FEC	K=7 convolutional code
Coding Rates	½, 2/3 and ¾
Number of Subcarriers	52
OFDM Symbol Duration	4.0 μs
Occupied Bandwidth	16.6 MHz

Table 2.1 Summary of the major parameters of the IEEE 802.11a standard

The block diagram, as specified by the standard [8] is shown below:

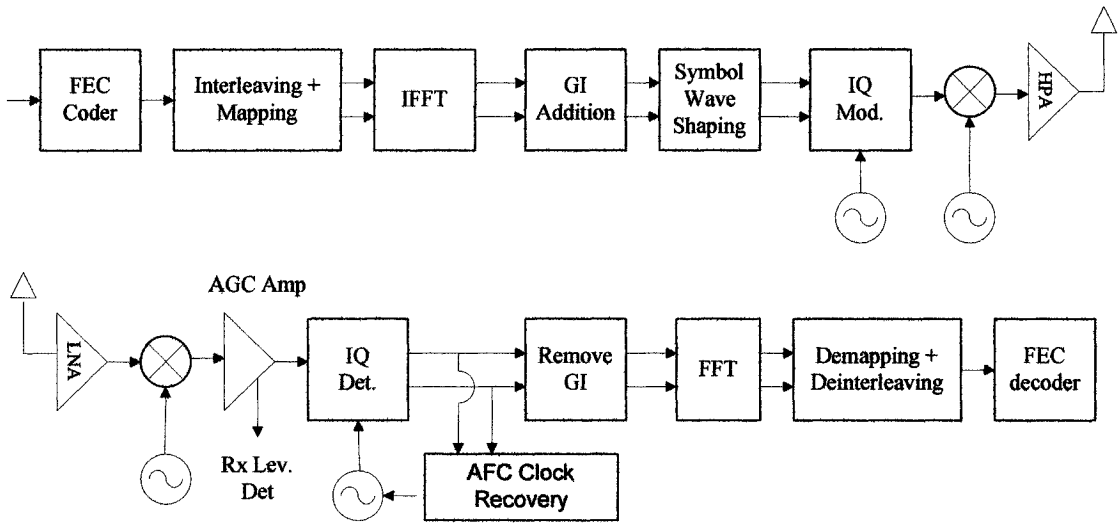

Fig 2.1 Block diagram of the transmitter and receiver of the IEEE standard 802.11a [8]

- Before the binary data is fed to the forward error correction (FEC) encoder, it is passed to a pseudorandom scrambler of length 127. This is done to prevent long strings of 1's or 0's which could be destructive to the timing recovery process at the receiver.
- The scrambled sequence is then passed to a FEC encoder. The convolutional encoder is (2, 1, 7) and uses the generator polynomials $g_0=133_8$ and $g_1=171_8$. Higher coding rates are achieved by puncturing the encoder output. For example to achieve a coding rate of 2/3, one bit out of every four coded bits is deleted from the output. This is compensated at the receiver by inserting dummy zeros in place of the omitted bits.
- The coded sequence is passed to an 8×6 block interleaver (interleaver depth is 48). The depth is determined by the number of subcarriers which is 48 by standard.
- The interleaved data is divided into groups prior to the mapping procedure. These newly formed symbols are called the number of bits per subcarrier, N_{BPSC}. They are of length 1, 2, 4 or 6 according to which modulation method is used: BPSK, QPSK,

16 QAM or 64 QAM. The mapping is done according to Gray-coded constellations and the output consists of complex symbols $d = (I + jQ) \times K_{MOD}$, where K_{MOD} is a normalization factor of values $(1, 1/\sqrt{2}, 1/\sqrt{10}, 1/\sqrt{42})$ according to each modulation method, respectively.

- The symbols are then passed to 64-IFFT block where not all the subcarriers are used. This is due to the fact that the bandwidth is restricted to 20 MHz and there should be no leakage outside this bandwidth. Although windowing is used, the edge subcarriers should still not be used to effectively reduce any leakage outside the desired bandwidth. Also, the center subcarrier should not be used because it is DC and could be distorted by the DC offsets of the ADC and DAC. The complex symbols are divided into groups of 48 symbols and mapped to the remaining subcarriers. Four pilot subcarriers are also added to complete the 52 subcarrier set. The pilot subcarriers are used to recover the phase distortion to the carrier signal during transmission.
- For each OFDM block, a cyclic extension of the symbol itself is pre-pended to the block. This is called the cyclic prefix (CP). Its length should be larger than the maximum delay of the channel and is equal to 16 samples by standard. This ensures that any distortion that occurs echoes within the guard interval, thus totally eliminating inter-symbol and inter-carrier interference (ISI and ICI).
- The signal is then up-converted for transmission according to the center frequency of the desired bandwidth.

The opposite operation is done at the receiver. However, other issues need to be taken care of before the data can be correctly demodulated. These issues are timing synchronization, carrier phase recovery and channel estimation. As mentioned before,

phase recovery can be taken care of by inserting pilot subcarriers in each OFDM block, which provide efficient tracking of the carrier phase. To achieve timing synchronization and channel estimation a preamble is inserted at the beginning of each packet before transmission. The structure of the preamble is shown below.

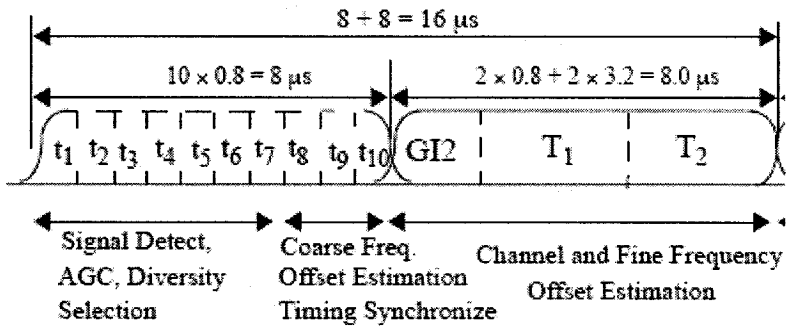

Fig. 2.2 Preamble structure as provided by the standard [8]

The parts labeled t_1 to t_{10} are called short training symbols and are used for coarse frequency estimation and timing synchronization. They are followed by T_1 and T_2 which are the two long training sequences used mainly for channel estimation. They are pre-pended by a long guard interval similar to the CP explained before. The exact method for channel estimation or synchronization is not specified by the standard and is left to the system design engineer. Some of the methods used are listed in references [26] – [29]. Channel estimation will be studied in greater detail in Chapter 5.

The standard specifies the OFDM symbol duration to be 4 μsec. As we mentioned before, there are 64 IFFT samples and the standard specifies the CP to be of length 16 samples. The size of the CP would cover the duration of 0.8 μsec which is longer than the maximum delay of most applications. We have a total of 80 samples which gives a duration of $4\times10^{-6}/80 = 0.05$ μsec or a rate of 20 MHz. This means that, for example, if

64 QAM is used, we have 48×6 bits every 4 μsec, thus giving a bit rate of 72 Mbit/s. If a coding rate of ¾ is used, we can achieve a transmission rate of 54 Mbit/s, which is the maximum rate specified by the standard. The preamble consists of short training symbols of length equivalent to two OFDM symbols or 8 μsec. Then we have two long training symbols, each of length 3.2 μsec. They are pre-pended by a long guard interval 32 samples long or 1.6 μsec. This is because it is vital to have the long training symbols completely free of ISI from short training symbols. The extended preamble has a total length of 16 μsec. A summary of the timing parameters is listed in the following table [8].

Parameter	Value
N_{SD}: Number of Data Subcarriers	48
N_{SP}: Number of Pilot Subcarriers	4
N_{ST}: Total Number of Subcarriers	52 ($N_{SD} + N_{SP}$)
Δ_F: Subcarrier Frequency Spacing	0.3125 MHz (=20MHZ/64)
T_{FFT}: IFFT/FFT Period	3.2 μs ($1/\Delta_F$)
$T_{preamble}$: Preamble Duration	16 μs ($T_{SHORT}+T_{LONG}$)
T_{SIGNAL}: Duration of the SIGNAL OFDM Symbol	4.0 μs ($T_{GI}+T_{FFT}$)
T_{GI}: GI Duration	0.8 μs ($T_{FFT}/4$)
T_{GI2}: Training Symbol GI Duration	1.6 μs ($T_{FFT}/2$)
T_{SYM}: Symbol Interval	4 μs ($T_{GI}+T_{FFT}$)
T_{SHORT}: Short Training Sequence Duration	8 μs ($10\times T_{FFT}/4$)
T_{LONG}: Long Training Sequence Duration	8 μs ($T_{GI2}+2\times T_{FFT}$)

Table 2.2 Summary of the standard's timing related parameters [8]

The following table shows different combinations of coding and modulation schemes to achieve different data rates specified by the standard [8].

Data Rate (Mbits/s)	Modulation	Coding Rate (R)	Coded Bits per Subcarrier (N_{BPSC})	Coded Bits per OFDM Symbol (N_{CBPS})	Data Bits per OFDM Symbol (N_{DBPS})
6	BPSK	1/2	1	48	24
9	BPSK	3/4	1	48	36
12	QPSK	1/2	2	96	48
18	QPSK	3/4	2	96	72
24	16-QAM	1/2	4	192	96
36	16-QAM	3/4	4	192	144
48	64-QAM	2/3	6	288	192
54	64-QAM	3/4	6	288	216

Table 2.3 Different combinations of coding and modulation to achieve different data rates [8]

2.2 Walsh Functions: Properties and Decoding Methods

Walsh functions are applied in many systems and are the core of any CDMA system [9]. Walsh defined these functions as a set of orthogonal, normalized and complete functions. In CDMA systems they are used in both forward and reverse links. In the forward link each user is assigned a function out of a set of a 64 Walsh functions. Since the functions are orthogonal they can be easily separated at the receiver. In the reverse link the functions are used as a 64-ary orthogonal modulation code. The set of N time functions $\{W_j(t);\ t \in (0, T),\ j = 0, 1, \ldots, N-1\}$ defined as Walsh functions possess the following properties:

1. $W_j(t)$ always has a value of either $\{+1,-1\}$ except at discontinuities.
2. All functions start with a value +1. Thus, $W_j(0) = 1$ for all j.
3. In a specific $W_j(t)$, there are j zero crossings in the interval (0,T);
4. $\int_0^T W_j(t)\, W_k(t)\, dt = \begin{cases} 0 \text{ if } j \neq k \\ T \text{ if } j = k \end{cases}$

5. Each function is either even or odd with respect to its midpoint.

If we use the conversions +1 → "0" and -1 → "1", we will be able to use the familiar concept of equivalence between logical operations such as the modulo-2 addition and waveform multiplication. After conversion the functions are called Walsh sequences. Walsh functions or sequences could be generated using several methods such as using Rademacher functions [9] or using the inherent symmetry properties of Walsh functions themselves. However, the most famous way of generating Walsh functions is by using Hadamard matrices.

A Hadamard matrix is a square matrix whose elements are taken from the set {+1,-1} (or equivalently {0, 1}). A distinction of any Hadamard matrix is that the first row and the first column will always contain only +1's (or the logic element 0). The rows and columns of the matrix are mutually orthogonal. The Hadamard matrix of order two is given by

$$\mathbf{H}_2 = \begin{pmatrix} 1 & 1 \\ 1 & -1 \end{pmatrix} = \begin{pmatrix} 0 & 0 \\ 0 & 1 \end{pmatrix}$$

Higher order matrices are found by repeating the above matrix as follows:

$$\mathbf{H}_{2N} = \begin{pmatrix} \mathbf{H}_N & \mathbf{H}_N \\ \mathbf{H}_N & \overline{\mathbf{H}_N} \end{pmatrix}$$

where $\overline{\mathbf{H}_N}$ is the complement of H_N. For example:

$$\mathbf{H}_4 = \mathbf{H}_2 \times \mathbf{H}_2 = \begin{pmatrix} 1 & 1 & 1 & 1 \\ 1 & -1 & 1 & -1 \\ 1 & 1 & -1 & -1 \\ 1 & -1 & -1 & 1 \end{pmatrix} \quad \mathbf{H}_8 = \mathbf{H}_2 \times \mathbf{H}_4 = \begin{pmatrix} 1 & 1 & 1 & 1 & 1 & 1 & 1 & 1 \\ 1 & -1 & 1 & -1 & 1 & -1 & 1 & -1 \\ 1 & 1 & -1 & -1 & 1 & 1 & -1 & -1 \\ 1 & -1 & -1 & 1 & 1 & -1 & -1 & 1 \\ 1 & 1 & 1 & 1 & -1 & -1 & -1 & -1 \\ 1 & -1 & 1 & -1 & -1 & 1 & -1 & 1 \\ 1 & 1 & -1 & -1 & -1 & -1 & 1 & 1 \\ 1 & -1 & -1 & 1 & -1 & 1 & 1 & -1 \end{pmatrix}$$

We can see from all the previous matrices that, unlike Walsh functions, Hadamard functions are not indexed according to the number of sign changes. A method to convert between the two indexes will be mentioned in Chapter 3. A complete list of the Hadamard functions of order 64 and their Walsh equivalent indexes are given in [9].

Walsh functions could also be generated using basis vectors. Walsh sequences of order $N=2^K$ form a K-dimensional vector space over GF(2). For example, in the reverse link of IS-95 system, the Walsh functions used could be considered a (64, 6) block code with a generator matrix given by

$$
\begin{pmatrix}
0000000000000000000000000000000011111111111111111111111111111111 \\
0000000000000000111111111111111100000000000000001111111111111111 \\
0000000011111111000000001111111100000000111111110000000011111111 \\
0000111100001111000011110000111100001111000011110000111100001111 \\
0011001100110011001100110011001100110011001100110011001100110011 \\
0101010101010101010101010101010101010101010101010101010101010101
\end{pmatrix}
$$

2.2.1 The Symmetry Properties of Walsh Functions

One of the most interesting things about Walsh functions is that they possess inherent symmetry properties that could be exploited in the generation and decoding process. In the proposed system these properties will be used to produce a low complexity block coding scheme. To illustrate these properties, consider the set of 8^{th} order Walsh codes shown in Table 2.4.

Index J	Sequence	Walsh Sequence
0	000	$W_0 = 00000000$
1	001	$W_1 = 00001111$
2	010	$W_2 = 00111100$
3	011	$W_3 = 00110011$
4	100	$W_4 = 01100110$
5	101	$W_5 = 01101001$
6	110	$W_6 = 01011010$
7	111	$W_7 = 01010101$

Table 2.4 Complete Walsh sequences of order 8

If we take any of the above sequences we will find:

- The sequence has either even or odd symmetry about the midpoint of the interval (0, T).
- The sequence has the same symmetry about the midpoints of the sub-intervals (0, T/2) and (T/2, T). This process continues K times until the midpoints of all the subintervals are finished (T/N, 3T/N, …, (N-1)T/N where $N = 2^K$).

For example if we take $W_5 = 01101001$, we find the sequence has odd symmetries about the axis at $T/2^K = T/2^3 = T/8$

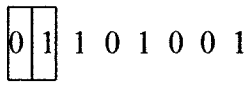

even symmetries about T/4

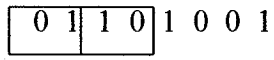

an odd symmetry about T/2

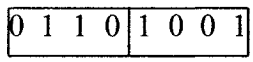

The symmetry properties are also reflected in the respective index sequence $J = (j_1, j_2, \ldots, j_K)$. That is, if $j_k = 1$ the sequence has odd symmetry about the axis $T/2^{K-k+1}$, otherwise, if $j_k = 0$ the sequence has even symmetry about that axis. For W_5, the index sequence is (101). As we can see, $j_1 = 1$ implying an odd symmetry about T/8, $j_2 = 0$ indicating an even symmetry about T/4, and $j_3 = 1$ an odd symmetry about T/2. This is how we can use the symmetry properties to generate Walsh functions instantly.

2.2.2 Decoding Walsh Functions

As we mentioned before, Walsh functions are used as block codes in the reverse CDMA link. Therefore, it becomes the function of the receiver to decide which function out of

the Walsh set has been transmitted. There are many ways to achieve this. The most straight forward way is to compare the received sequence with all the sequences in the set and decide on whichever sequence is the closest out of all comparisons. This is called correlation decoding which is the method usually used for most block coding schemes. It is defined as

$$\{W_j(t), W_k(t)\} = \int_0^T W_j(t)\, W_k(t)\, dt$$

or, for binary sequences

$$\{X, Y\} = \sum_{i=1}^{N} x_i\, y_i$$

For example, consider the Walsh set of order 8. Assuming we receive the sequence Y=01000010, comparing Y with each of the eight sequences, we find that $\{Y, W_0\} = 4$ which is the maximum out of the eight correlations. Therefore, the receiver decides that W_0 was sent.

An equivalent to correlation is to use Hamming distances and choose the sequence with minimum Hamming distance. In the previous example, the Hamming distance between Y and W_0 is 2, which is the minimum out of the eight sequences. Therefore, again the receiver chooses W_0.

We can notice in the above example that two errors occurred and were corrected. Since this type of encoding/decoding operation can be seen as a block code, it has an error correction capability of

$$t = \left\lfloor \frac{d_{min} - 1}{2} \right\rfloor$$

where d_{min} is the minimum distance of the code defined as min D (W_j, W_k), $j \neq k$ and the operation $\lfloor x \rfloor$ represents nearest integer less than or equal to x. In the (64, 6) code used in CDMA systems, $d_{min} = 32$ and therefore, the error correction capability $t = 15$.

2.2.2.1 Fast Walsh Transform Decoding

The disadvantage of correlation decoding is that as the code gets bigger, the decoding process becomes very complicated and could produce large delays. A more efficient method is the fast Walsh transform (FWT) [9] which exploits the inherent symmetry properties of Walsh codes to achieve efficient decoding. The method is based on reversing the Walsh generation process using the symmetry properties. It was mentioned before that in a sequence $J = (j_1, j_2, \ldots, j_K)$, the Walsh sequence will have either odd or even symmetry about the axis $T/2^{K-k+1}$ if j_k is equal to 1 or 0, respectively. In real life communications, errors occur, thus changing the values of the received bits. To perform decoding we use the majority decision rule. First, we assign a value of +1 for identical pairs and a value of -1 to opposite pairs. To illustrate this process, let's take the received sequence Y = 0101 1010 as an example. If we examine the symmetry about the central axis we find that all pairs are identical and thus we conclude that the symmetry measure is +1×4 (even symmetry). In the received sequence Y=0101 1011 the symmetry measure is 1+1+1-1=2. Therefore, by the majority decision rule we have even symmetry and an error has been made. For the code set of order eight we know that each code except W_0 has a weight of 4. We then observe that we have five 1's in the received sequence and therefore, we decide that the last bit is in error and can be corrected.

To illustrate the full decoding process, we again use an example. Take the above received sequence Y = 0101 1011. We start by examining the symmetry about the axis in the first set

$$0 \mid 1 \quad 0 \mid 1 \quad 1 \mid 0 \quad 1 \mid 1$$

The symmetry measure is found as -1 + (-1) + (-1) +1 = -2 and the majority symmetry is odd. This implies that $j_1 = 1$ and $J = (1, j_2, j_3)$. Then we examine the symmetry about the next set

$$0 \quad 1 \mid 0 \quad 1 \quad 1 \quad 0 \mid 1 \quad 1$$

The symmetry measure is -1 + (-1) + (-1) +1 = -2 and the majority symmetry is odd. Therefore $j_2 = 1$ and $J = (1, 1, j_3)$. Finally, we examine the symmetry about the last axis

$$0 \quad 1 \quad 0 \quad 1 \mid 1 \quad 0 \quad 1 \quad 1$$

The symmetry measure is 1 + 1 + 1 + (-1) = 2 and the majority symmetry is even. Therefore, $j_3 = 0$ and $J = (1, 1, 0)$ which is the correct sequence for $W_6 = 0101\ 1010$ and a single error has been corrected. The above algorithm can be summarized as follows:

For a set of Walsh sequences of order $N = 2^K$

1. Correlate every group of bits of length 2^{k-1} with the reverse of the following group of length 2^{k-1}, where $k = 1,2,\ldots, K$.
2. Take the sum of the correlation measures.
3. Decide whether the majority symmetry is odd or even according to whether the sum is negative or positive, respectively.
4. For odd symmetry, decide j_k as 1. For even symmetry, decide j_k as 0

This can be put in closed form as

$$\sum_{i=0}^{N/2^j-1} \{(r_{2^j.i+1}, r_{2^j.i+2}, \ldots\ldots, r_{2^j.i+2^{j-1}+1}) , (r_{2^j.i+2^j}, r_{2^j.i+2^{j-1}}, \ldots\ldots, r_{2^j.i+2^{j-1}+1})\}$$

$$= \begin{cases} > 0 \rightarrow x_j = 0 \\ = 0 \rightarrow \text{pick } x_j = 0 \text{ or} 1 \\ < 0 \rightarrow x_j = 1 \end{cases}$$

2.3 MIMO Systems

The idea to equip a communication system with multiple antennas at both the transmitter and the receiver is becoming widely popular. A system with multiple antennas can be designed to increase capacity, improve performance and increase throughput. MIMO systems prove to be very effective in combating multipath fading and increasing the signal to noise ratio (SNR) at the receiver. They use the effects of fading (instead of trying to mitigate them) to their benefit to increase spectral efficiency and capacity. A MIMO system can be seen as a combination of multiple single input single output (SISO) systems. Therefore, the capacity in turn is a combination of several SISO systems. It has been proved also [11] that capacity grows linearly with the number of antennas.

This section provides an introductory note to MIMO systems. Preliminary terms will be introduced and brief descriptions of different MIMO system designs will be presented. These designs will be detailed in Chapters 3 and 4.

2.3.1 Diversity Gain

Diversity schemes are techniques used to combat multipath fading. According to [10], diversity is simply providing replicas of the transmitted signal to the receiver. By doing this we increase the probability that at least one of the received signals is not in deep fade. To this end, the designer has to ensure that the individual signal paths between each transmit/receive antenna pair fades independently. Therefore, if a single path is in deep fade, there is a higher probability that the next one will not be so. The higher the number of signal replicas, the more the number of independent fading paths and the easier it is to combat fading. The number of individual paths is called the diversity order. There are

several ways to provide the transmit signal replicas. Mainly the multiple signals are transmitted over time, frequency or space.

2.3.1.1 Temporal Diversity

In this type of diversity several replicas of the signal are provided over time [10]. The simplest and most straight forward way of achieving this is to repeatedly transmit the same signal until it is correctly received. A more practical way of providing temporal diversity is by using a combination of channel coding and interleaving. This can only be achieved if the duration of the interleaved symbol is large compared to the channel coherence time so that the channel provides enough time variations.

2.3.1.2 Frequency Diversity

In the case where the coherence bandwidth of the channel is small in comparison to the bandwidth of the signal, several replicas of the signal could be provided across the frequency spectrum ensuring that each frequency fades independently [10].

2.3.1.3 Spatial Diversity

Using multiple antennas at the transmitter at the receiver, independent replicas of the signal could be provided only if the antenna spacing is larger than the coherence distance of the channel. **Receive diversity** is when several versions of the same signal are coherently combined at the receiver to improve the performance. **Transmit diversity** is achieved using controlled redundancies at the transmitter that could be exploited, using

signal processing techniques, at the receiver side to improve signal quality [10]. Spatial diversity is a very popular form of diversity and we will later use it in our system.

2.3.2 Array Gain

When the transmitter or the receiver possesses perfect knowledge of the channel, they can weight the signal with coefficients such that there will be coherent combination at that side. This results in an increase of the SNR at the receiver, called array gain. When the transmitter has channel knowledge, the transmitted signal is weighed and the signal is coherently combined at the receiver. The array gain in this case is called transmitter array gain. On the other hand, if the receiver has the channel knowledge, the incoming signals can be coherently combined and the array gain is called receiver array gain [10].

2.3.3 The Diversity-Multiplexing Tradeoff in MIMO Systems

As it was mentioned before, MIMO systems can be used to increase capacity and throughput and to improve performance. Unfortunately, diversity and multiplexing gain lie at opposite sides of the scale. Multiplexing gain is defined [10] as the increase in capacity obtained from using multiple transmit and receive antennas at no additional power or bandwidth consumption. Diversity is obtained by transmitting replicas of the same signal, as explained before. In this case there is full correlation between the signals and the diversity order is equal to the number of paths. However, if we divide the data stream between the individual paths, instead of repeating the stream across the antennas, there will be no correlation between the transmitted streams and thus the throughput will increase achieving a multiplexing gain equal to the number of the independent streams. In

this case, however, there is no diversity, which is in contrast to the first case where we had a full diversity order but no multiplexing gain. There are several ways we can combine space and time coding to achieve diversity (such as space-time block coding) or multiplexing gains (such as layered space-time coding). These techniques will be discussed in detail in Chapters 3 and 4.

2.4 An Outlook on Systems Combining MIMO, OFDM and CDM

In this section, we will take a look at some of the work done by researchers for systems employing MIMO, OFDM and Walsh code spreading. We will categorize the systems according to which MIMO configuration they are using: Layered space time (LST) or space time block coding (STBC). Both configurations will be explained in greater detail in Chapters 3 and 4, respectively.

2.4.1 Systems Using LST Codes, OFDM and Walsh Code Spreading

The first system that we will investigate is the MIMO-OFDM-CDM system proposed in [15]. Different detection techniques were discussed and their performance was investigated through computer simulations. The block diagram of the system is shown in the following diagram.

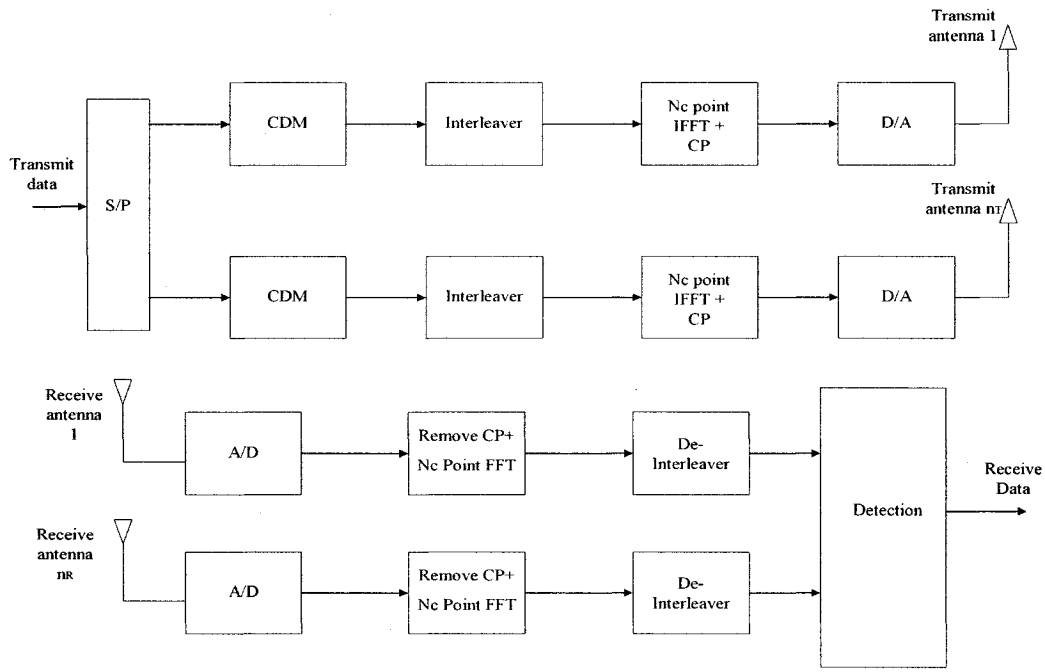

Fig 2.3 Transceiver structure of the MIMO-OFDM-CDM system [15]

In [15] a 2×2 system (two transmit and two receive antennas) with QPSK modulation is used. The bandwidth used is 20 MHz and the OFDM block has 64 subcarriers. The spreading lengths P are set to 2 and 4 and the interleaving depth is equal to the number of subcarriers N_c divided by the spreading length (N_c/P). The data at the receiver is given by

$$\mathbf{r} = \mathbf{H}\,\mathbf{d} + \mathbf{v}$$

Where **d** is the block of transmitted symbols and **H** is called the extended channel matrix given by

$$\begin{pmatrix} \mathbf{H}_{11}\mathbf{C} & \cdots\cdots & \mathbf{H}_{1M_T}\mathbf{C} \\ \vdots & \ddots & \vdots \\ \mathbf{H}_{M_R 1}\mathbf{C} & \cdots\cdots & \mathbf{H}_{M_R M_T}\mathbf{C} \end{pmatrix}$$

Where M_T and M_R are the number of transmit antennas and that of receive antennas, respectively, **C** is the spreading code and **v** the complex AWGN. The detection methods used in [15] are described as:

- **Linear receivers**: the received sequence is equalized by a matrix **A** as

$$\mathbf{y = Ar = AHd + Av}$$

The Equalization matrix **A** can be computed by many methods such as the ZF criterion given by $\mathbf{A} = \mathbf{H}^{\dagger}$ (where the superscript denotes the pseudo-inverse of **H**), or the MMSE criterion given by $\mathbf{A} = \sigma_d^2 \mathbf{H}^{H} (\mathbf{H}\mathbf{H}^{H} + \sigma_n^2 \mathbf{I}_{M_R})^{-1}$ where σ_n^2 is the noise variance and σ_d^2 is the data variance. The decision on the received sequence is given by $\hat{\mathbf{d}} = Q(\mathbf{y})$.

- **Lattice-Reduction-Aided (LRA) Receivers:** This receiver is based on finding a change of basis for the decision region of the columns of **H**. An algorithm to compute the function **F,** which transforms **H** into **H'**, has been proposed in [16] and is applicable for 2×2 systems. The purpose of the transform is to optimize the decision regions in order to minimize errors. This operation consists of:

1. Scaling, shifting and equalizing in the new basis such that

$$\mathbf{y} = (\mathbf{HF})^{\dagger} \times ½ \times [\mathbf{Hd + v + Hl}]$$

where ½ is a scaling factor (depending on the number of columns of **H**) and **l** is a shifting matrix given by $\mathbf{l} = [1+i, \ldots, 1+i]^T$ and $i = 1, \ldots M_T P$.

2. Slicing and returning to the original basis after undoing the scaling and the shifting by

$$\hat{\mathbf{d}} = 2\mathbf{F}Q(\mathbf{y}) - \mathbf{l}$$

Other detection techniques such as VBLAST, Partial Decision Feedback (PDF) and a proposed a hybrid LRA-PDF detection technique were also investigated in [15]. The simulation results will be shown in Chapter 3.

The second system to be reviewed is the MIMO-OFDM system proposed in [38], where the increased throughput and improved performance acquired from combining MIMO with an OFDM system based on the IEEE standard 802.11a was investigated. The block diagram of the system is shown in Fig. 2.4.

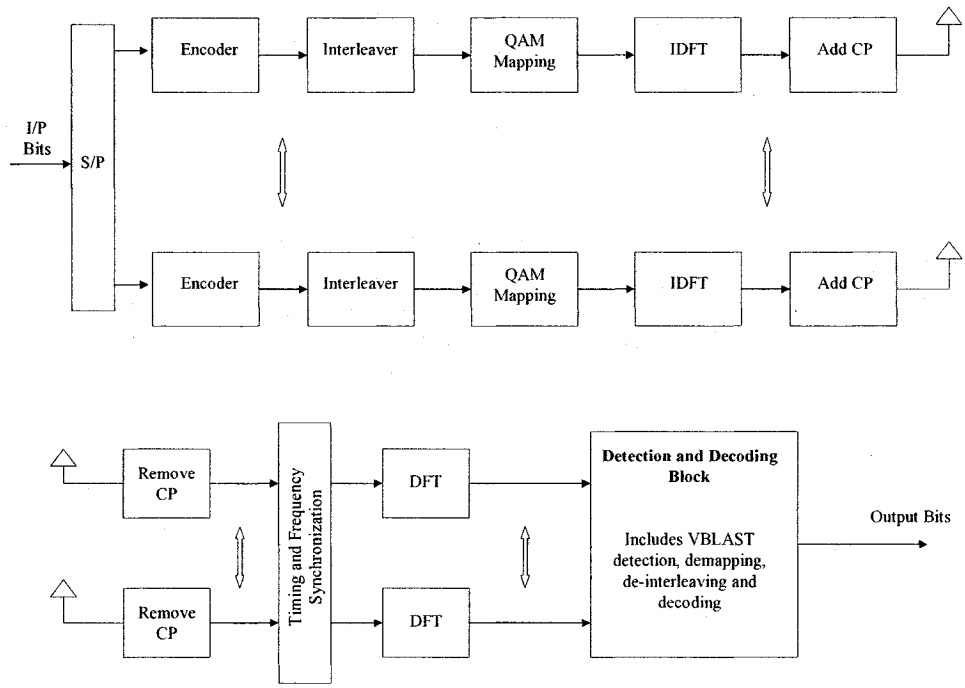

Fig. 2.4 Block diagram of the MIMO-OFDM system [38]

This system follows the parameters specified in the standard. For example, the bandwidth used is 20 MHz, the number of OFDM subcarriers is 64 and the guard interval is 800ns. Other detailed parameters can be found in [38]. Frame detection, time and frequency synchronization as well as channel estimation are achieved by using a preamble.

Synchronization tracking is achieved using pilot subcarriers. The paper showed how synchronization techniques can be extended for MIMO systems. Also, Two detection methods based on per-antenna-coding (PAC) are discussed (PAC is sometimes known as horizontal coding), namely, PAC soft-output maximum likelihood detection (SOMLD) and PAC VBLAST. The proposed synchronization and detection techniques are verified using computer simulations and initial measurements of the implemented system. Simulation results show that VBLAST achieves a better performance than SOMLD, especially at low SNRs. Initial measurements show that when we use a 3×3 system the throughput approximately doubles compared to the 1×1 system, while theoretically the throughput value should have tripled. This is due to the coupling between the branches of the transmitter and the receiver and due to the fact that the MIMO channels assumed are not well conditioned (they are not i.i.d channels).

2.4.2 Systems Using STBC, OFDM and Walsh Code Spreading

The first system that we will discuss here is the STBC MC-CDMA system proposed in [14]. Computer simulations were used to compare the performance of the system using different detection techniques. The block diagram is shown in Fig. 2.5.

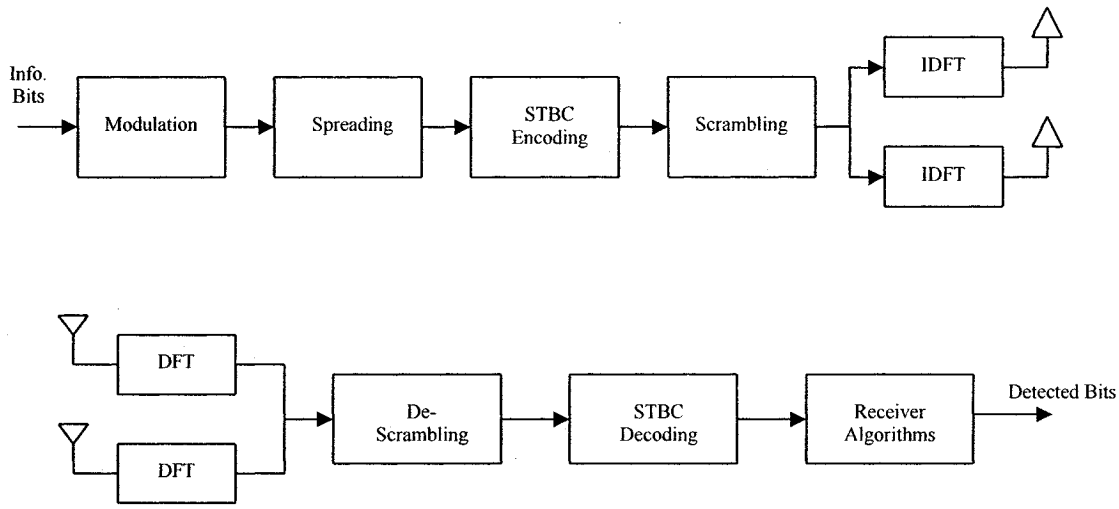

Fig 2.5 Transceiver structure of the STBC MC-CDMA system [14]

The system uses QPSK modulation with 512 OFDM subcarriers. The number of users is 32 and the length of the Walsh sequences is also 32 (fully loaded system). Two antenna configurations are used, namely, 2 ×1 and 2×2. The bandwidth is 5 MHz and the carrier frequency is 2.56 GHz. The received sequence after DFT is given by

$$\mathbf{r} = \mathbf{U}\,\mathbf{b} + \mathbf{v}$$

where **b** is the transmitted user symbols, **v** is complex AWGN and **U** is given by

$$\begin{pmatrix} \mathbf{FH_{11}F^{-1}CS} & \mathbf{FH_{12}F^{-1}CS} \\ \mathbf{-(FH_{12}F^{-1}CS)^*} & \mathbf{(FH_{11}F^{-1}CS)^*} \end{pmatrix}$$

F and $\mathbf{F^{-1}}$ are the DFT and IDFT matrices given by $F^{-1}(p,q) = \frac{1}{\sqrt{P}} e^{j(2\Pi/P)pq}$ $0 \le p,q \le P-1$ and P is the length of the spreading codes. **C** is the scrambling code matrix and **S** is the spreading code matrix. $\mathbf{H_{11}}$ and $\mathbf{H_{12}}$ are the channel matrices from their respective transmit to receive antennas. In the paper three receiver algorithms are discussed:

1. **Maximum Ratio Combining (MRC)**: the output of the MRC receiver is given by

$$\mathbf{y}_{MRC} = \mathbf{U}^{\mathbf{H}}\,\mathbf{r}$$

where the superscript "H" denotes the Hermitian transpose. The detected symbols are then derived from

$$\hat{\mathbf{b}}_{MRC} = \text{dec}(\mathbf{y}_{MRC})$$

where (dec) is the decision based on the modulation symbol.

2. **Minimum Mean Square Error (MMSE):** it works in a similar way to MRC except that

$$\mathbf{y}_{MMSE} = \mathbf{U}^{H} (\mathbf{U}\,\mathbf{U}^{H} + \sigma^2\,\mathbf{I}_P)^{-1}\,\mathbf{r}$$

where σ^2 is the noise variance and I_P is an P × P identity matrix. Therefore,

$$\hat{\mathbf{b}}_{MMSE} = \text{dec}(\mathbf{y}_{MMSE})$$

3. **EM based detection and PIC:** First we define user sets for the received vector as

$$\mathbf{x}_k = \mathbf{U}_k\,\mathbf{b}_k + \mathbf{v}_k \qquad k = 1, \ldots\ldots, K$$

where K is the number of users. The noise is decomposed into K components such that $\sum_{k=1}^{K} \mathbf{v}_k = \mathbf{v}$. Therefore, $\mathbf{Q}_k = \beta_k\,\mathbf{Q}$, where $\mathbf{Q}_k$ and $\mathbf{Q}$ are the covariance matrix of $\mathbf{v}_k$ and that of $\mathbf{v}$, and β_k are real valued coefficients such that $\sum_{k=1}^{K} \beta_k = 1$ with $\beta_k \geq 0$. Now $\mathbf{r}$ is related to $\mathbf{x}_k$ by

$$\mathbf{r} = \sum_{k=1}^{K} \mathbf{x}_k = \sum_{k=1}^{K} (\mathbf{U}_k\,\mathbf{B}_k + \mathbf{v}_k) = \sum_{k=1}^{K} \mathbf{U}_k\,\mathbf{b}_k + \mathbf{v}$$

The expectation step is given by

$$\hat{\mathbf{x}}_k = \mathbf{U}_k\,\hat{\mathbf{b}}_k^{(n)} + \beta_k\,[\,\mathbf{r} - \sum_{i=1}^{K} \mathbf{U}_i\,\hat{\mathbf{b}}_i^{(n)}\,]$$

and the maximization step is given by

$$\hat{\mathbf{b}}_k^{(n+1)} = \underset{\mathbf{b}_k}{\operatorname{argmin}} \left\| \hat{\mathbf{x}}_k - \mathbf{U}_k \mathbf{b}_k \right\|^2$$

which shows that this is an iterative procedure. The initial condition for $\mathbf{b}_k$ could be taken as the output for the MRC receiver and β_k can be found by experimentation. Simulations are carried out in two channel models for vehicular and pedestrian situations and the results will be shown in Chapter 4.

The second system to be investigated is the STBC-OFDM-CDM system suggested in [37]. The performance of this system is studied under time varying channels in which imperfect system parameters were taken into account. The block diagram of the system is shown in Fig. 2.6 [37].

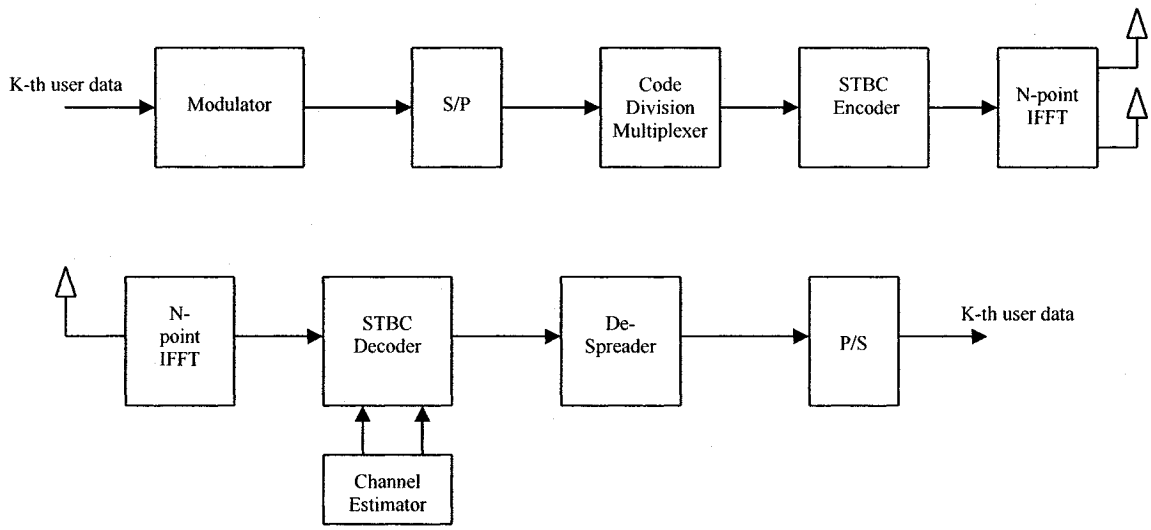

Fig. 2.6 Block diagram of the STBC-OFDM-CDM system [37]

The system uses BPSK modulation and 64 OFDM subcarriers. The code length is 32 with varying number of users. Two antenna configurations are considered: 1×1 and 4×1. First, an expression for the BER is derived taking into account parameters such as residual

carrier frequency offset and imperfect channel parameters in a Rayleigh fading channel. Then the performance of the system was investigated using computer simulations and the results show that the system performs best in slowly fading channels. The results also show that as the number of users increase, the multiple access interference increase (MAI) and can cause performance degradation. The simulation results will be further discussed in Chapter 4.

2.5 Conclusions

In this chapter, some background materials supporting the new systems to be proposed in the following chapters have been presented. The chapter started with a brief description of the IEEE 802.11a OFDM physical layer including the structure of the system and the block diagram as specified by the standard as well the preamble structure. Then some of the theory behind Walsh functions and their properties, as well as some of the decoding methods including fast Walsh transform (FWT) were discussed. These properties will be later used in our systems. MIMO systems and their characteristics as well as different configurations have also been discussed. Some of the work done by researchers in combining MIMO, OFDM and CDM was also presented. Some insight was provided on the several areas explored by scientists such as detection techniques. We have also showed how different blocks are combined to improve performance, reduce complexity or increase throughput. In the following chapters, we will propose systems where new combinations will be introduced to achieve superior performance and reduced complexity compared to the systems that we have studied in this chapter.

Chapter 3

Proposed MIMO-OFDM System with Walsh Block Coding and VBLAST Algorithm

In this chapter we present the first configuration of our proposed system which combines MIMO-VBLAST, OFDM and Walsh block coding. In the system, the idea of using Walsh sequences as a block coding scheme will be exploited. The chapter starts with a detailed block diagram of the system with a detailed description of the functions of each block and an overview of layered space-time (LST) codes and the VBLAST algorithm. Then we offer a detailed simulation study of the proposed system including simulations under several coding gains, different antenna configurations, coding schemes, different channel delays, and different propagation environments, two variations of the VBLAST algorithm (namely ZF-VBLAST and MMSE-VBLAST) and in the presence of an interleaver. Finally, the chapter offers a comparison between the proposed system and similar former systems in terms of complexity and performance.

3.1 Overview of Layered Space-Time Coding

In this section we will take a look at LST codes which will be employed in the system introduced in this chapter. It was mentioned in Chapter 2 that there exists a trade-off between diversity and multiplexing gain. LST codes sacrifice part of the diversity order to achieve higher multiplexing gain and were first proposed in [13] by Foschini. Rather than trying to eliminate the effects of multipath fading, LST codes regard the delay spreads as data routes. The individual paths from the transmit antennas to the receive antennas are independent of each other and thus sending uncorrelated data on these paths ensures orthogonal transmission. In these techniques, the main data stream is split into multiple lower rate streams (the number of streams equal the number of transmit antennas M_T). Each stream is individually modulated and transmitted from its respective antenna. Thus, these techniques achieve a multiplexing gain equal to the number of transmit antennas M_T. There is no diversity at the transmitter as it possesses no knowledge of the channel. However, channel knowledge could be incorporated at the receiver, leading to receiver diversity.

There are many ways in which we can implement LST codes. Of these methods are: horizontal encoding, diagonal encoding and threaded space-time coding [10]. However, vertical encoding is the method that has gained the most attention, particularly, BLAST (Bell Labs Layered Space-Time) architectures such as VBLAST and DBLAST. The VBLAST algorithm is gaining more popularity as it achieves high capacities and good performance compared to other techniques. In this architecture, the data is encoded, interleaved and modulated before it is split into the individual streams. This means that each encoded symbol is spread across all the antennas. If (R) is the coding rate and N_{BPSC}

is the number of bits per subcarrier depending on the modulation used, then the signaling rate becomes $R*N_{BPSC}*M_T$ bits/transmission which means that the increase in the number of transmit antennas provides a linear increase in the transmission rate. The problem with this technique is the complicated joint decoding process due to the scattering of the encoded bits across the antennas. In [30] the VBLAST algorithm was introduced which is a non-linear detection algorithm that employs symbol cancellation to improve performance. This algorithm will be explained in detail later in this chapter.

3.2 System Structure and Block Description

Fig. 3.1 shows the block diagram of the first configuration of our proposed system which we will study in this chapter. The following sections provide detailed description of the structure of the system.

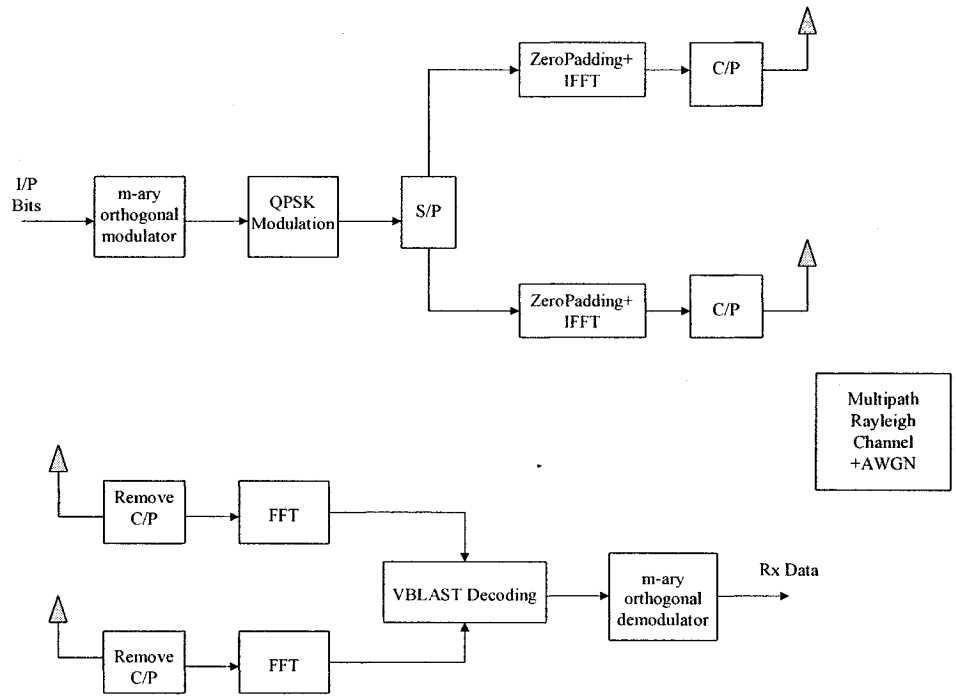

Fig 3.1 Block diagram of the proposed system with VBLAST configuration

3.2.1 Transmitter Structure

- First, we generate a number of random bits. Note that our Walsh encoder and the OFDM blocks work with a specified integer number of input bits. Therefore, the number of bits input to the encoder should be an integer multiple of the OFDM symbols and the number of bits that are accepted in each encoding operation. Since in reality we probably have no control over the number of input bits, we generate a random number of bits and afterwards we pad them to achieve that integer number.
- After padding, the symbols are fed to an m-ary orthogonal modulator. The encoding operation is very similar to a mapping operation. The orthogonal modulator or Walsh encoder takes each six input bits in a row and computes one of 64 sequences from a table of Walsh sequences according to the rule

$$S = c_0 + 2c_1 + 4c_2 + 8c_3 + 16c_4 + 32c_5 \quad (1)$$

where (c_0, c_1, ..., c_5) are the input coded symbols and S is the number index of the Walsh sequence chosen to be output. This method of operation was inspired by the IS-95 CDMA system which uses the same method in the reverse link [9] to provide the receiver with a measure of coherence over a six-symbol period. This method can also be used as a block coding scheme with high correcting capabilities as we mentioned in Chapter 2. The Walsh sequences used by this method are indexed according to the number of sign changes. We would like to use the Hadamard matrices to generate the orthogonal sequences as they are the most popular and simplest generation method. Hadamard sequences, however, are not indexed according to the number of sign changes, as we mentioned in Chapter 2. To convert between the two indexes, we use the following operation [9] instead of (1):

$$P_5 = c_0 \tag{2}$$

$$P_{4-j} = \text{xor}\,(c_j, c_{j+1}) \qquad j = 0, 1, \ldots, 4 \tag{3}$$

where (p_0, p_1, ..., p_5) is the binary equivalent of an index in the Hadamard table corresponding to the same sequence in the Walsh table. Later in our simulations we will use three sets of codes: (64, 6), (32, 5) and (16, 4). In the (32, 5) code we take 5 bits in a row and use them to choose one of 32 Walsh sequences and in the (16, 4) we take 4 bits in a row and use them to choose one of 16 Walsh sequences. Walsh functions were explained in detail in Chapter 2.

- The output sequences are then passed to a QPSK modulator which uses gray code constellation mappings to choose one of the four phases [pi/4, 3*pi/4, -3*pi/4, -pi/4] corresponding to the vector [00, 10, 11, 01].
- The modulated data stream is then separated into a number of lower rate streams equal to the number of transmit antennas.
- Each stream then passes to a 64-IFFT OFDM block where they are zero padded and converted to the time domain as required by the IEEE standard 802.11a which was explained in Chapter 2 (only 48 subcarriers are used as specified by the standard).
- At this point, a cyclic prefix is generated from each OFDM block and prepended to each data stream. The cyclic prefix's size is 16 symbols as specified by the standard.
- Finally, the preamble is generated and prepended to the signal. The preamble will be used by the receiver for channel estimation. The preamble structure will be explained in Chapter 5 which deals with channel estimation. The simulations undertaken in this chapter assume perfect knowledge of the channel and so the preamble is not used

here. However, it is still added so that the whole structure does not deviate from the standard.

A flowchart that summarizes the transmitter's subtasks is shown as follows:

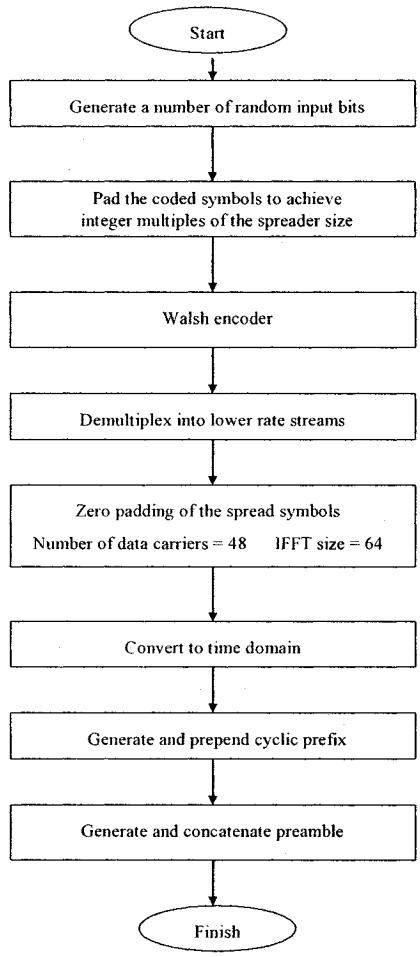

Fig 3.2 Flowchart for subtasks in the transmitter

3.2.2 Channel Structure

The channel considered in this chapter is a multipath Rayleigh channel, whose envelope has a probability distribution function given by [40]

$$p(x) = \frac{1}{\Omega_p} \exp\left\{\frac{-x}{\Omega_p}\right\} \tag{4}$$

where Ω_p is the total envelope power. The channel is assumed to be quasi-static, namely, it stays constant through the transmission of one packet. The maximum delay spread is 100ns which is the average delay spread of most applications (later we simulate the performance of the system under different channel delays and fading environments). The following table shows the maximum channel delays of different propagation environments [36].

Environment	Maximum Delay Spread (ns)
Large Building (e.g. Stock Exchange)	120
Meeting Room (5m×5m)	55
Office Building	130
Indoor Sports Arena	120
Factory	125
Office Building: Single Room Only	30
Airport	120
Warehouse	129
Cafeteria	75
Shopping Center	200

Table 3.1 Typical maximum channel delays for several environments [36]

From the table, we can deduce that the maximum delay increases as the propagation environment becomes larger. Other factors also contribute to the maximum delay of the channel such as the number of reflective or refractive objects in the medium. This is why the largest channel delay can be found in shopping center, where the signal travels the farthest distance and could be reflected more often than in other mediums. The smallest channel delay can be found in the single room office building.

To simulate the effect of the channel on the transmitted signal first the channel impulse response (CIR) is randomly generated for each channel so that the channels are independent of each other. The number of channels is equal to the product of the number of transmit and receive antennas $M_T \times M_R$. Then, for every path from each transmitter to each receiver, the transmitted signal is convoluted with the corresponding CIR. After that, additive white gaussian noise (AWGN) is added.

3.2.3 Receiver Structure

- First, the cyclic prefix is removed and disregarded and the preamble is extracted. The training carriers and the data carriers then pass to a 64-FFT block where they are converted back to the frequency domain. Since we apply zero padding at the transmitter, the 48 data carriers have to be extracted out of the block of 64 received carriers. This whole process is repeated for each receive antenna.
- Now that all the data carriers have been extracted, they are passed to a VBLAST decoder. As we mentioned earlier in this chapter, joint detection has to be performed since each symbol is spread across all transmit antennas. The idea behind VBLAST lies in the application of symbol cancellation. This was proposed in [30] by Foschini, Wolniansky, Golden and Valenzuela for a single carrier system. The decoder first extracts the strongest out of all the received streams and proceeds with the rest. This makes recovery easier as the strongest sources of interference are being removed one after another. The process is called successive interference cancellation (SIC). As an example, consider the single carrier communication system [30] shown in Fig. 3.3:

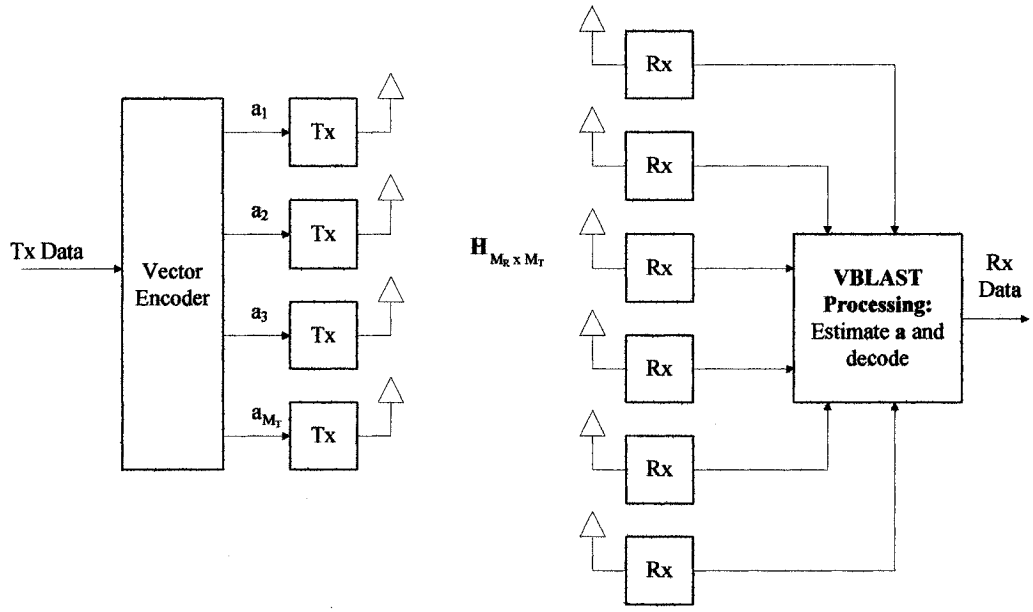

Fig 3.3 Simplified single carrier VBLAST diagram [30]

As shown, the QAM transmitters transmit the symbol vector $\mathbf{a}=(a_1, a_2, \ldots, a_{M_T})^T$, where "T" denotes the transpose operation. Each receive antenna receives a combination of signals from all transmit antennas. The received signal vector containing all the signals received by M_R antennas can be written as

$$\mathbf{r}_1 = \mathbf{Ha} + \boldsymbol{\nu} \tag{5}$$

where $\mathbf{H}$ is the $M_R \times M_T$ ($M_T \leq M_R$) channel matrix whose elements h_{ji} represents the complex transfer functions from transmit antenna i to the receive antenna j and $\boldsymbol{\nu}$ is a noise vector. The order each stream is chosen is very important. At each stage, the stream which gives the best post-detection SNR is chosen. This leads to the maximization of the worst SNR over all orderings. The transmitted symbol with the smallest post-detection SNR will determine the performance of the system.

First, linear nulling is applied by weighing the received vectors using any known method such as zero forcing (ZF) or minimum mean squared error (MMSE) to form a linear combination of the components of $\mathbf{r}_1$ to yield the decision statistic y_{k_1}

$$y_{k_1} = \boldsymbol{w}_{k_1}^{T} \boldsymbol{r}_1 \tag{6}$$

For example, if ZF is used the weight vector $\boldsymbol{w}_i^T$ ($i = 1, 2, \ldots, M_T$) is chosen to satisfy the condition

$$\boldsymbol{w}_{k_i}^{T} (\boldsymbol{H})_{k_j} = \delta_{ij} \tag{7}$$

where $(\mathbf{H})_{k_j}$ is the k_j^{th} column of $\mathbf{H}$ and δ_{ij} is the kroenecker delta function . The unique vector satisfying the above equation is the k_i^{th} row of $(\mathbf{H}_{k_{j-1}}^{-})^{\dagger}$ where $\mathbf{H}_{k_j}^{-}$ is obtained by setting columns $k_1, k_2, \ldots k_j$ of $\mathbf{H}$ to zero and "†" denotes the pseudoinverse operation. After the nulling operation is performed a slicing operation is applied on y_{k_1} according to the modulation method used to retrieve the transmitted symbol $\hat{a}_{k_1}$

$$\hat{a}_{k_1} = Q(y_{k_1}) \tag{8}$$

The detected symbol is then used to form a new vector which will be removed from the original received vector for interference cancellation resulting in the modified vector

$$\boldsymbol{r}_2 = \boldsymbol{r}_1 - \hat{a}_{k_1} (\boldsymbol{H})_{k_1} \tag{9}$$

The new vector will be used to detect the second symbol a_2. This process is repeated for M_T times until the last symbol a_{M_T} is recovered. The process is summarized as follows

Initialization:

$i = 1$

$\mathbf{G}_1 = \mathbf{H}^{\dagger}$

Recursion:

$k_j = argmin \, \| (\mathbf{G}_i)_j \|^2$ where $j \notin \{k_1 \; k_2 \; \ldots\ldots \; k_{i-1}\}$

$$w_{k_i} = (G_i)_{k_i}$$

$$y_{k_i} = w_{k_i}^T r_i$$

$$\hat{a}_{k_i} = Q(y_{k_i})$$

$$r_{i+1} = r_i - \hat{a}_{k_i} (H)_{k_i}$$

$$G_{i+1} = (H_{k_i}^{-})^{\dagger}$$

$$i = i + 1$$

where $(\mathbf{G}_i)_j$ is the j^{th} row of $\mathbf{G}_i$.

The above process detects symbols from a multiple antenna system but with a single carrier. Since we are using a multiple carrier system (OFDM) we need to apply one VBLAST detector for each subcarrier to correctly receive all the symbols [17]. So the aforementioned process is repeated for each of the 48 subcarriers.

- The detected symbols are then passed to an m-ary orthogonal demodulator where a fast Walsh transform (FWT) operation which exploits the symmetry properties of Walsh codes is performed to retrieve the transmitted symbols from the table of Walsh sequences according to which code was used. FWT was explained in Chapter 2.

A flowchart that summarizes the receiver's subtasks is shown below:

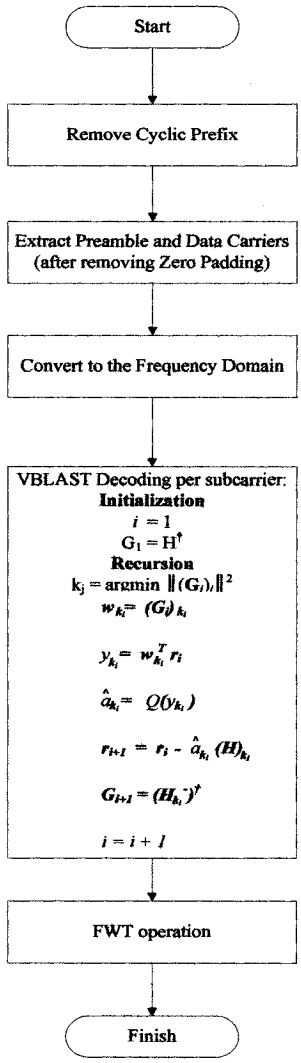

Fig 3.4 Flowchart for subtasks in the receiver

3.3 Performance and Complexity Study of the Proposed System

In this section we will investigate the performance of the system using computer simulations of different channel conditions and system parameters. We will also compare our system to previous systems in terms of performance and computational complexity.

3.3.1 Performance Study

We will examine the performance of the proposed system by simulating its bit error rate (BER). The tool used for the simulation is MATLAB ver7.0. In this chapter perfect channel knowledge is assumed at the receiver. The model simulates a packet transmission system and each packet has one set of preambles (one preamble from each transmit antenna) although the preambles are not used in this chapter. In each simulation we will find the average BER at each SNR by counting the number of received bits in error and dividing by the total number of transmitted bits.

3.3.1.1 Experiment 1: Performance of Block Coded System

In this experiment we study the performance of our system with comparison to a similar system without using the proposed Walsh block coding scheme. For this simulation we use a 2×4 system which means that, according to [10], we have a diversity of order M_R-M_T+1 = 3. The Walsh code used in this system is the (64, 6) code and the results are shown in Fig. 3.5.

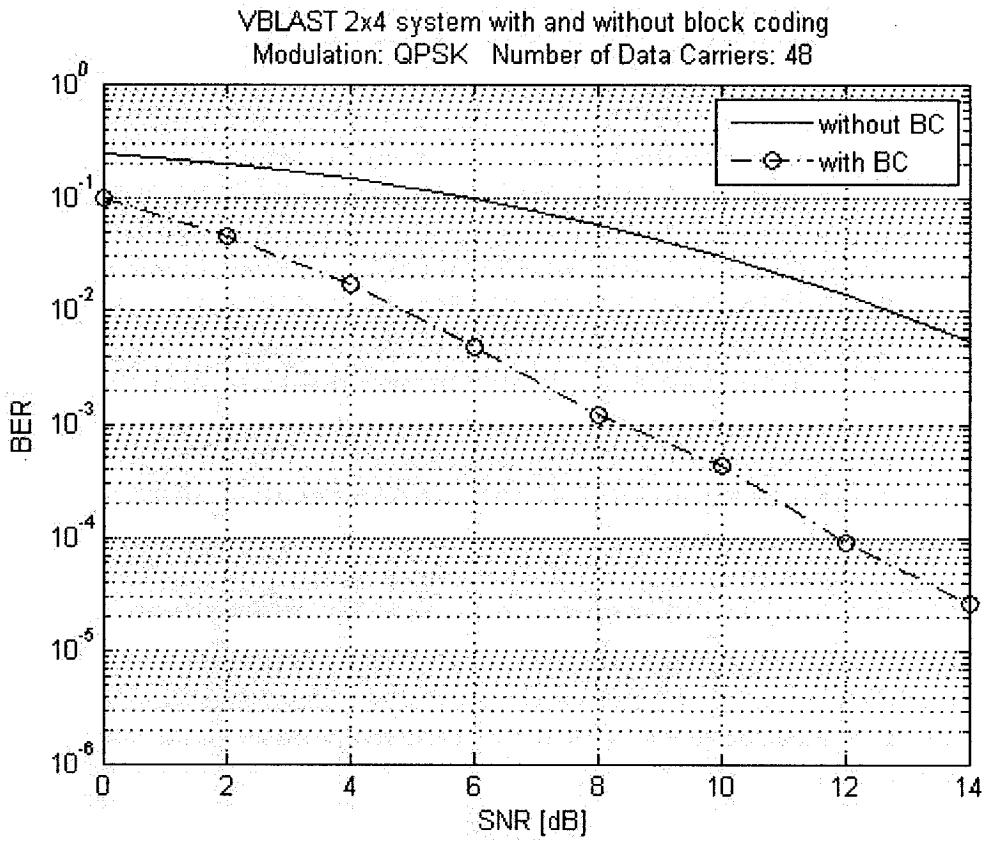

Fig 3.5 BER plots of our VBLAST system with and without Walsh block coding

The simulation results show a significant improvement in the BER performance of the system with the proposed Walsh spreading. This is because the (64, 6) code has an error correcting capability of 15 as discussed in Chapter 2, which makes it a very powerful code.

3.3.1.2 Experiment 2: Comparison with Convolutional-Coded System

In this experiment we compare the performance of the proposed system to that of a similar system with convolutional coding instead of our block coding scheme. The block diagram of the modified system is shown below.

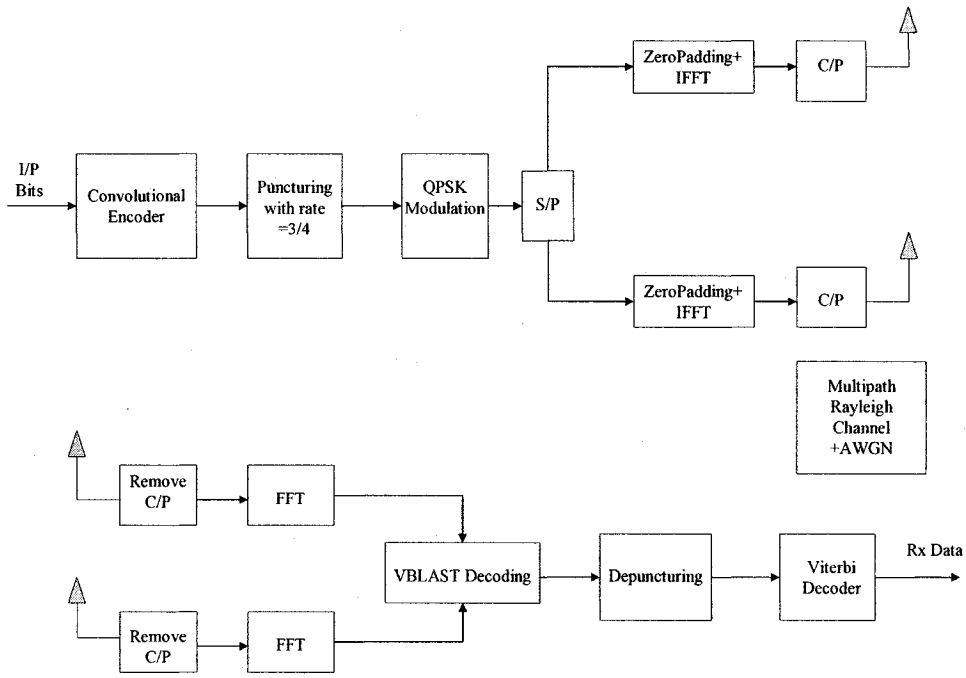

Fig 3.6 Block diagram of the VBLAST system using convolutional coding instead of our block code

We use the convolutional code specified by the standard, which was previously discussed in Chapter 2, and the puncturing rate is ¾. Previous research has shown that combining VBLAST with convolutional coding does not necessarily improve performance, especially in quasi-static environments such as the one used with our system [41]. This is because of the limited performance of the convolutional codes in these environments, since there is not enough multipath diversity for the decoder to properly decide on the decoded symbols. For this experiment, we use the 2×4 antenna configuration and for the system that uses our block coding scheme, we use the (16, 4) code. We also simulate the packet error rate (PER) of both systems for comparison. The BER and PER plots are shown in the following figure.

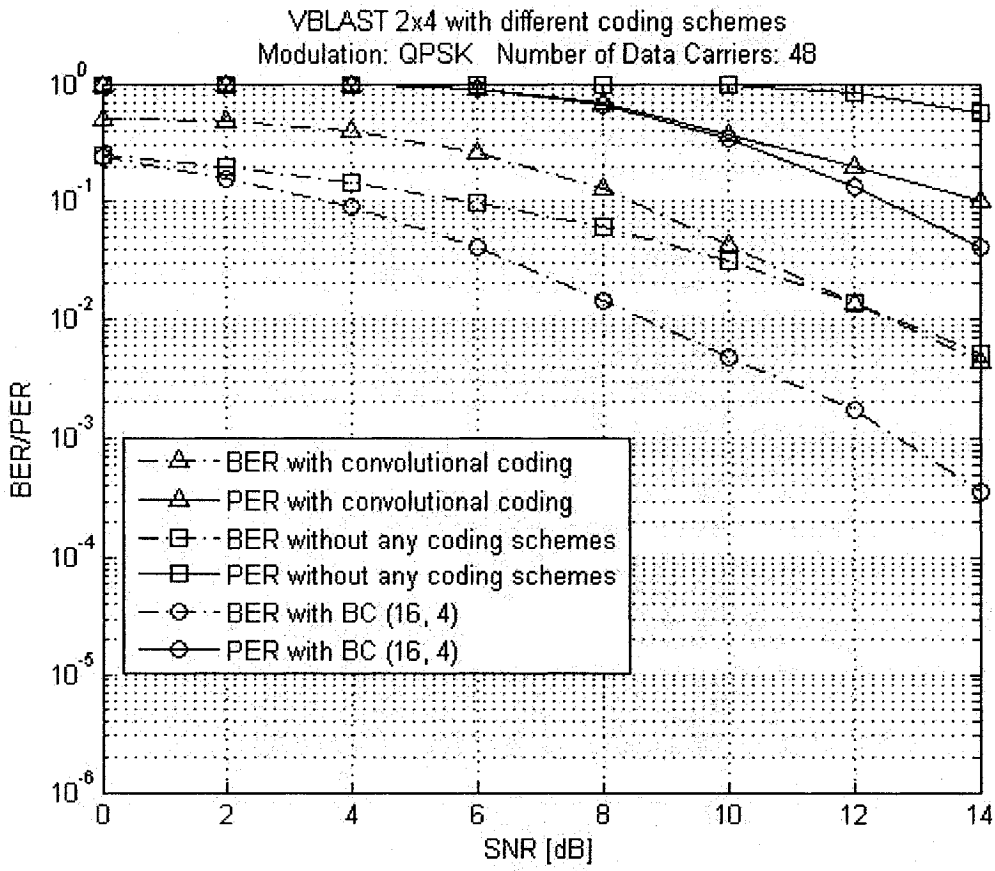

Fig. 3.7 BER and PER plots of the VBLAST system with different coding schemes

Simulation results confirm the fact that the convolutional code does not improve the BER performance of the VBLAST system, although it improves the PER. However, we can clearly see that our block coding scheme achieves better BER and PER results with VBLAST than the convolutional code. This is because of the error propagation problem inherently present with VBLAST. Since VBLAST uses SIC, each step assumes that the previously decoded symbols are correct and therefore, an error that occurs in the decoding of one symbol could affect the decoding of the following symbols. Since the Viterbi decoder uses a tree-search algorithm that depends on several symbols in a row, error propagation could impair the performance of the convolutional code. In contrast,

our FWT decoder does not use the tree-search algorithm and therefore, the error propagation problem does not have the same effect on our block code. In addition, this implies that our scheme is more immune to burst errors than the convolutional code.

3.3.1.3 Experiment 3: Interleaved System

In this experiment we compare the performance of our system (whose block diagram is shown in Fig. 3.1) to the convolutional-coded VBLAST system (whose block diagram is shown in Fig. 3.6) after adding an interleaver. For both systems, we add the interleaver directly before the QPSK modulator and add the de-interleaver directly after the VBLAST decoder. The interleaving depth is 48, as specified by the standard, which is the same as the number of data subcarriers. For this simulation, we use the same convolutional code, block code and antenna configuration as the ones used in Experiment 2 and we simulate the BER and PER of both systems. The results are shown in Fig. 3.8.

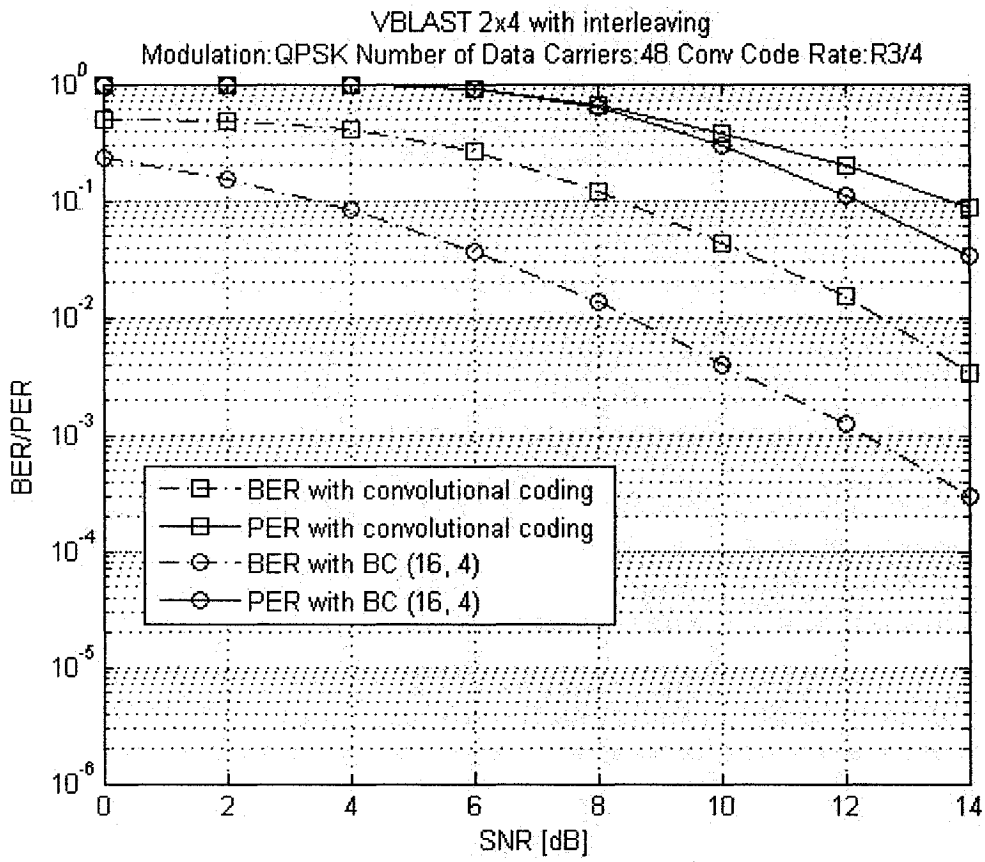

Fig. 3.8 BER and PER plots of VBLAST system with interleaving and either convolutional or block coding

Simulation results show performance improvement of the VBLAST system with both convolutional and block coding schemes after adding the interleaver in both BER and PER plots. We can also see that our block coding scheme outperforms convolutional coding after adding the interleaver. This is because the interleaving operation is effective in combating burst errors.

3.3.1.4 Experiment 4: Different Code Sizes

In this experiment we investigate the performance of our system using different code sizes. Fig. 3.9 shows the BER plots using (64, 6), (32, 5) and (16, 4) codes and the 2×4 antenna configuration.

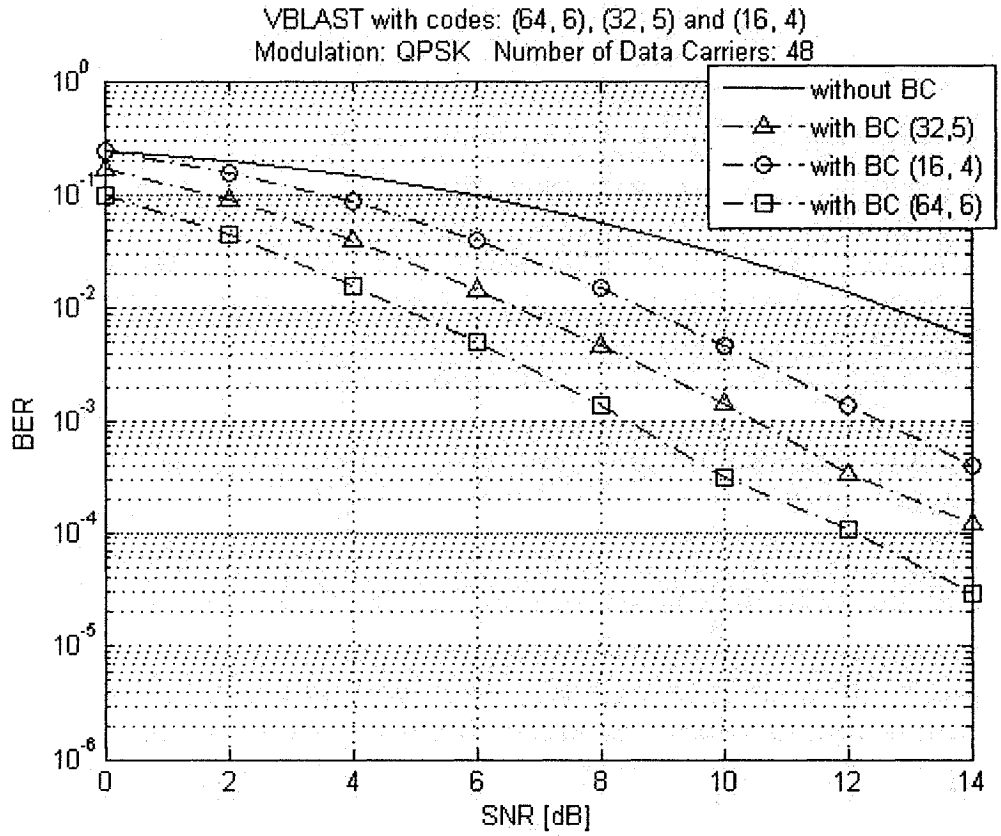

Fig 3.9 BER plots of our VBLAST system with different coding gains

Simulation results show that as we increase the code size the performance improves. The improvement is approximately the same when we change the code size from 16 to 32 and from 32 to 64. This is because as we double the code size the number of errors corrected also approximately doubles. It is known that the number of corrected errors for the (16, 4) code is 3, for the (32, 5) is 7 and for the (64, 6) is 15. However, it takes the receiver one extra step to decode the sequences each time the code size doubles and hence it is up to

the design engineer to tradeoff the performance and complexity when choosing a block code.

3.3.1.5 Experiment 5: Different Antenna Configurations

This experiment investigates the performance of our system using different antenna configurations. For the simulations we will use 2×2, 2×3 and 2×4 systems. The 2×2 system achieves a diversity order of only 1 and is not considered to be a practical system. However, it is simulated for purposes of comparison. The Walsh code used for all the simulations in this experiment is the (64, 6) code. The results are shown in the following figure.

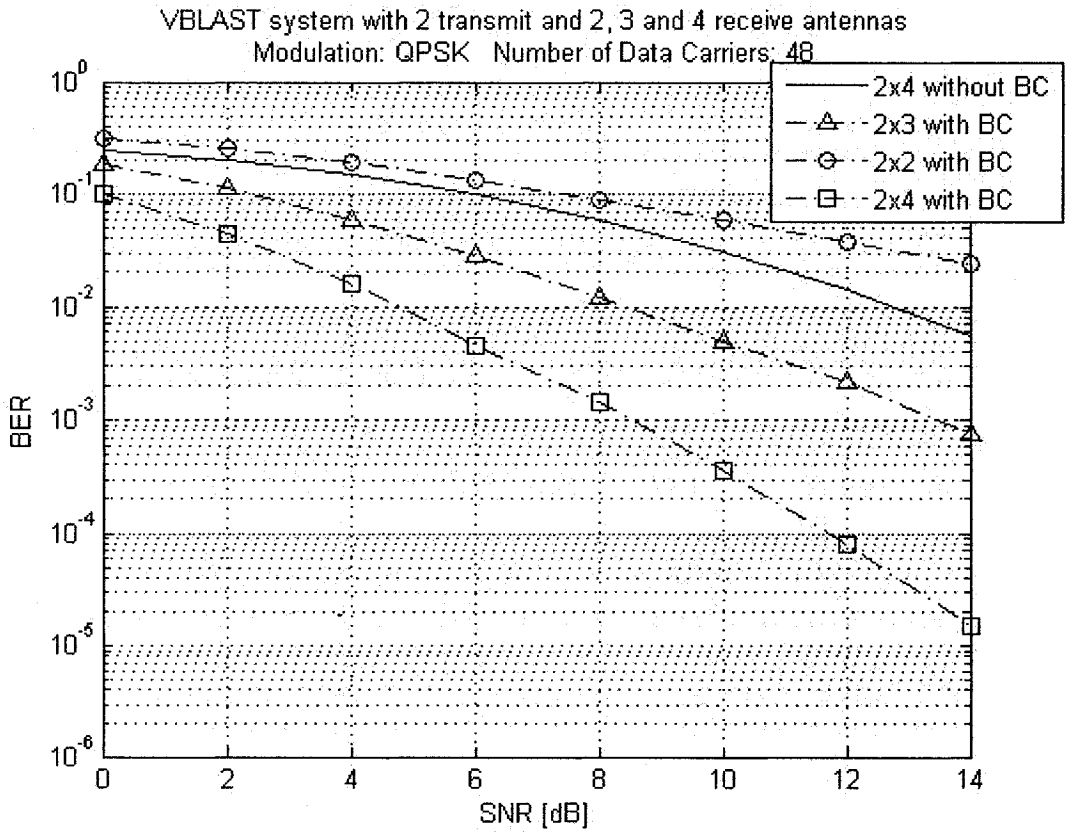

Fig 3.10 BER plots of our VBLAST system with different antenna configurations

The simulation shows that as we increase the number of receive antennas the performance improves. This is due to the fact that more receive antennas lead to higher diversity. The 2×3 system has a diversity order of 2 and the 2×4 system has a diversity order of 3, as we mentioned before. The 2×2 system even achieves a performance similar to that of the 2×4 system without using the proposed spreading. However, from the figure we can see that the performance improvement decreases as we go from 2 to 3 or from 3 to 4 receive antennas. This is because the diversity order increases by one for each extra receive antenna and so the diversity order doubles as we move from 2 to 3 antennas but it does not double as we go from 3 to 4. Also, as we increase the number of antennas the complexity increases since more FFT and VBLAST decoding operations are required.

3.3.1.6 Experiment 6: Different Maximum Channel Delays

In this experiment we will simulate the system under different values of the maximum channel delay. Three channels with delays of 50 ns, 100ns and 200ns, respectively, are considered. The system used is a 2×4 system and the code is (32, 5). The results are shown in Fig. 3.11.

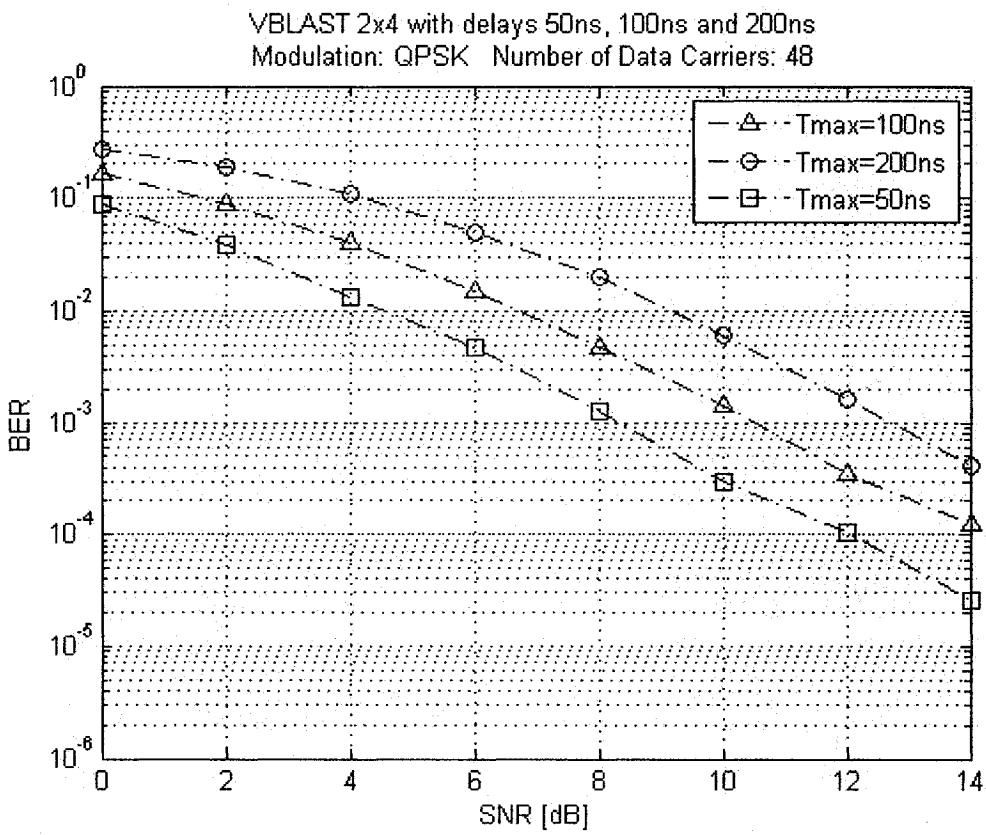

Fig 3.11 BER plots of our VBLAST system with different channel delays

As expected, the channel delay increases the performance becomes worse. This is because the VBLAST system uses the multipaths as individual channels and therefore, more interference occurs as the maximum delay increases and the performance becomes worse. Moreover, if the channel delay is more than the length of the cyclic prefix (800ns), there will be a drastic drop in performance due to the occurrence of inter-carrier and inter-symbol interference (ICI and ISI). However, as we can see from Table 3.1, most channel delays are less than this value and therefore, it is practical to assume that the situation will not occur for most cases.

3.3.1.7 Experiment 7: Different Fading Environments

In this experiment we will investigate the performance of our system under different types of propagation environments, namely, Ricean with several K factors and Rayleigh fading (which was used in all the previous experiments). The envelope of the Ricean channel has probability distribution given by [40]

$$p(x) = \frac{(K+1)}{\Omega_p} \exp\left\{-K - \frac{(K+1)x}{\Omega_p}\right\} I_0\left\{2\sqrt{\frac{K(K+1)x}{\Omega_p}}\right\} \quad x \geq 0 \quad (10)$$

where I_0 is the Bessel function of order 0 and K is the Rice factor defined as the ratio of the power of the line of sight (LOS) path of the channel to the power of the fading paths. We can deduce from Equation (10) that if K=0, the equation becomes identical to Equation (4) for Rayleigh fading. The value of K is influenced mainly by the amount of scattering in the environment. The K factor has a smaller value in rich scattering environments (ideally Rayleigh environments), and its value increases in poor scattering environments implying that the LOS component becomes more powerful. $K=\infty$ implies a non-fading channel. For this experiment we use the (16, 4) code and 2×4 antenna configuration. The BER plots are shown in the following figure.

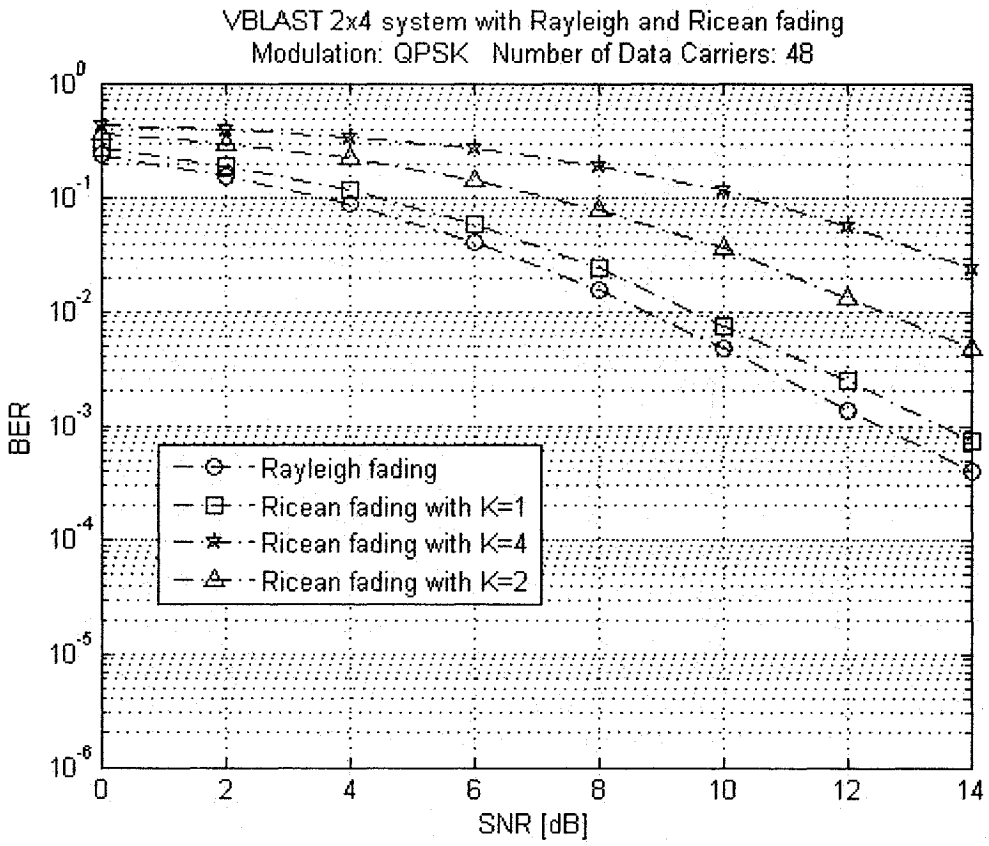

Fig. 3.12 BER plots of the VBLAST system under Rayleigh and Ricean fading with different K factors

Simulation results show that the system performs better under Rayleigh fading than Ricean fading. We can see from Fig. 3.12 that the performance with K=1 Ricean fading is only slightly worse than Rayleigh fading. However, we can also see that the performance deteriorates rapidly with K=2 and K=4 as the multipath fading components become less powerful in comparison to the LOS component.

3.3.1.8 Experiment 8: Different Nulling Methods

In this experiment we will study the performance of the system using different nulling methods. In all the previous simulations we used the ZF method. We now examine the performance of our system using the ZF versus that using MMSE. When using the

MMSE technique the VBLAST algorithm has to be modified, so we use $\mathbf{G} = (\mathbf{H}^{\mathbf{H}}\mathbf{H} + \sigma_n^2 \mathbf{I}_{M_T})^{-1} \mathbf{H}^{\mathbf{H}}$. We will use a 2×4 system with a code (64, 6). The results are shown below.

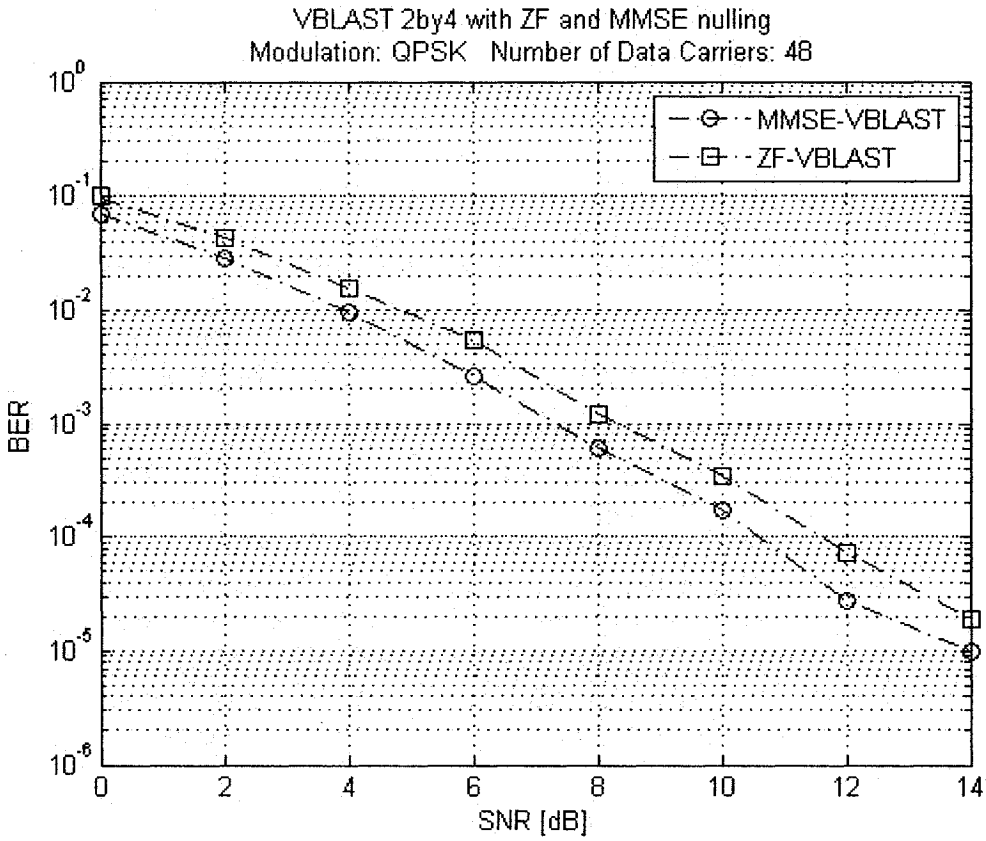

Fig 3.13 BER plots of our VBLAST system with ZF and MMSE nulling techniques

Simulation results have shown an improvement by using the MMSE technique. This is because the mean estimator averages out the noise while the ZF estimator does not take noise into consideration. However, this comes with extra complexity as we have to perform an inverse matrix operation and also the noise variance has to be estimated somehow at the receiver. In this experiment we have assumed that the variance is known.

3.3.2 Comparison of the Proposed System to Previous Systems

We now will compare the complexity as well as performance of the proposed system to that of former systems.

3.3.2.1 Comparison 1: MIMO-OFDM-CDM System

The first system we will examine is the MIMO-OFDM-CDM system proposed in [15] which we previously discussed in Chapter 2. The diagram of the transmitter and the receiver is shown again in the following figure for the purpose of comparison.

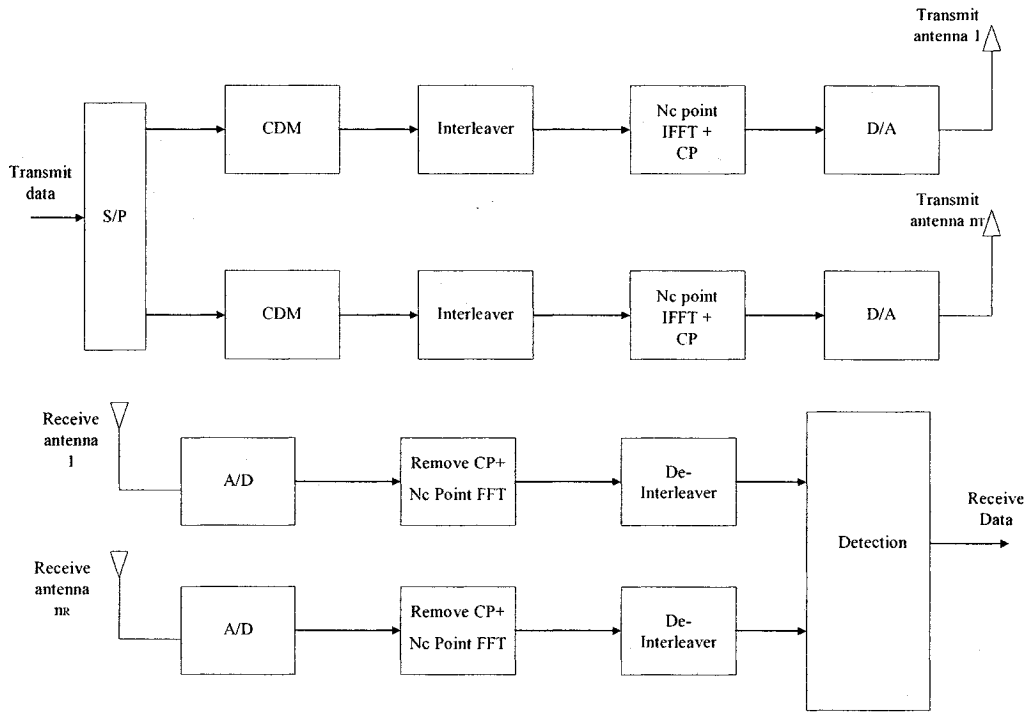

Fig 3.14 Transmitter and receiver structure of the MIMO-OFDM-CDM system in [15]

As we mentioned in Chapter 2, the system uses 2 transmit and 2 receive antennas (2×2 system) and as we can see from Fig. 3.14 there are no FEC techniques employed. The input data is split and each stream passes to a CDM block which works in a different way

than our Walsh block encoder. The system in [15] uses a maximum code length of 4 and therefore, we have 4 multiplications per CDM block giving a total of 8 multiplications over 2 CDM blocks. Our Walsh encoder has a maximum of six steps when using the (64, 6) code and so, our coding block has lower complexity than the CDM blocks in [15]. In addition, we can see from Fig. 3.14 that the transmitter uses two interleavers (one per layer). Therefore, our transmitter has lower complexity than the one in [15]. A similar argument could be applied at the receiver. Our Walsh decoder employs an FWT operation which has a maximum of 6 steps for the (64, 6) code. The despreading operation in [15] again has a total of 8 multiplications over two de-spreading blocks. Therefore, our receiver has a lower complexity than the one in [15]. The results of the simulations of the performance of the MIMO-OFDM-CDM adopted from [15] are shown in Fig. 3.15.

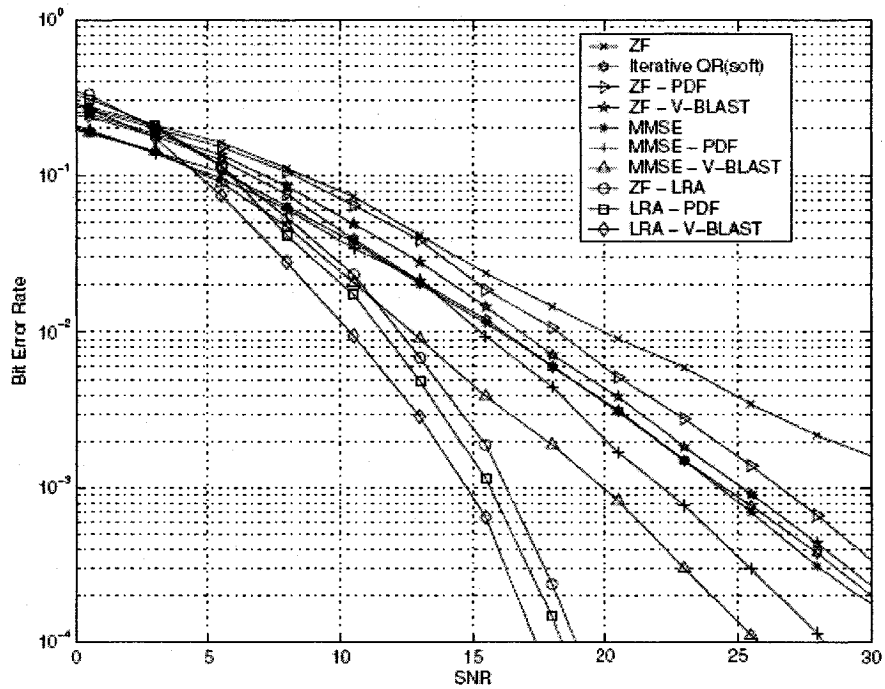

Fig. 3.15 Simulation results for the MIMO-OFDM-CDM system [15]

Although the paper compares different detection techniques, by looking at the curve for the ZF-VBLAST which is the detection technique employed in our system we find that the proposed system has much better performance, so implying that our system is superior on both aspects of complexity and performance.

3.3.2.2 Comparison 2: MIMO-OFDM System

The next system to be investigated is the coded MIMO-OFDM system proposed in [31]. Fig. 3.16 shows the block diagram of the transmitter and receiver.

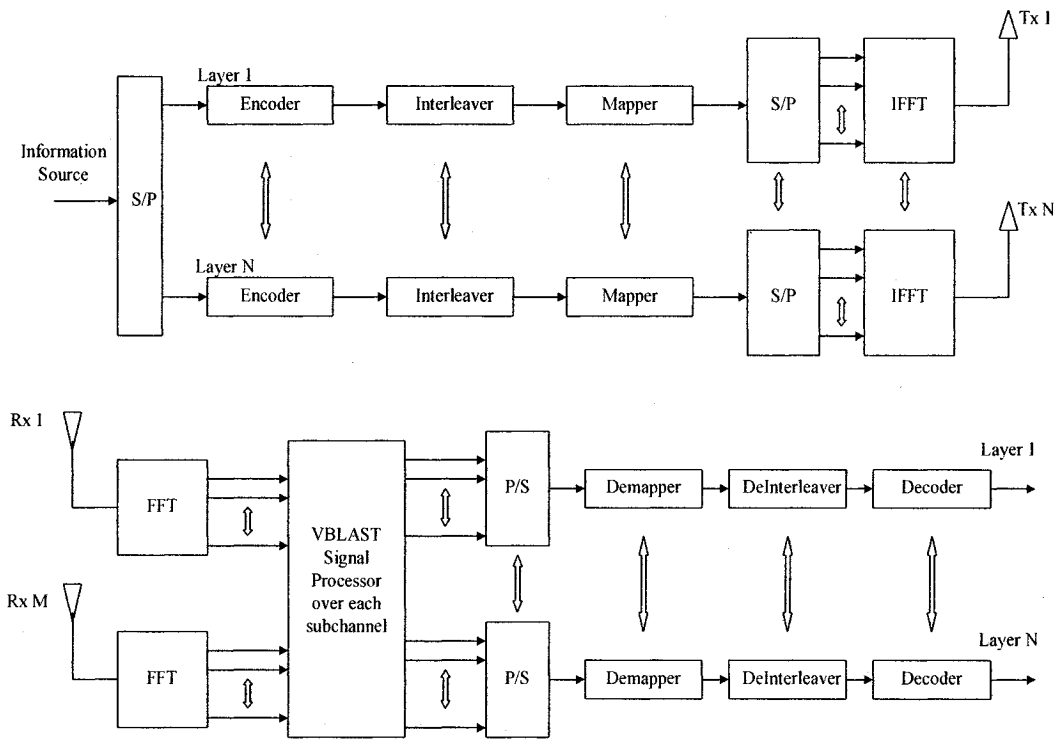

Fig. 3.16 Transmitter and receiver structure of the MIMO-OFDM system in [31]

The system in [31] uses a 4×4 antenna configuration and we can easily deduce that our system has a lower complexity than the one in [31]. This is because our system employs

only one Walsh encoder at the transmitter which has lower complexity than the combined convolutional encoding and interleaving operations done in [31]. In addition to that, the system in [31] uses one convolutional encoder, interleaver and mapper per layer. Our receiver only has one FWT decoder which has lower complexity than the demappers, deinterleavers and decoders used per layer at the receiver in [31].

3.3.2.3 Comparison 3: MIMO MC-CDMA System

The last system to be discussed is the MIMO MC-CDMA system discussed in [18]. The transceiver structure is shown in the following figure.

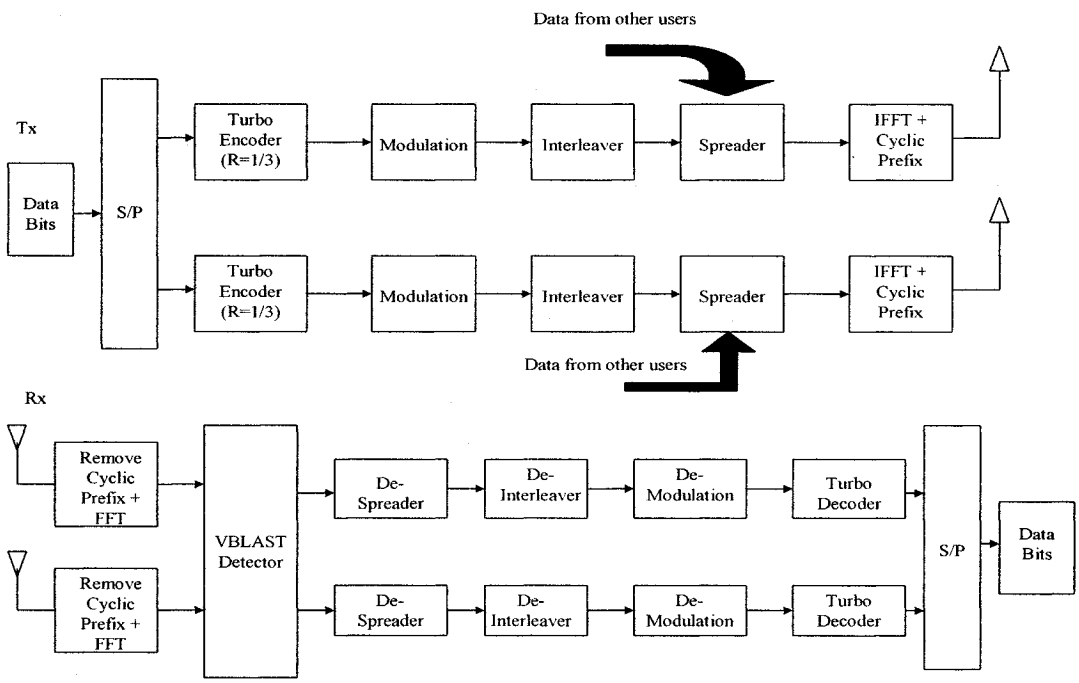

Fig 3.17 Transmitter and receiver structure of the MIMO MC-CDMA system in [18]

Similar to the previous system, the transmitter has separate encoders, modulators, interleavers and spreaders for each layer, and so the transmitter structure has higher

complexity than the proposed system even if the spreaders have less complexity than the proposed encoder. Also, the receiver in Fig. 3.17 has one demodulator, deinterleaver and despreader per layer. Therefore, we can deduce again that our system has lower complexity than the one in [18].

3.4 Conclusions

In this chapter a MIMO-OFDM system that utilizes the VBLAST algorithm in combination with a Walsh block coding scheme has been presented. Although this coding method was inspired by the IS-95 system, it is used in our system for the purpose of improving the performance and the implementation of the encoder and decoder have been simplified to provide a low complexity and high performance block code. The block diagram of the system has been shown with a detailed description of each block's functionality. We have also presented a brief review of LST codes as well as the VBLAST algorithm that represent the MIMO configuration used in this chapter.

A simulation study of the performance of the system was carried out using different coding techniques, code sizes, antenna configurations, delay spreads, two variations of the VBLAST algorithm, types of fading environments and in the presence of an interleaver. Computer simulations show that the proposed block coding scheme outperforms convolutional coding in both BER and PER, because our FWT decoder does not use the tree-search algorithm employed by the Viterbi decoder which makes it more immune to the error propagation problem inherently present with VBLAST. Adding an interleaver also improved the performance of the proposed system on both BER and PER aspects. We have also seen that the performance improves as the code size increases due

to the higher error correction capability. It has also been shown that as the number of receive antennas increase the performance improves as the result of increasing diversity. By increasing the maximum channel delay, we observed that the performance of the system deteriorates due to the increased multipath fading effects. It has also been shown that MMSE-VBLAST achieves better performance than the ZF-VBLAST since it averages out the noise introduced by the channel. Finally, we have seen that the system performs better in rich scattering environments, such as Rayleigh fading environments, than in poor scattering environments, such as Ricean fading environments with high K factors. The proposed system was also compared to some of the previous LST systems, showing the superiority of our system in both performance and computational complexity.

Finally, we can conclude that the proposed coding scheme is well suited for VBLAST systems as demonstrated by the performance analysis and the complexity comparisons. However, one drawback arises which is the bandwidth consumption that increases when large size block codes are used. It is therefore the job of the design engineer to trade-off performance for higher data rates. Nevertheless, the system offers promising potential as it achieves very good performance results and maintains a low computational complexity.

Chapter 4

Proposed MIMO-OFDM System with Walsh Block Coding and STBC Configuration

In the previous chapter, a system combining MIMO-VBLAST, OFDM and Walsh block coding scheme has been proposed. In this chapter, a similar system using MIMO-STBC instead of VBLAST will be studied. STBC aims to improve the performance of the system rather than increasing the transmission rate as in the case of VBLAST. The chapter starts with a block diagram of the system with a detailed description of each block followed by an overview of STBC techniques. We then present a performance study of the new system through computer simulations under different system parameters such as different coding gains, coding schemes different number of antennas, channel delays, types of fading environments and in the presence of an interleaver. Finally, we compare the computational complexity as well as the performance of the system to that of a few existing systems.

4.1 Overview of STBC Techniques

In this section, space-time block coding (STBC) techniques will be briefly reviewed. These codes rely on spreading data streams across time and space to combat multipath fading and improve link quality. The idea is to transmit orthogonal versions of the signal to the receiver so that if the power of one path fades significantly, the receiver will still be able to recover the signal through other paths. This is called diversity, as we have previously mentioned in Chapter 2. STBC codes provide full order diversity of $M_T \times M_R$ (where M_T is the number of transmit antennas and M_R the number of receive antennas). These codes started with the famous Alamouti code [12] which provides simple transmit diversity without the need for feedback from the receiver to deliver channel state information (CSI) to the transmitter. The code also needs no bandwidth expansion since the data is spread across time and space. It operates as follows:

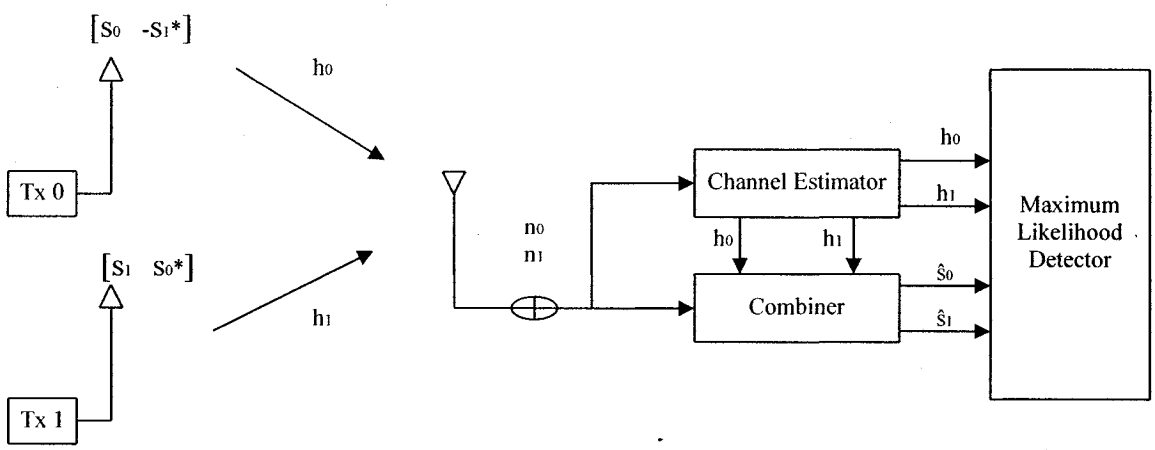

Fig 4.1 Simplified 2×1 communication system using the Alamouti code [12]

At the transmitter of the system shown in Fig. 4.1 [12], the space-time encoder takes the modulated symbols and encodes them according to the matrix

$$\begin{pmatrix} s_0 & -s_1^* \\ s_1 & s_0^* \end{pmatrix}$$

At the first symbol period, antenna 0 transmits s_0 and antenna 1 transmits s_1. At the second symbol period antenna 0 transmits $-s_1^*$ and antenna 1 transmits s_0^*. Thus, the symbols are transmitted across time and space. We can see that it takes two symbol periods to transmit two symbols so there is no bandwidth expansion. Assuming fading is constant across two symbols we have

$$h_0(t) = h_0 = \rho_0 e^{j\theta 0} \tag{1}$$

$$h_1(t) = h_1 = \rho_1 e^{j\theta 1} \tag{2}$$

the received signals at each symbol period are a superposition of the two transmitted signals and are given by

$$r_0 = h_0 s_0 + h_1 s_1 + v_0 \tag{3}$$

$$r_1 = -h_0 s_1^* + h_1 s_0^* + v_1 \tag{4}$$

the combiner shown in Fig. 4.1 uses the channel estimates to build a combined signal as follows

$$\hat{s}_0 = h_0^* r_0 + h_1 r_1^* \tag{5}$$

$$\hat{s}_1 = h_1^* r_0 - h_0 r_1^* \tag{6}$$

combining the equations (1) - (6), we get

$$\hat{s}_0 = (\rho_0^2 + \rho_1^2) s_0 + h_0^* v_0 + h_1 v_1^* \tag{7}$$

$$\hat{s}_1 = (\rho_0^2 + \rho_1^2) s_1 - h_0 v_1^* + h_1^* v_0 \tag{8}$$

which are used by the maximum likelihood decoder to recover the transmitted symbols. The use of these codes was extended to the case of multiple antennas by Tarokh, Jafarkhani and Calderbank in [32], where space time codes were generalized by applying the theory of orthogonal designs. All the codes achieve full diversity of order $M_T \times M_R$ and simple maximum likelihood decoding can be used to recover the signals. The theory

of orthogonal designs [32] states that linear processing of an orthogonal matrix $\mathbf{\epsilon}$ is possible only if the entries of modulated symbols x_1, x_2, ..., x_n and their conjugates x_1^*, x_2^*,...., x_n^* follow the rule

$$\mathbf{\epsilon}.\mathbf{\epsilon}^H = c\,(|x_1|^2 + |x_2|^2 + \ldots.. + |x_n|^2)\,\mathbf{I}_{M_T}$$

where "H" is the Hermitian transpose, c is a constant and I_{M_T} is the $M_T \times M_T$ identity matrix. The rate of an STBC code is given by

$$R = k/p$$

where k is the number of modulated symbols in the transmit matrix and p the number of symbol periods taken to transmit the whole matrix. The spectral efficiency of STBC codes is given by

$$\eta = r_b/B = r_s mR/r_s = km/p \quad \text{bits/s/Hz}$$

where r_b is the bit rate, r_s is the symbol rate B is the bandwidth and m is the number of bits per signal constellation. For real signal constellations such as M-ASK, there exist STBC codes if and only if the number of transmit antennas $M_T = 2$, 4 or 8. These codes are given in detail in [32]. For complex signal constellations, the only full rate code that exists is the Alamouti code explained before. If more transmit antennas are required, some of the bandwidth will have to be sacrificed and the processing at the receiver becomes more complex. These higher order codes are called sporadic codes and are given in [32].

4.2 System Structure and Block Description

Fig. 4.2 shows the block diagram of the STBC based configuration of our system. Comparing with Fig. 3.1, we can see that there are several common blocks. Therefore, to avoid repetition, in the following sections only the blocks that are different in the two systems will be highlighted.

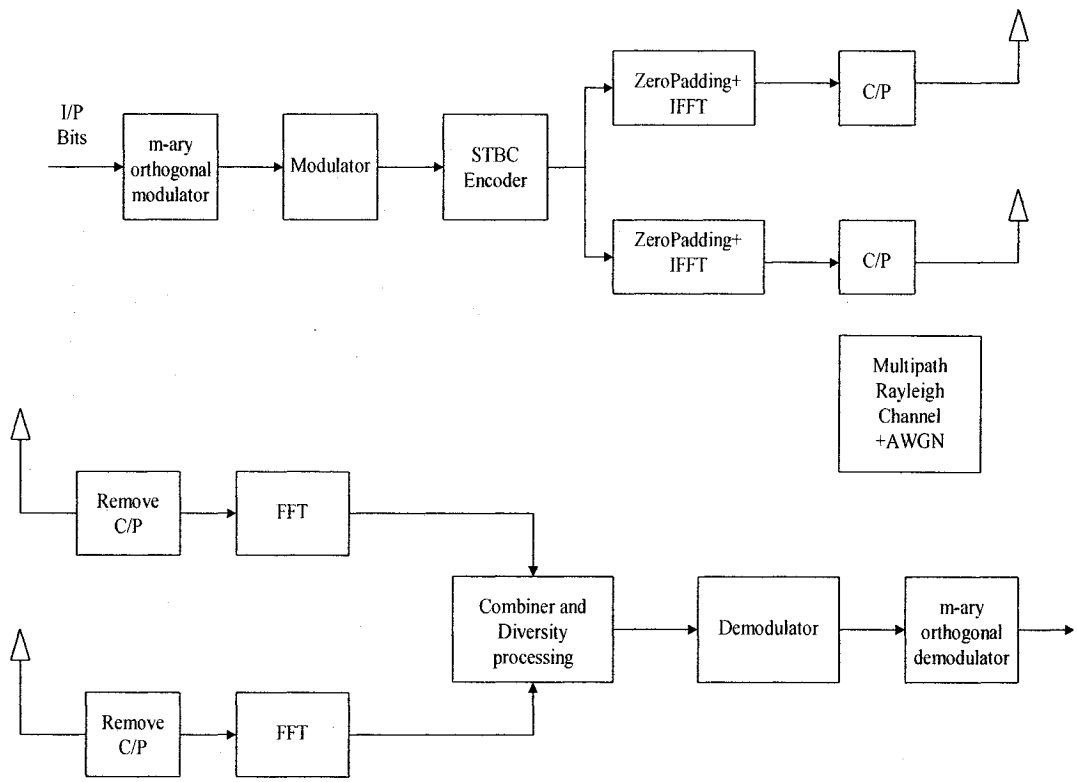

Fig 4.2 Block diagram of the proposed system with STBC configuration

4.2.1 Transmitter Structure

The STBC transmitter works exactly the same way as the VBLAST transmitter explained in Chapter 3, except for the part concerned with diversity. The VBLAST transmitter simply splits the data streams across the transmit antennas, while the STBC transmitter has an extra block called the STBC encoder. It takes the modulated symbols and maps them according to the aforementioned Alamouti matrix after generating the necessary conjugates. The simulations in this chapter assume 2 transmit antennas and 1, 2 or 4 receive antennas.

4.2.2 Channel Structure

The channel considered in this chapter is again a quasi-static multipath Rayleigh fading channel with a maximum delay spread of 100ns (later we simulate the system under different channel delays and fading environments). However, the channel works in a different way from the VBLAST channel. As it was mentioned in Chapter 3, the VBLAST encoding scheme uses the delay spreads as routes from the transmitter to the receiver and each route is completely independent from the other. In other words we have a number of independent channels equal to the product of the number of transmit and receive antennas. However, for STBC encoding the process is different. All signals from all transmit antennas go through the same channel. The transmitted signals are forced to be orthogonal through the channel by means of STBC encoding. Therefore, to simulate how this channel works, each transmitted signal is convoluted with the same CIR, rather than different CIRs as in Chapter 3, and AWGN is added afterwards.

4.2.3 Receiver Structure

- The first part of the receiver is the same as the VBLAST counterpart. The cyclic prefix is removed; the preamble is extracted and passed along with the data to a 64-FFT block where they are converted back to the frequency domain.
- The next block is the combiner. This block takes on the task of linear processing on the incoming signals (after OFDM demodulation). In case we have one receive antenna, the necessary calculations to obtain $\hat{s}_0$ and $\hat{s}_1$ are those shown before. If we have 2 receive antennas, the combining process is repeated across each antenna and the results are combined. Otherwise if we have 4 receive antennas, the process is repeated 4 times and the results are combined.
- The signals are then passed to a QPSK demodulator where a slicing operation is performed to recover the transmitted Walsh codes.
- The bits are then passed to an m-ary orthogonal demodulator where a FWT operation takes place to decode the transmitted Walsh codes and obtain back the transmitted bits.

4.3 Performance and Complexity Study of the Proposed System

In this section, the performance of our system will be investigated through computer simulations under different channel conditions and system parameters. Afterwards, we will provide comparisons of our system to previous systems in terms of performance and computational complexity.

4.3.1 Performance Study

In this sub-section, we will examine the performance of the system by simulating its BER. Again, all the simulations in this chapter assume perfect channel knowledge at the receiver.

4.3.1.1 Experiment 1: Performance of Block Coded System

In this simulation, we examine the performance of the proposed system compared to a similar system without using Walsh spreading. We use the (64, 6) block code and a 2×2 antenna configuration. Since STBC achieves a full diversity, the diversity order here is 4. The code rate of this STBC code is 1 and its spectral efficiency is (2×2/2 = 2) as explained before. Fig. 4.3 shows the BER plots from this experiment.

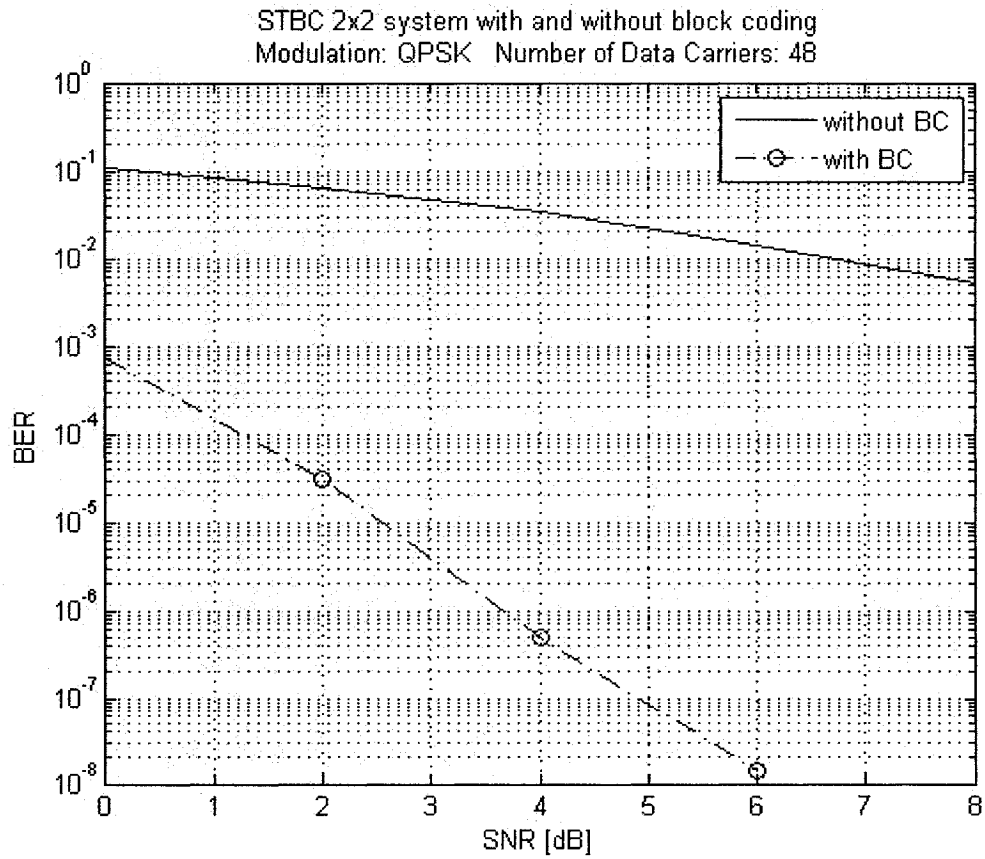

Fig 4.3 BER plots of our 2×2 STBC system with and without Walsh block coding

We can see that a significant performance improvement has been achieved with the proposed block coding scheme. The performance improvement is even greater with STBC compared to that using VBLAST. This is because STBC achieves full order diversity compared to the sub-optimal diversity order when VBLAST is used. More specifically, the system using STBC yields a BER of 10^{-8} at an SNR of 6 dB, as seen in Fig. 4.3.

4.3.1.2 Experiment 2: Comparison with Convolutional-Coded System

In this experiment we compare the performance of the proposed system to that of a similar system that uses convolutional coding. The block diagram of the STBC system with convolutional coding is shown in the following figure.

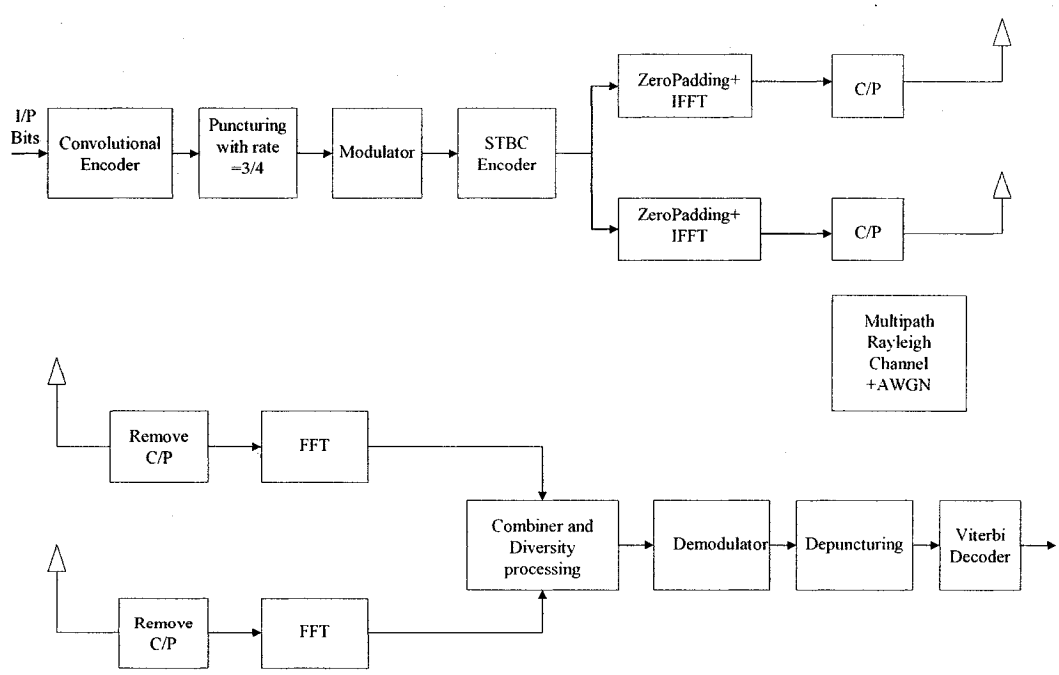

Fig. 4.4 Block diagram of STBC system using convolutional coding instead of our block code

We use the same convolutional code that was used with Experiment 2 in Chapter 3. However, in contrast to VBLAST, it is expected that convolutional coding enhances the performance of STBC. For this experiment, we use 2×2 antenna configuration and the (16, 4) code with the system that employs our block coding scheme. We simulate the BER and PER of both systems and the results are shown in Fig. 4.5.

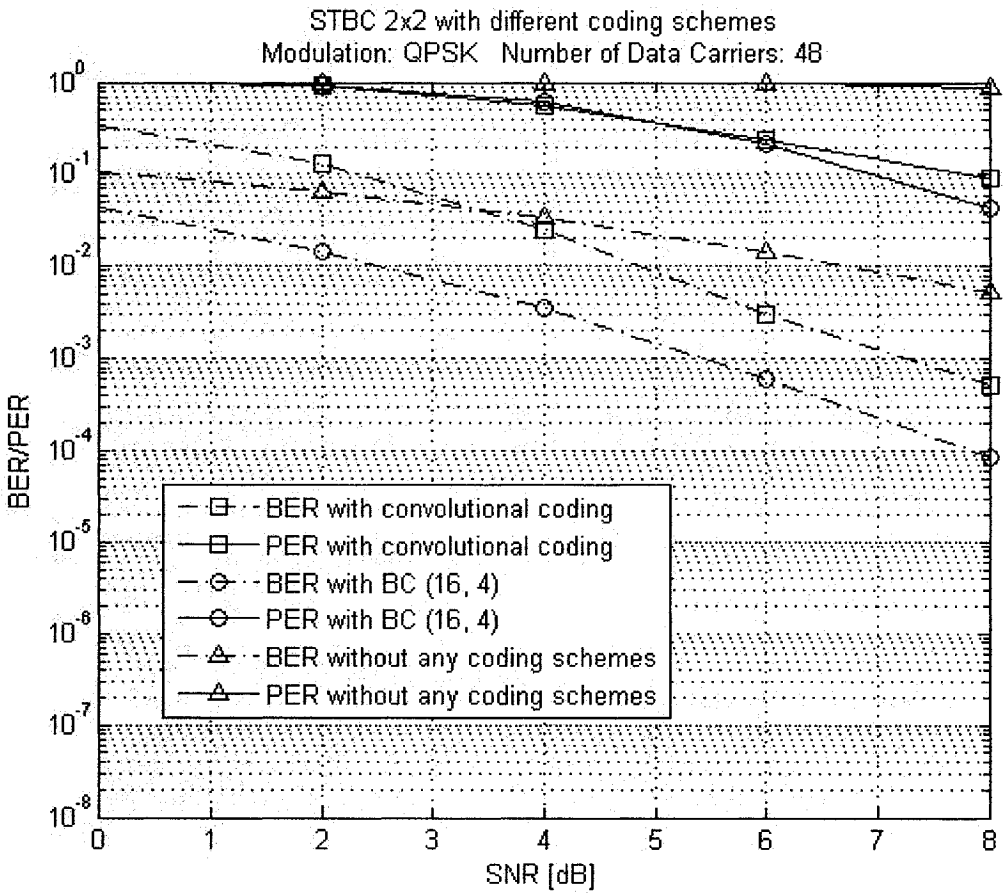

Fig. 4.5 BER and PER plots of the STBC system with different coding schemes

The simulation results show that convolutional coding improves the BER and PER performance of STBC, especially, at high SNR. We can also see that combining STBC with our block code achieves even better results than both convolutional-coded and

uncoded STBC systems on both BER and PER aspects implying that our block code is more effective against burst and random errors.

4.3.1.3 Experiment 3: Interleaved System

In this experiment we investigate the BER and PER performance of convolutional and block coding schemes with the STBC system after adding an interleaver. For both systems we add the interleaver before the QPSK modulator and add the de-interleaver after the demodulator. For both systems we use 2×2 antenna configuration and for the proposed system we use the (16, 4) code. The simulation results are shown in the following figure.

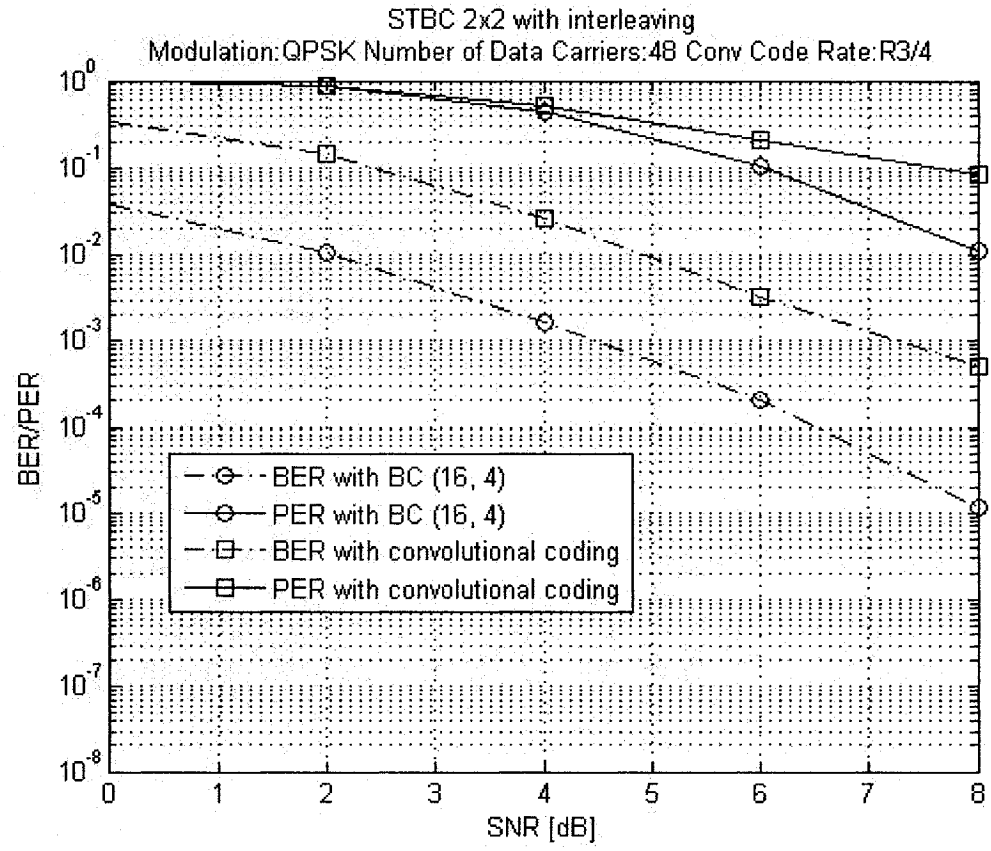

Fig. 4.6 BER and PER plots of the STBC system with interleaving and either convolutional or block coding

Simulation results show that the BER and PER performance improves after adding the interleaver. We can also see that our interleaved block coding scheme outperforms interleaved convolutional coding. Comparing with Fig. 3.8, we can see that more performance improvement is acquired from combining interleaving with STBC than with VBLAST.

4.3.1.4 Experiment 4: Different Code Sizes

In this experiment we study the performance of the system under different code sizes. We now use (64, 6), (32, 5) and (16, 4) codes and 2×2 antenna configuration. The simulation results are shown in Fig. 4.7.

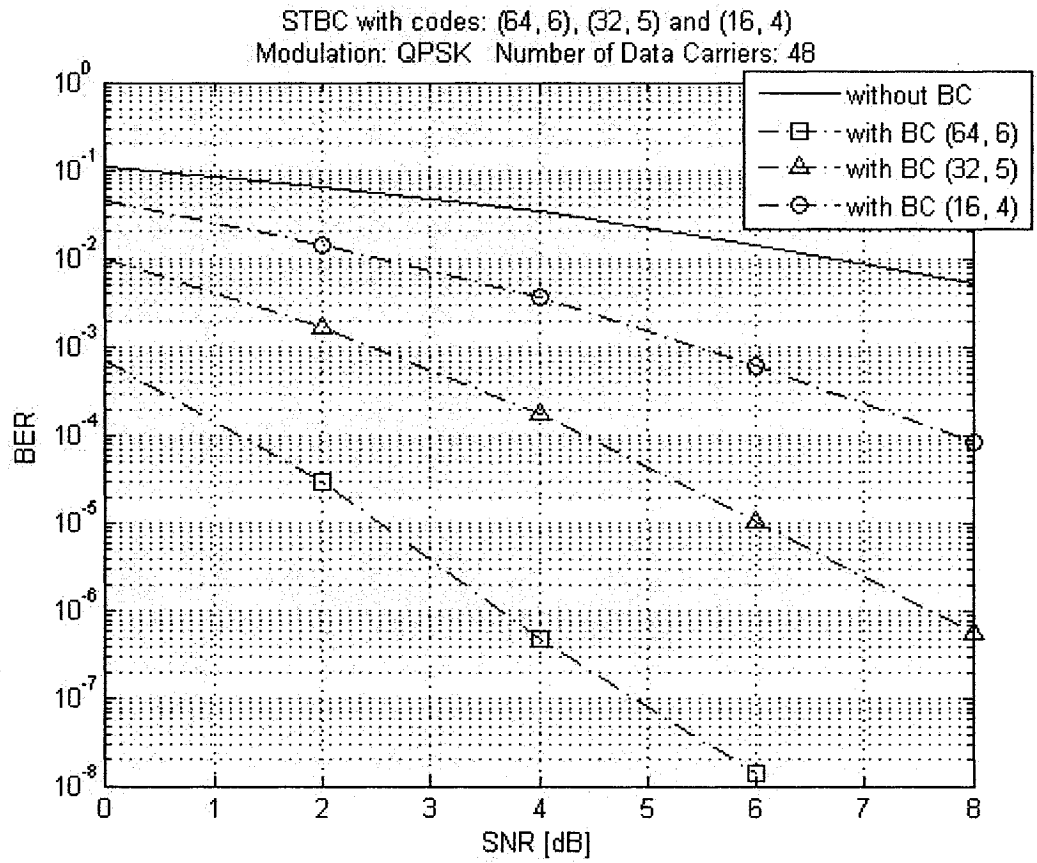

Fig 4.7 BER plots of our STBC system with different coding gains

The simulation results show that as the code size increases the performance improves. Basically, the improvement is the same as we double the code size from 16 to 32 and from 32 to 64. Again, the performance improvement achieved with each code is larger with STBC than with VBLAST.

4.3.1.5 Experiment 5: Different Antenna Configurations

In this experiment we study the performance of the system under different antenna configurations. We use a Walsh code of size (32, 5) and simulate 2×1, 2×2 and 2×4 antenna configurations. The simulation results are shown below.

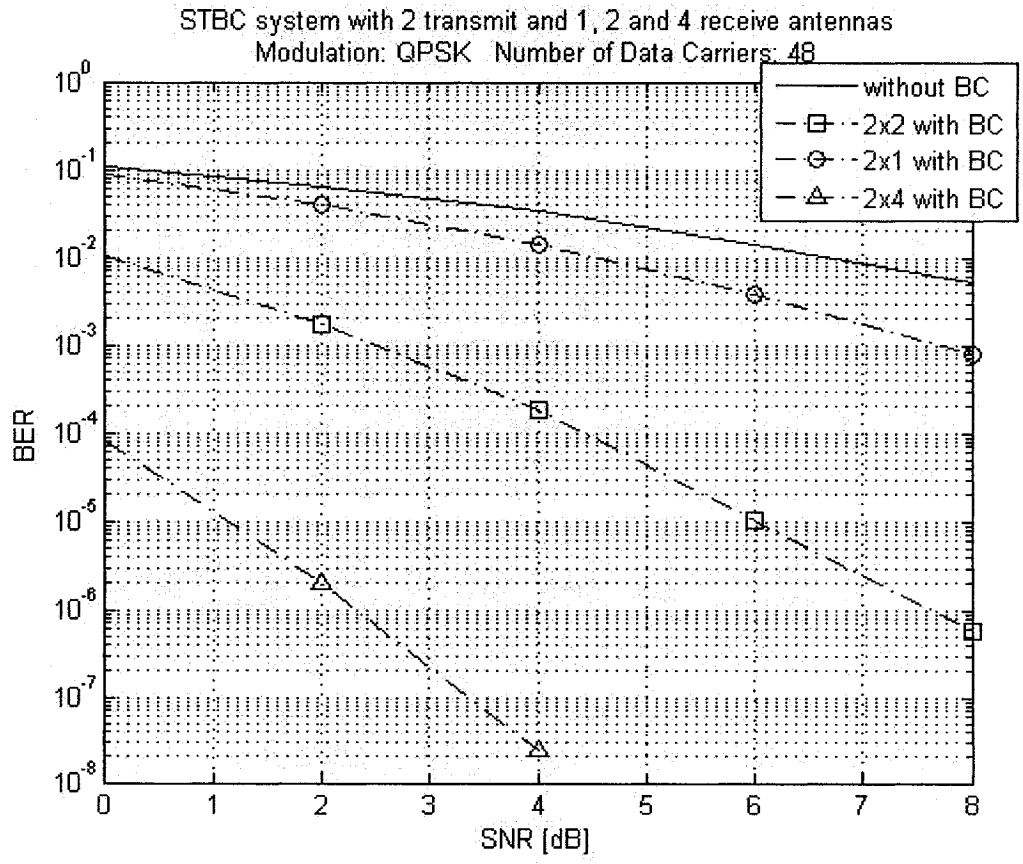

Fig 4.8 BER plots of our STBC system with different antenna configurations

Similar to the VBLAST system, the BER performance improves as we increase the number of receive antennas. However, unlike VBLAST, STBC achieves a full order diversity of $M_T \times M_R$ and therefore, the 2×1 system achieves a diversity order of 2, the 2×2 system a diversity order of 4 and the 2×4 system a diversity order of 8. From the figure we can see that the BER improvement is the same as we move from 1 to 2 and from 2 to 4 receive antennas. This is because the diversity order doubles as the number of antennas doubles. Even the 2×1 system still has a better performance than the 2×2 system without using the proposed Walsh spreading. However, the complexity increases as we increase the number of receive antennas, since the signal combining operations have to be performed at each receive antenna, which in turn need more FFT blocks for each extra antenna.

4.3.1.6 Experiment 6: Different Maximum Channel Delays

In this experiment we study the system performance under different maximum channel delays. We will use a Walsh code of size (64, 6) and simulate the system under maximum delays of 50ns, 100ns and 200ns. The following figure shows the simulation results from this experiment.

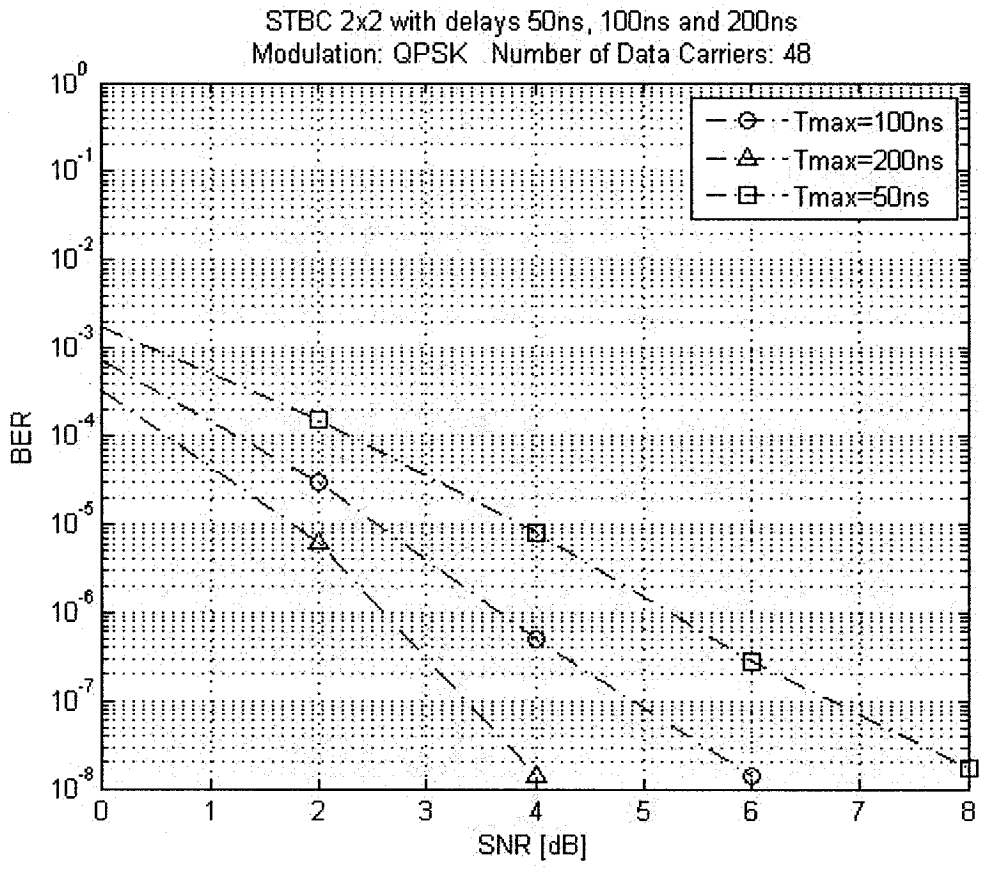

Fig 4.9 BER plots of the STBC system with different channel delays

This experiment has shown very interesting results, namely, as we increase the maximum delay the performance actually is improved. This is because with STBC, we have more paths from the transmitter to the receiver as the maximum delay increases. The STBC uses these extra paths to provide the receiver with more versions of the transmitted signal and so higher diversity order is achieved. Note that this advantage was not available in the VBLAST system. On the other hand, similar to VBLAST, the channel delay in the STBC system has to be less than the duration of the cyclic prefix. Otherwise, interference would occur.

4.3.1.7 Experiment 7: Different Fading Environments

In this experiment, we study the performance of the system under different types of fading environments, namely, Rayleigh and Ricean fading with several K factors. We use the 2×2 antenna configuration and the (16, 4) code. The BER plots are shown in Fig. 4.10.

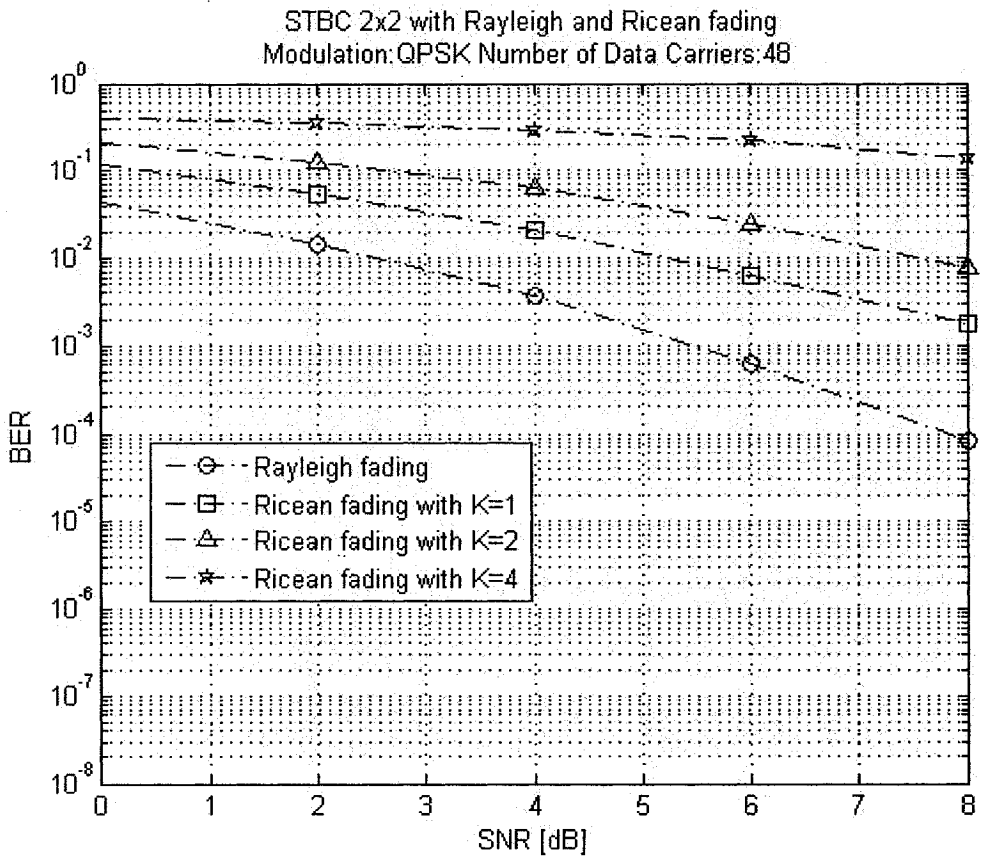

Fig. 4.10 BER plots of the STBC system under Rayleigh and Ricean fading with different K factors

Simulation results show that the system performs better under Rayleigh fading than Ricean fading. The BER performance deteriorates rapidly as the K factor becomes higher and the scattering becomes poorer. Comparing with Fig. 3.12, we can see that the performance of the STBC system deteriorates more rapidly than VBLAST under high K

factors. This is because the STBC system relies on the scattering in the environment to improve the system performance, in contrast to VBLAST which uses the scattering to increase data rate, thus making its performance more immune to the decreased scattering present with high Ricean K factors.

4.3.2 Comparison of the Proposed System to Existing Systems

We now compare the computational complexity and performance of the proposed system to some of the existing systems.

4.3.2.1 Comparison 1: STBC OFDM-CDM System

Consider the STBC OFDM-CDM system proposed in [37], which was previously mentioned in Chapter 2. The block diagram of the transmitter and receiver is shown below for comparison purpose.

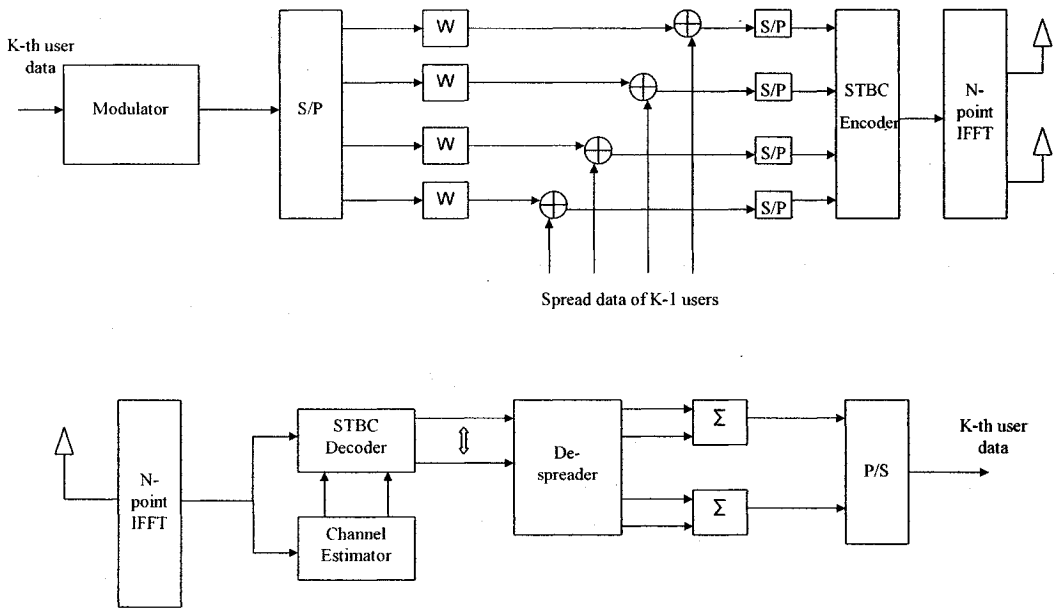

Fig. 4.11 Block diagram of the STBC-OFDM-CDM system in [37]

By examining Fig. 4.11 we find that the system in [37] has similar blocks to our system but uses different spreading techniques. A maximum code size of 32 (32 users) is used in [37] and therefore, 32 multiplications and 32 additions (where the data of the other users is added) are required at the transmitter. For the (32, 5) code, our system needs only 5 steps at the transmitter and receiver and so gives a much lower complexity. The simulation results of the system in [37] are shown below.

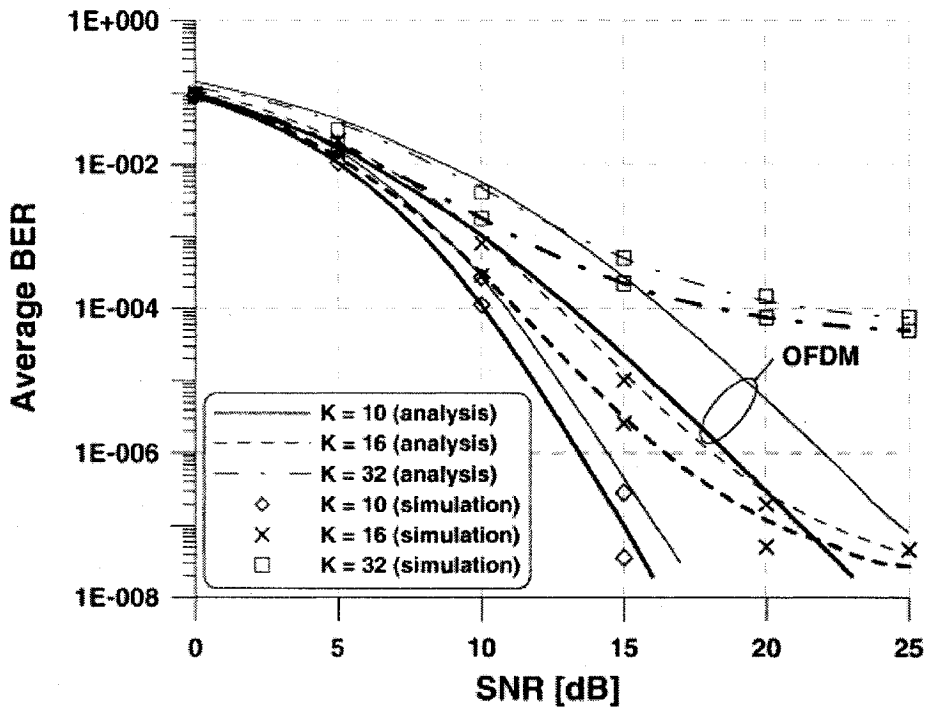

Fig. 4.12 BER plots of the STBC-OFDM-CDM system [37]

By examining Fig. 4.12 we find that the system achieves the best performance when K=10 (lowest number of users) and the performance deteriorates as the number of users increase due to the increased MAI. Comparing with Fig. 4.7, we can see that our system achieves a better performance even when using the smallest code: (16, 4). At an SNR of 8 dB our system has a BER of 10^{-4} while the system in [37] gives a BER of about 10^{-3}.

4.3.2.2 Comparison 2: STBC MC-CDMA System

The second system considered for comparison is the STBC MC-CDMA system discussed in [14]. The block diagram of the transmitter and receiver is shown in the following figure.

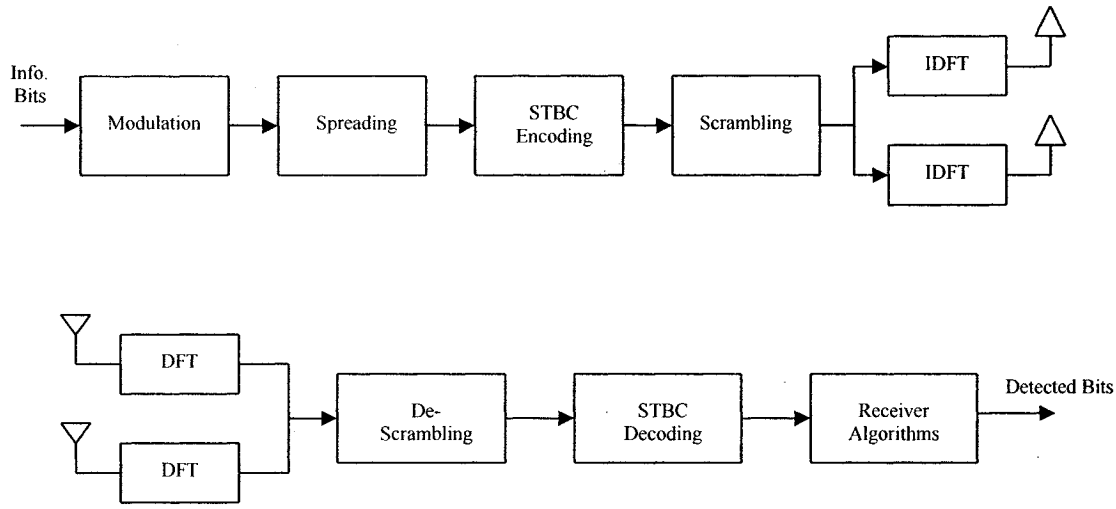

Fig 4.13 Transmitter and receiver structure of the STBC MC-CDMA system in [14]

As we previously mentioned in Chapter 2, the above system uses 2×1 and 2×2 systems with Walsh sequences of length 32. It does not use any FEC mechanisms and uses a scrambler. Although the spreader in [14] has a lower complexity than the proposed one, the overall complexity of our transmitter is less than that in [14] since we are not using any scrambling operations. At the receiver, a similar argument can be made: Both systems use similar blocks except that a descrambling block is employed in [14] which implies that our receiver has a lower complexity, even though our decoding block has a higher complexity compared to the despreader in [14]. Fig. 4.14 shows the simulation results of the system in [14].

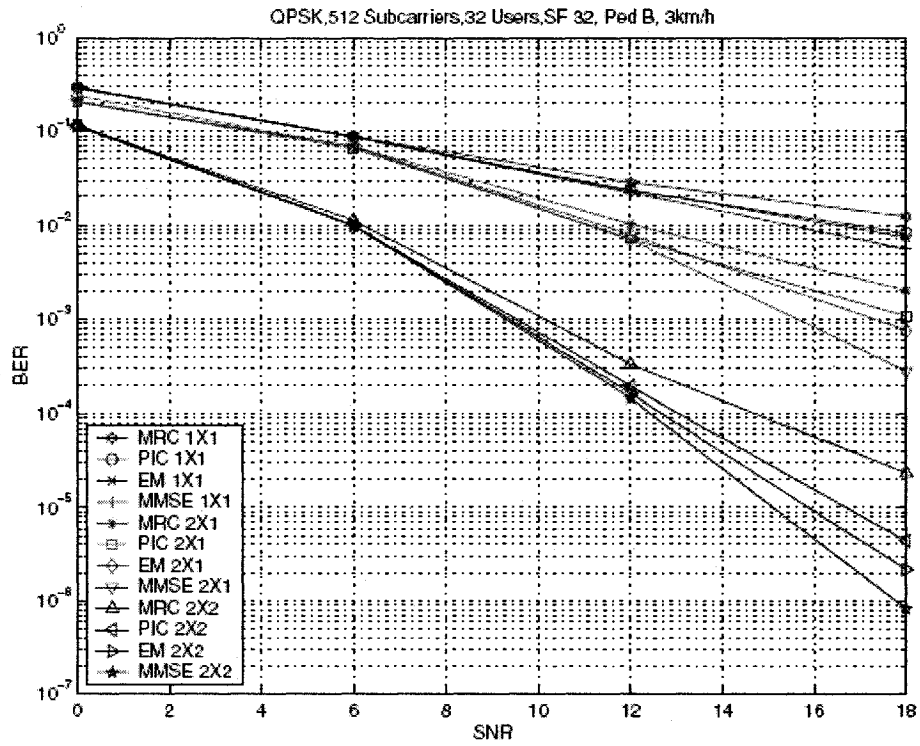

Fig 4.14 Simulation results of the STBC MC-CDMA system [14]

We can clearly see that the proposed system has a significant performance improvement over that in [14] even for the case of the 2×2 MMSE system. From Fig. 4.8 we can see that our system reaches a BER of 10^{-6} at 7.5 dB for a code size of 32 while the system in [14] reaches the same BER at 18 dB. Therefore, our system is superior in terms of performance and computational complexity.

4.3.2.3 Comparison 3: MIMO-OFDM System

Another system under study is the MIMO-OFDM system used in [33]. The block diagram of its transmitter and the receiver is shown in Fig. 4.15.

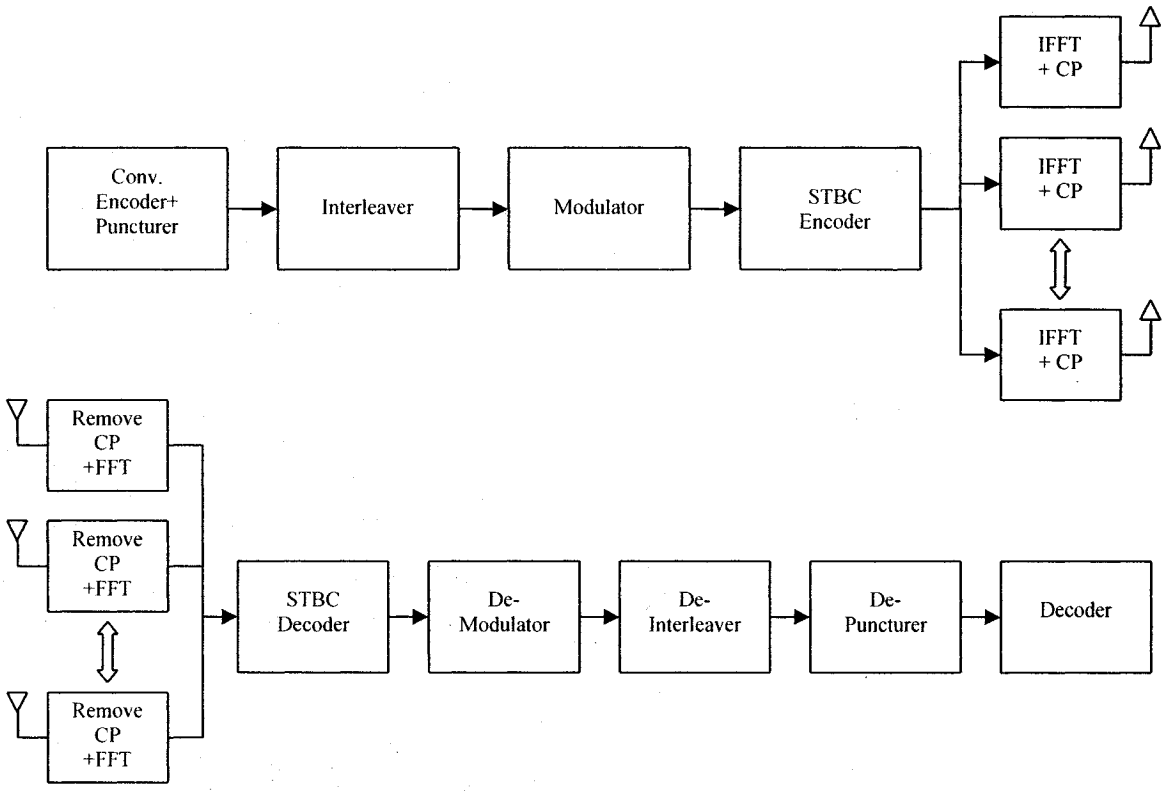

Fig 4.15 Transmitter and receiver structure of the MIMO-OFDM system in [33]

The system in [33] uses a 2×2 antenna configuration. Its transmitter uses a convolutional encoder and an interleaver instead of a spreader. However, the complexity of encoder plus interleaver is higher than that of our proposed transmitter. Similarly, the receiver in [33] has no despreader but has a de-interleaver and a decoder which means that it has higher complexity than the receiver in our system. The simulation results for the system in [33] are shown below.

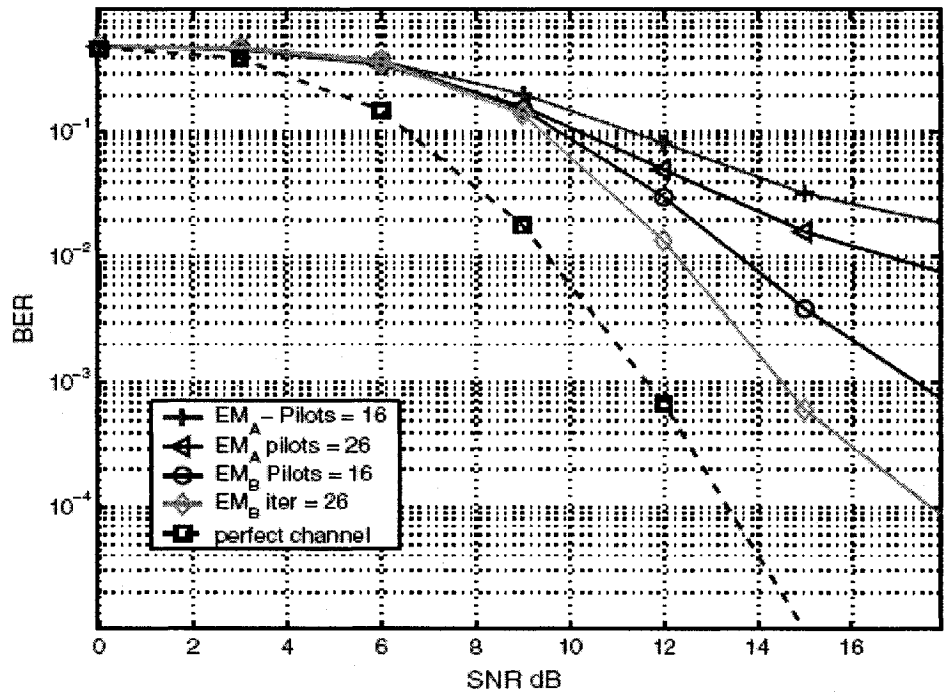

Fig 4.16 Simulation results of the MIMO-OFDM system [33]

It is seen from Fig. 4.7 and Fig. 4.16 that in the perfect channel case, our system gives a much better BER performance than that in [33]. For example, when a Walsh code of size 16 is used, the BER of our system is 10^{-4} at an SNR of 8dB whereas that of the system in [33] is only 0.5×10^{-2}.

Finally, from all the previous comparisons we can conclude that our system achieves both a better BER performance and a lower computational complexity than some of the existing systems without using the Walsh block coding scheme.

4.4 Conclusions

In this chapter, we have presented the second configuration of our MIMO-OFDM system using STBC and Walsh block coding. We provided the system block diagram with a detailed description of each block. We have also provided a brief review of STBC techniques as well as their implementation in our system.

A performance study of the proposed system has also been carried out, showing detailed simulation results under different channel delays, fading environments, coding schemes, code sizes, antenna configurations and in the presence of an interleaver. It has been seen that the performance improvement from the STBC configuration is even better than that from using VBLAST, as a result of exploiting the full order diversity in the STBC system. The main differences we have seen between STBC and VBLAST is that the performance of the STBC system improves with convoultional coding and the performance improvement increases with the proposed block coding scheme. It has also been shown that the performance of the system with STBC improves as the channel delay increases, since STBC uses the streams as a source of diversity to enhance system performance. Simulating the system under different fading environments has shown that the system performs best under Rayleigh fading and the performance deteriorates rapidly under Ricean fading with high K factors because of the poor scattering. Finally, we have compared our system to a few previous systems in terms of both BER performance and computational complexity. The comparisons have shown that our system is superior in both aspects.

Chapter 5

The Performance of the Proposed Systems with Channel Estimation Techniques

In Chapters 3 and 4 the VBLAST and STBC configurations of our proposed system have been studied. In order for these techniques to achieve diversity and array gain, channel knowledge has to be known at the receiver. In Chapters 3 and 4, we assumed that the receiver has perfect channel knowledge. In reality, the channel parameters have to be estimated and therefore, errors might occur. In this chapter some common channel estimation techniques will be implemented in the proposed system. The objective is to evaluate the performance of the proposed system in a more practical situation. We will start by reviewing the criteria for preamble design, followed by a brief description of a few channel estimation methods, namely, LS, MMSE and the FFT method which will be used in our system. A performance study of our system with these estimation techniques will then be provided.

5.1 A Brief Overview of Channel Estimation Techniques and Preamble Design

5.1.1 Criteria for Preamble Design

Channel estimation is usually achieved by employing training symbols at the transmitter that are known to the receiver. A packet of training symbols, called the preamble is appended to each data packet prior to transmission. This preamble will be mutated by the channel according to its parameters. The receiver extracts the preamble from the received packet and, since the training symbols are known at the receiver, it could use any channel estimation method to determine the channel parameters. However, for this method to work the channel has to be constant for the duration of the preamble (quasi-static) which we already assume. Therefore, this method is valuable in slow fading channels. For fast tracking, pilot symbols are used (this method will not be discussed in this thesis). As far as MIMO systems are concerned, the signals transmitted from the antennas should be made orthogonal to each other in order to estimate the CIR from each receive to each transmit antenna. There are three ways to achieve this goal [10]:

Time orthogonality: which is achieved by allowing each antenna to transmit alone to ensure there is no interference at the receiver.

Frequency orthogonality: This is done by assigning a specific frequency to each antenna and using the appropriate separation methods at the receiver. This however uses more bandwidth than other methods.

Code orthogonality: By using some coding methods, we can make the dot product of the training symbols equal to zero, thus ensuring orthogonality. This will require more complicated processing at the receiver.

In our system we use training symbols that are orthogonal in time. This is the most popular method as it is efficient and easy to implement. In Chapter 2, we had discussed the preamble structure adopted by the IEEE standard 802.11a. The same structure will be employed in this chapter for the training sequence.

5.1.2 Brief Review of Some Common Channel Estimation Techniques

There are several ways to process the information carried by the preamble and to estimate channel parameters. In this section we will go over some of these techniques.

5.1.2.1 Least Squares (LS) Estimation

Assuming we transmit a matrix of training symbols $\mathbf{P} = [\mathbf{p}_1, ..., \mathbf{p}_L]$ of size $M_T \times L$ and where L, the number of training symbols in the preamble transmitted from each antenna, is greater than or equal to the number of transmit antennas M_T ($L \geq M_T$). The matrix of received signals (**S**) can be given by [34]:

$$\mathbf{S} = \mathbf{HP} + \mathbf{V} \tag{1}$$

where $\mathbf{S} = [\mathbf{s}_1, ..., \mathbf{s}_L]$ is the $M_R \times L$ matrix of received signals and M_R is the number of receive antennas, **H** is the $M_R \times M_T$ complex channel matrix and **V** is the $M_R \times L$ zero-mean noise matrix. The LS channel estimates are found by minimizing the error matrix $\mathcal{E}^2$ [10]

$$\mathcal{E}^2 = (\mathbf{S} - \mathbf{P}\,\mathbf{H})^H(\mathbf{S} - \mathbf{P}\,\mathbf{H}) \tag{2}$$

The estimates that minimize Equation (2) are given by

$$\hat{\mathbf{H}} = (\mathbf{P}^H \mathbf{P})^{-1} \mathbf{P}^H \mathbf{S} \tag{3}$$

which can be written as

$$\hat{\mathbf{H}}_{LS} = \mathbf{S}\mathbf{P}^{\dagger} \tag{4}$$

In case the preambles are orthogonal, then at any time only one antenna is transmitting and **P** is unitary. Therefore, Equation (1) can be rewritten as

$$s_{j,k} = h_{j,i,k}\, p_{i,k} + v_{j,k} \qquad i = 1, \ldots, M_T,\ j = 1, \ldots, M_R \text{ and } k = 0,1, \ldots, L-1 \tag{5}$$

where $s_{j,k}$ is the k^{th} received symbol at receive antenna j, $h_{j,i,k}$ is the channel coefficient from receive antenna j to transmit antenna i which affects the symbol k, $p_{i,k}$ is the k^{th} transmitted symbol from antenna i and $v_{j,k}$ is the AWGN that affects the symbol k. Therefore, the LS channel estimates for the symbol k can be found by

$$\hat{h}_k = p_k^H\, s_k = p_k^{-1}\, s_k = h_k + \hat{v}_k \qquad k=0, 1, \ldots, L-1 \tag{6}$$

where $\hat{v}_k = p_k^{-1}\, v_k$. It is the job of the designer to find out the optimum set of preambles that minimizes the channel mean square error (MSE). If we assume that the power of the training symbols is constrained by [34]

$$\|\mathbf{P}\|^2 = C \tag{7}$$

where C is a given power constant. Therefore, we have to find **P** which minimizes

$$\min E\{\|\mathbf{H} - \hat{\mathbf{H}}_{LS}\|^2\} \quad \text{subject to } \|\mathbf{P}\|^2 = C \tag{8}$$

using the fact that $E\{\mathbf{V}^H \mathbf{V}\} = \sigma_n^2 M_R \mathbf{I}$, where σ_n^2 is the received noise power and **I** is the identity matrix, $E\{\|\mathbf{H} - \hat{\mathbf{H}}_{LS}\|^2\}$ can be written as

$$J_{LS} = E\{\|\mathbf{H} - \hat{\mathbf{H}}_{LS}\|^2\} = \sigma_n^2 M_R\, tr\{(\mathbf{P}\mathbf{P}^H)^{-1}\} \tag{9}$$

where "tr" denotes the trace of the matrix. We can use the Lagrange multiplier method to solve Equation (8). By Substituting Equation (9) into Equation (8), we can solve Equation (8) by minimizing the function

$$L(\mathbf{P}, \mu) = \mathrm{tr}\{(\mathbf{P}^H \mathbf{P})^{-1}\} + \mu\,(\mathrm{tr}\{\mathbf{P}^H \mathbf{P}\} - C) \tag{10}$$

After some algebraic work [34], we can find that the optimal training matrix has to satisfy

$$\mathbf{P}\mathbf{P}^H = C/M_T\,\mathbf{I} \tag{11}$$

where $\mathbf{I}$ is the identity matrix. Therefore, any training matrix with orthogonal rows of the same norm $\sqrt{(C/M_T)}$ is optimum.

5.1.2.2 Minimum Mean Square Error (MMSE) Channel Estimation

The MMSE channel estimator is given by [34]

$$\hat{\mathbf{H}}_{MMSE} = \mathbf{S}\,(\mathbf{P}^H \mathbf{R}_H \mathbf{P} + \sigma_n^2 M_R \mathbf{I})^{-1} \mathbf{P}^H \mathbf{R}_H \tag{12}$$

This estimator takes into account the channel correlation matrix $\mathbf{R}_H$. In all previous simulations we assumed that the transmitted data streams are uncorrelated and independent [10] which is not the situation in reality. As Antenna correlation may cause performance degradation, it should be taken into account. For 2 transmit antenna systems, its correlation matrix is given by:

$$\begin{pmatrix} 1 & \alpha \\ \alpha & 1 \end{pmatrix}$$

where α is the correlation factor between receive antennas, which takes values between 0 (uncorrelated) and 1 (fully correlated). The MMSE estimator also takes into account the noise power and averages it out. The disadvantage of this method is that the channel correlation matrix and the noise power have to be known at the receiver which introduces

an increase in complexity. In this chapter, we assume that these parameters have already been estimated at the receiver. The performance of the MMSE estimator is characterized by the error $\mathcal{E} = \mathbf{H} - \hat{\mathbf{H}}_{MMSE}$ [34], where $\mathcal{E}$ has zero mean and its correlation matrix given by

$$\mathbf{R}_{\mathcal{E}} = E\{\mathcal{E}\,\mathcal{E}^{H}\} = (\mathbf{R}_{H}^{-1} + \sigma_n^{-2} M_R^{-1}\,\mathbf{P}\mathbf{P}^{H})^{-1} \tag{13}$$

Then, the MMSE estimation error is given by

$$J_{MMSE} = E\{\| \mathbf{H} - \hat{\mathbf{H}}_{MMSE} \|^2\} = tr\{\mathbf{R}_{\mathcal{E}}\} \tag{14}$$

To minimize this error function the transmit power constraint is given by $tr\{\mathbf{P}\mathbf{P}^{H}\} = C$. Using the Lagrange multiplier method, we can solve Equation (14) by minimizing the function

$$L(\mathbf{P}, \mu) = tr\{(\mathbf{R}_{H}^{-1} + \sigma_n^{-2} M_R^{-1}\,\mathbf{P}\mathbf{P}^{H})^{-1}\} + \mu\,(tr\{\mathbf{P}\mathbf{P}^{H}\} - C) \tag{15}$$

Again, making a computational effort the optimal training matrix can be chosen to satisfy

$$\mathbf{P}\mathbf{P}^{H} = 1/M_T\,(C + \sigma_n^2 M_R\, tr\{\mathbf{R}_{H}^{-1}\})\mathbf{I} - \sigma_n^2 M_R\,\mathbf{R}_{H}^{-1} \tag{16}$$

The equation shows that at high SNR ($\sigma_n^2/C \rightarrow 0$) the category for choosing the MMSE training matrix approaches the category for choosing the LS training matrix.

5.1.2.3 The FFT Method

The FFT method is not a channel estimation method on its own; rather it refines the channel estimates produced by any of the above methods. The method works as follows [35]

1. First, the channel estimates are found using any of the aforementioned methods. These are called coarse channel estimates. Assuming LS is used; the estimates are

given by Equation (6). Assuming all **P**'s are unitary and the training symbols are orthogonal, the variance of the noise in the coarse channel estimates would remain unchanged.

2. Improve the coarse estimates by converting them to the time domain using an L-point IFFT operation. This is equivalent to multiplying the estimates by $\mathbf{F}^{-1}$ where **F** is the Fourier transform matrix given by

$$\begin{pmatrix} 1 & 1 & \dots & 1 \\ 1 & \omega & \dots & \omega^{L-1} \\ 1 & \omega^2 & \dots & \omega^{2(L-1)} \\ \Updownarrow & & & \Updownarrow \\ 1 & \omega^{L-1} & \dots & \omega^{(L-1)^2} \end{pmatrix}$$

and $\omega = e^{j2\Pi/L}$. From the matrix we can see that **F** is unitary.

3. The converted estimates given by $\{g_{i,j,k}\}$ $i = 0, 1, \dots, M_T$; $j = 0,1, \dots, M_R$ and k=0, 1, …, L-1 are passed to a rectangular window such that

$$\hbar_{i,j,k} = \begin{cases} g_{i,j,k} & 0 \le m \le (C_p\text{-}1) \\ 0 & m \ge C_p \end{cases} \qquad (17)$$

where C_p is the maximum delay of the channel, which is typically chosen to be equal to the length of the cyclic prefix.

4. The resulting estimates are then converted back to the frequency domain using an L-point FFT operation

$$\hat{h}_{i,j} = FFT_L \{ \hbar_{i,j} \} \qquad (18)$$

The result of this whole operation is that the noise variance is finally reduced to $\sigma^2 C_p/L$.

5.2 Simulation Results

In this section the performance of our system will be simulated using the aforementioned channel estimation techniques, in which both STBC and VBLAST configurations are considered. The channel model and the system parameters used for the simulation are the same as the ones used in Chapters 3 and 4. Rayleigh fading is assumed in all the experiments in this chapter.

5.2.1 Experiment 1: Effect of FFT Method

In the first experiment, the effect of the FFT method on channel estimation will be investigated. We consider the STBC configuration in our system with 2×2 transmit and receive antennas and the (32, 5) Walsh code. We use LS channel estimation to compute the initial coarse channel estimates. The simulation results are shown in Fig. 5.1.

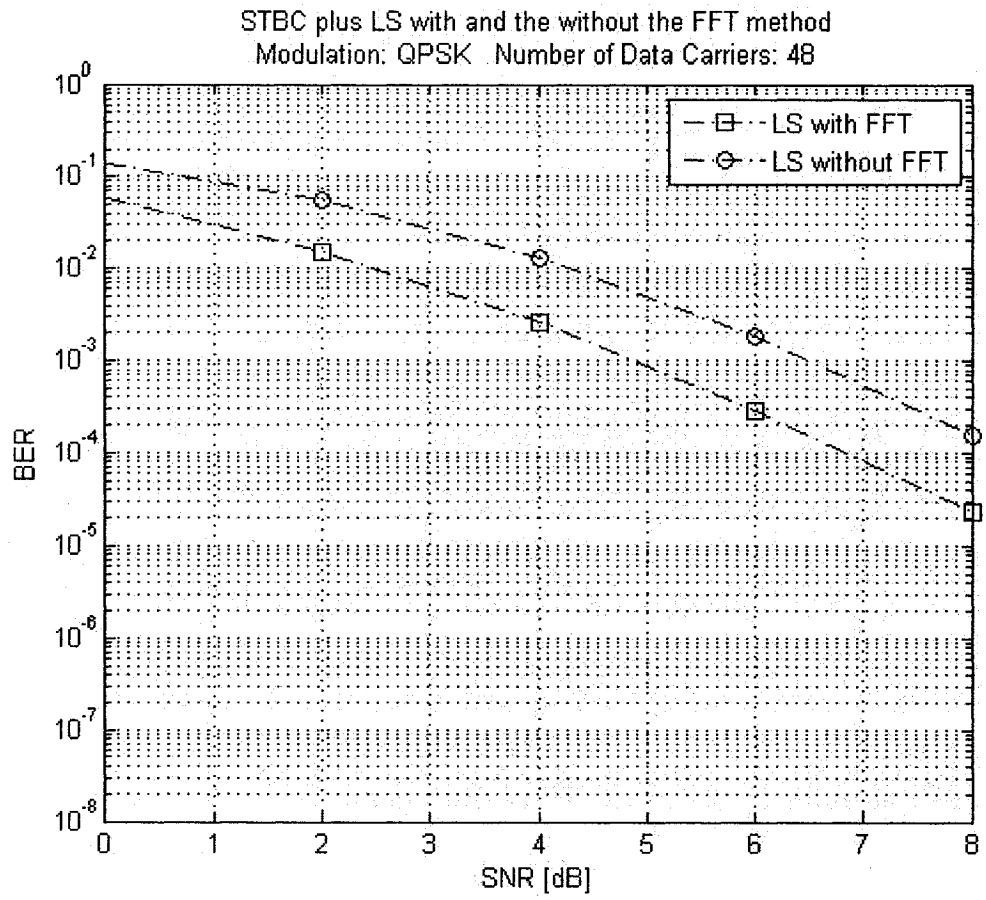

Fig 5.1 BER plots of our STBC system using LS channel estimation with and without the FFT method

From Fig. 5.1 we can see that the FFT method improves the performance of LS channel estimation by approximately 2 dB. Since the size of the cyclic prefix is 16 samples and 48 training symbols are used, the noise variance is reduced to 1/3 of its original value. Furthermore, the FFT method is easy to implement and does not instigate a drastic increase in complexity as only 3 extra steps are needed after the original channel estimation method takes place.

5.2.2 Experiment 2: Channel Estimation with STBC

In this experiment the effect of channel estimation on the STBC configuration of our system is investigated. The same system parameters used in Experiment 1 are applied here. We would like to compare the performance of the system with perfect channel knowledge to the same system using channel estimation. Both LS and MMSE channel estimation techniques are examined, each accompanied by the FFT method. The simulation results are shown in the following figure.

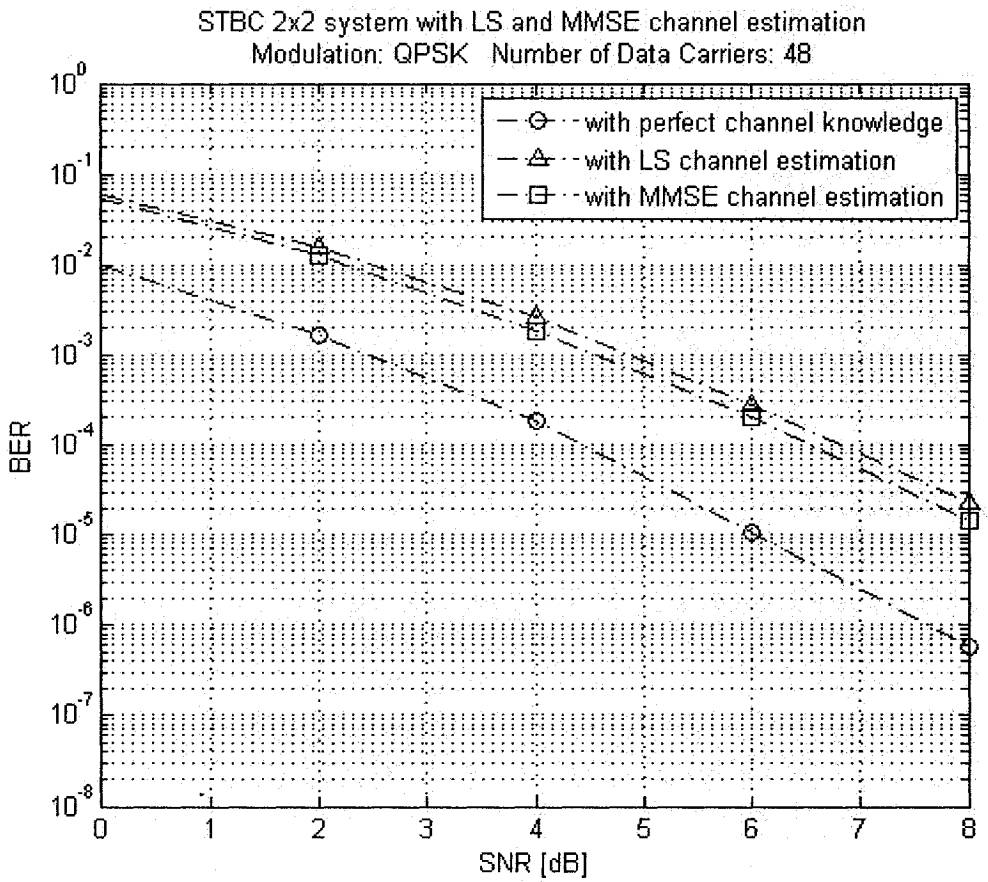

Fig 5.2 BER plots of our STBC system with LS and MMSE channel estimation

As we can see from the figure, there is approximately 2 dB difference between the performance of the system with perfect channel knowledge and the one with LS channel estimation. This shows why channel estimation techniques have to be carefully designed for each system. We can also see from the figure that MMSE achieves performance results that are very close to LS which makes the increased complexity, resulting from the estimation of the noise variance in MMSE, unjustified.

5.2.3 Experiment 3: Channel Estimation with VBLAST

In this experiment, we consider the VBLAST configuration of our system for computer simulation. We use 2×4 transmit and receive antennas with the (16, 4) code. As in Experiment 2, we want to examine both LS and MMSE estimation techniques with the FFT method and we will compare both cases to the one with perfect channel knowledge. The simulation results are shown below.

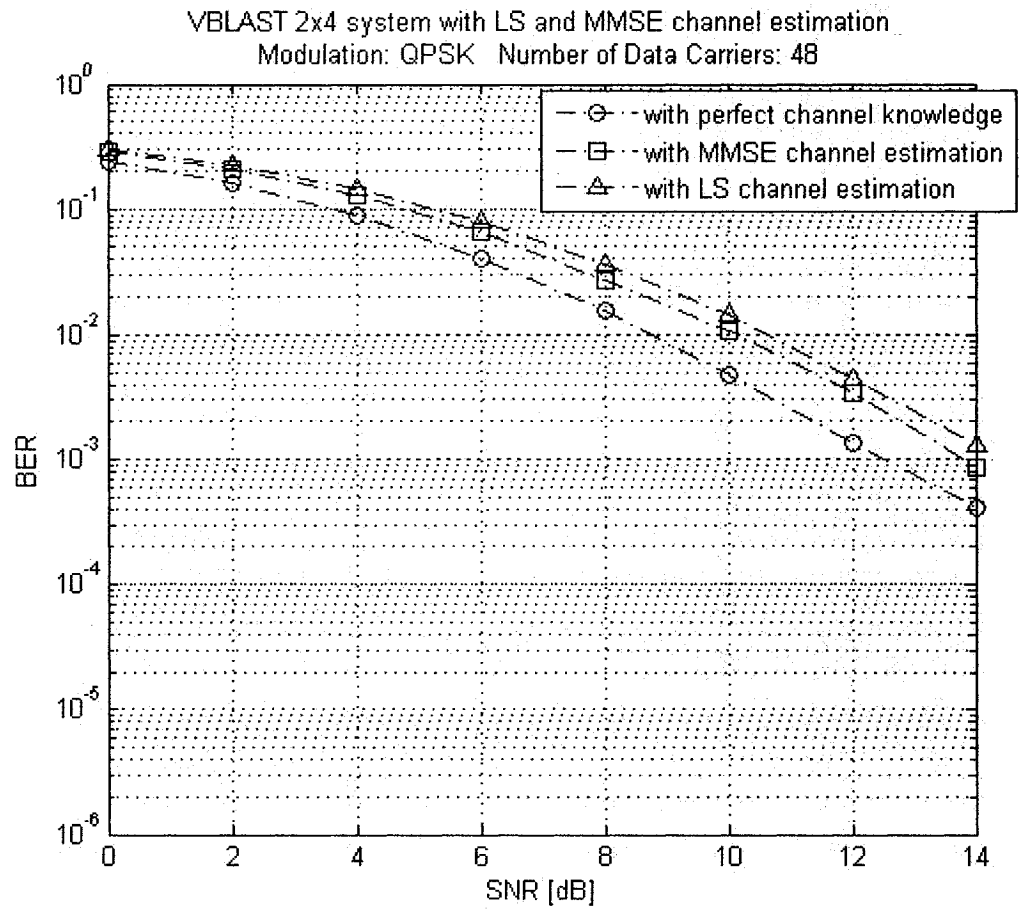

Fig 5.3 BER plots of our VBLAST system with LS and MMSE channel estimation

We can see that the results in this experiment are concurrent with the ones in experiment 2. Again, MMSE achieves close performance results to LS. These results confirm those already published in other literature [41].

5.3 Conclusions

In this chapter, the performance of the proposed system has been investigated using different channel estimation techniques. First, the general criteria for preamble design for MIMO systems were previewed and the preamble structure used in our system was

described. A brief visit of some of the typical channel estimation techniques, namely, LS and MMSE has also been presented. We have then explained the FFT method which is used to refine the estimates produced by one of the above mentioned methods.

The performance of our system using the aforementioned techniques has been investigated through computer simulations. The first experiment showed how the FFT method would improve the estimates produced by LS channel estimation. In Experiment 2, we considered the STBC configuration in our system and compared its performance with perfect channel knowledge to that using LS and MMSE channel estimation algorithms accompanied by the FFT method. Simulations showed that MMSE achieves performance results that are very close to LS, even though noise variance was taken into account. In Experiment 3, we examined the effects of the same techniques used in Experiment 2 on the VBLAST configuration of our system. Simulation results also showed that these techniques have similar effects on VBLAST as on STBC. This leads to the conclusion that the increased complexity in MMSE, arising from estimating the noise variance and the channel correlation matrix at the receiver, is unjustified. Using LS channel estimation plus the FFT method achieves good performance results without drastically increasing the computational complexity.

Chapter 6

Conclusions and Future Research Directions

6.1 Conclusions

In this thesis a high-performance and low-complexity MIMO-OFDM system has been presented in which Walsh code spreading has been implemented as block coding in the system. A performance study of the proposed system was undertaken by considering both VBLAST and STBC configurations as well as different channel estimation techniques. Computer simulations and comparisons have shown that the proposed system outperforms some of the existing systems without using Walsh block coding in terms of both system performance and computational complexity.

In Chapter 2, some fundamental techniques for modern wireless communication systems including: MIMO, OFDM and Walsh spreading have been reviewed. A brief description of the physical layer of the IEEE standard 802.11a has been given, including the key parameters of the standard as well as the main blocks on which the system is based. Some properties of Walsh functions as well as some of the code generation methods have been

reviewed. Some of the terms defining MIMO systems and the imbedded tradeoff found in MIMO techniques between diversity and multiplexing gain have also been examined. Finally, some of the previous works in the combination of the three techniques, namely, OFDM, MIMO and CDM have been discussed.

In Chapter 3, the first configuration of our system which combined MIMO-VBLAST, OFDM and the proposed Walsh block coding scheme has been presented. A detailed explanation of the system's block diagram was given with an overview of the VBLAST algorithm. Then, a performance study of the system was carried out by considering different system parameters and channel conditions. The simulation results have shown that the proposed system achieves better performance results than its convolutional-coded counterpart. This is due to the fact that the performance of the Viterbi decoder (associated with convolutional coding) is impaired by the error propagation problem inherently present with VBLAST, while the proposed block coding scheme does not experience that problem. The proposed system still outperforms the convolutional-coded system even after adding an interleaver. This makes the proposed block coding scheme more suitable for VBLAST systems, and since most of the blocks used in our design follow the IEEE standard 802.11a, the system can be easily implemented. We have also seen that as the block code's size increases the performance improves. This, however, comes with the expense of some bandwidth consumption. It is up to the design engineer to trade-off performance for the target data rate. However, since the proposed system has lower computational complexity than typical layered space-time systems, as demonstrated through comparisons, therefore the design problem becomes more flexible as the data rates can easily be increased using higher order modulations or more transit antennas.

In Chapter 4, the proposed system using the MIMO-STBC configuration has been studied. In contrast to VBLAST, which aims to increase data rates, STBC is intended to improve performance and enhance the link quality. After a short review of the STBC codes for complex and real constellations, the system's structure has been outlined and the differences between the VBLAST system and STBC have been elaborated. Then, a performance study of the system has been conducted in a similar manner as the one done in Chapter 3. The proposed system has showed even more improved performance than VBLAST due to the exploitation of higher diversity orders with STBC. A significant difference was observed between VBLAST and STBC when the systems were simulated using different channel delays. Compared to VBLAST, the performance of STBC is seen to improve as the delay increases under the condition that the maximum delay is still smaller than the cyclic prefix. This is because the STBC uses the channel paths as a source of diversity that improves the performance. It has also been shown that the system achieves optimum performance in rich scattering environments, namely, Rayleigh environments and the performance deteriorates rapidly in poor scattering environments, namely, Ricean fading with high K factors. This leads to the conclusion that the STBC configuration of the proposed system is more suited for applications were the performance is limited by the effects of multipath fading and were high data rates are not required. However, since the proposed system has low computational complexity, as demonstrated in Chapter 4, higher data rates can be achieved using higher order modulations and small block code sizes.

Finally, in Chapter 5, the performance of the proposed system has been investigated using different channel estimation techniques. The criteria for preamble design and the

structure of the preamble used in the proposed system have been outlined. Some of the existing channel estimation techniques such as LS, MMSE and the FFT method employed to improve the performance of any channel estimation method has been studied. Simulation results have shown that LS channel estimation is not sufficient for MIMO systems if used on its own. It has also been shown that by using LS plus the FFT method, satisfactory performance results are achieved without a drastic increase in computational complexity thus making these techniques suitable for both STBC and VBLAST systems.

6.2 Future Research Directions

Although the techniques addressed in this thesis are relatively new, they have become very popular among researchers and a lot of work has been done on this topic. However, there are some key points that could prove useful to the future development of the system proposed in this thesis:

- All the simulations in this thesis were under the assumption of perfect timing synchronization and offset estimation at the receiver. However, in reality these issues have to be addressed carefully. Therefore, future work can be done to investigate the performance of our system using different synchronization and phase recovery techniques. Some of these techniques are listed in [26]-[29].
- We have mentioned that there is a tradeoff between diversity and multiplexing gain when we choose STBC or LST codes. The idea of combining both MIMO techniques has been studied in [39] and proves to be efficient in achieving a good compromise in

performance and data rates. Using this combination might be very useful to our system.

- Our system is designed for a single user and so, in order to apply it in mobile networks it has to be extended to a multiple user system. There are several techniques to achieve this goal namely, TDMA, FDMA or CDMA, out of which CDMA is the latest access scheme implemented in networks worldwide. OFDM itself could also be extended as a multiple access scheme which is known as OFDMA. Our system would have to be tested with some of these schemes before it is implemented in real world.
- In our simulations we assumed a slow fading channel. Since this is not always the situation, one has to study the system under fast fading channels as well.
- In Chapter 1, we mentioned that the two main problems facing OFDM are: its sensitivity to synchronization errors and the peak-to-average power ratio (PAPR) problem. Although there has been is a lot of research done in these aspects, still more work is needed.
- Although VBLAST is considered to be a very efficient decoding method for LST codes, its performance is considered suboptimal. Therefore, more work is needed to improve its performance and to further decrease its computational complexity.

References

[1] K.R Santhi, V.K. Srivastava, G. S. Kumaran and A. Butare, "Goals of true band's wireless next wave (4G-5G)," *IEEE Vehicular Technology Conference (VTC),* volume 4, October 2003, page(s):2317 – 2321.

[2] H.-B Lim, "Beyond 3G: issues and challenges," *IEEE Potentials,* volume 21, issue 4, October 2002, page(s):18 – 23.

[3] J. Hu and W. W. Lu, "Open Wireless Architecture – the core to 4G mobile communications," *IEEE International Conference on Communications Technology (ICCT),* volume 2, April 2003, page(s):1337 – 1342.

[4] H. Yang, "A road to future broadband wireless access: MIMO-OFDM-Based air interface," *IEEE Communications Magazine,* volume 43, issue 1, January 2005, page(s):53 – 60.

[5] A. Doufexi, S. Armour, M. Butler, A. Nix, and D. Bull, "A study of the performance of HIPERLAN/2 and IEEE 802.11a physical layers," *IEEE Vehicular Technology Conference (VTC),* volume 1, May 2001, page(s):668 – 672.

[6] S. O'Leary, "Hierarchical transmission and COFDM systems," *IEEE transactions on Broadcasting,* volume 43, issue 2, June 1997, page(s):166 – 174.

[7] G. Lawton, "Is MIMO the future of wireless communications?" *Computer Magazine, IEEE Computer Society,* volume 37, issue 7, July 2004, page(s):20 – 22.

[8] IEEE Standard 802.11a – 1999 "Supplement to IEEE standard for information technology telecommunications and information exchange between systems - local and metropolitan area networks - specific requirements. Part 11: wireless LAN Medium Access Control (MAC) and Physical Layer (PHY) specifications: high-speed physical layer in the 5 GHz band."

[9] J. S. Lee and L. E. Miller, *CDMA Systems Engineering Handbook,* Norwood, MA: Artech House, 1998.

[10] M. Jankiraman, *Space-Time Codes and MIMO Systems,* Norwood, MA: Artech House, 2004.

[11] G. J. Foschini and M. J. Gans, "On limits of wireless communications in a fading environment when using multiple antennas," *Wireless Personal Communications,* 1998, page(s): 6:311-355.

[12] S. M. Alamouti, "A simple transmit diversity technique for wireless communications," *IEEE Journal Select Areas in Communication,* volume 16, No. 8, October 1998, page(s): 1451 – 1458.

[13] G. Foschini, "Layered Space-Time Architecture in Wireless Communications in a Fading Environment using Multielement Antennas," *Bell Labs Technical Journal,* Autumn 1996, page(s): 41-59.

[14] S. Iraji and J. Lilleberg, "Interference cancellation for space-time block-coded MC-CDMA systems over multipath fading channels," *IEEE Vehicular Technology Conference (VTC),* volume 2, October 2003, page(s): 1104 – 1108.

[15] J. Adeane, M. R. D. Rodrigues, I. Berenguer and I. J. Wassell, "Improved detection methods for MIMO-OFDM-CDM communication systems," *IEEE Vehicular Technology Conference (VTC),* volume 3, September 2004, page(s): 1604 – 1608.

[16] I. Berenguer, J. Adeane, I. J. Wassell, and X. Wang, "Lattice-reduction-aided receivers for MIMO-OFDM in spatial multiplexing systems," *Personal, Indoor and Mobile Radio Communications PIMRC,* volume 2, September 2004, page(s): 1517 – 1521.

[17] Z. Lei, P. Xiaoming and F. P. S. Chin, "V-BLAST receivers for downlink MC-CDMA systems," *IEEE Vehicular Technology Conference (VTC),* volume 2, October 2003, page(s): 866 – 870.

[18] P. Xiaoming, Z. Lei and F. P. S. Chin, "Performance comparison of different MIMO configurations for downlink MC-CDMA systems," *IEEE Communications Systems (ICCS),* September 2004, page(s): 281 – 285.

[19] G. D. Pantos, A. G. Kanatas and P. Constantinou, "Performance evaluation of OFDM transmission over a challenging urban propagation environment," *IEEE Transactions on broadcasting,* volume 49, issue 1, March 2003, page(s): 87 – 96.

[20] B. J. Choi, L. Hanzo, and M. S. Munster, *OFDM and MC-CDMA for Broadband Multi-User Communications, WLANs and Broadcasting,* New York, J. Wiley and Sons Inc., 2003.

[21] R. Prasad, *OFDM for wireless communications systems,* Norwood, MA: Artech House, 2004.

[22] Y. Sun, "Bandwidth-Efficient Wireless OFDM," *IEEE Journal on Select Areas in Communications,* volume 19, No.11, November 2001, page(s): 2267 – 2278.

[23] Y. Li, and M. Kavehrad, "Effects of time selective multipath fading on OFDM systems for broadband mobile applications," *IEEE Communication Letters,* volume 3, No. 12, December 1999, page(s): 332 – 334.

[24] Z. Dlugaszewski, K. Wesolowski, and M. Lobeira, "Performance of several OFDM transceivers in the indoor radio channels in 17 GHz band," *IEEE Vehicular Technology Conference (VTC)*, volume 2, May 2001, page(s) 825 – 829.

[25] X. D. Yang, Y. H. Song, T. J. Owens, J. Cosmas and T. Itagaki, "Performance analysis of the OFDM scheme in DVB-T," *IEEE Proceedings of Emerging Technologies: Frontiers of Mobile and Wireless Communication,* volume 2, June 2004, page(s): 489 – 492.

[26] M.-H Hsieh and C.-H Wei, "A low-complexity frame synchronization and frequency offset compensation scheme for OFDM systems over fading channels," *IEEE Transactions on Vehicular Technology,* volume 48, issue 5, September 1999, page(s): 1596 – 1609.

[27] W. Songping and Y. Bar-Ness, "OFDM systems in the presence of phase noise: consequences and solutions," *IEEE Transactions on Communications,* volume 52, issue 11, November 2004, page(s): 1988 – 1996.

[28] V. P. G. Jimenez, M. J. F Garcia, F. J. G. Serrano and A. G. Armada, "Design and implementation of synchronization and AGC for OFDM-based WLAN receivers," *IEEE Transactions on Consumer Electronics,* volume 50, issue 4, November 2004, page(s): 1016 – 1025.

[29] Z. Zhang, K. Long, M. Zhao and Y. Liu, "Joint Frame Synchronization and Frequency Offset Estimation in OFDM Systems," *IEEE Transactions on Broadcasting,* volume 51, issue 3, September 2005, page(s): 389 – 394.

[30] P. W. Wolniansky, G. J. Foschini, G. D. Golden and R. A. Valenzuela, "V-BLAST: an architecture for realizing very high data rates over the rich-scattering wireless channel," *IEEE International Symposium on Signals, Systems and Electronics (ISSSE),* October 1998, page(s):295 – 300.

[31] L. Heunchul and L. Inkyu, "New approach for coded layered space-time OFDM systems," *IEEE International Conference on Communications (ICC),* volume 1, May 2005, page(s):608 – 612.

[32] V. Tarokh, H. Jafarkhani and A. R. Calderbank, "Space-time block codes from orthogonal designs," *IEEE Transactions on Information Theory,* volume 45, issue 5, July 1999, page(s):1456 – 1467.

[33] T. Y. Al-Naffouri, O. Awoniyi, O. Oteri and A. Paulraj, "Receiver design for MIMO-OFDM transmission over time variant channels," *IEEE Global Telecommunications Conference (GLOBECOM),* volume 4, December 2004, page(s):2487 – 2492.

[34] M. Biguesh and A. B. Gershman, "MIMO channel estimation: optimal training and tradeoffs between estimation techniques," *IEEE International Conference on Communications,* volume 5, June 2004, page(s):2658 – 2662.

[35] A. N. Mody and G. L. Stuber, "Parameter estimation for OFDM with transmit receive diversity," *IEEE Vehicular Technology Conference (VTC),* volume 2, May 2001, page(s):820 – 824.

[36] R. Van Nee and R. Prasad, *OFDM for wireless multimedia communications,* Norwood, MA: Artech House, 2000.

[37] Y. Younghwan, M. Kim, S. Hong, I. Hwang and H. Song, "Performance investigation of STBC-OFDM with code-division multiplexing in time-varying channels," *IEEE transactions on Broadcasting,* volume 50, No. 4, December 2004, page(s):408-413.

[38] A. Zelst and T. Shenk, "Implementation of a MIMO OFDM-based wireless LAN system," *IEEE transactions on Signal Processing,* volume 52, No.2, February 2004, page(s):483-494.

[39] M. H. bin Halmi and D. C. H. Tze "Adaptive MIMO-OFDM combining space-time block codes and spatial multiplexing," *IEEE Symposium on Spread Spectrum Techniques and Applications (ISSSTA),* September 2004, page(s): 444-448.

[40] G. Stuber, *Principles of Mobile Communication, Second Edition,* New York, Kluwer Academic Publishers, 2002.

[41] R. Trepkowski, *Channel Estimation Strategies for Coded MIMO Systems,* M.A.Sc. thesis, Virginia Polytechnic and State University, June 2004.

[42] S.M. Kay, *Fundamentals of Statistical Signal Processing: Estimation Theory,* Prentice Hall, Inc., 1993.

[43] A. H. El Mougy, W.-P Zhu, M. O. Ahmad, "A high performance MIMO-OFDM system with Walsh block coding," submitted for review to the journal of *Circuits, Systems and Signal Processing* in May 2006.

[44] A. H. El Mougy, W.-P Zhu, M. O. Ahmad, "A new channel coding scheme for MIMO-OFDM systems," submitted for review to the *International conference on Signal Processing* to be held on November 2006.